NATIONAL ACADEMY OF SCIENCES OF UKRAINE
Palladin Institute of Biochemistry

BIOTECHNOLOGIA ACTA

Vol. 8, No 6, 2015

BIMONTHLY

Editorial address:
Palladin Institute of Biochemistry of the NAS of Ukraine, 9 Leontovicha Street, Kyiv, 01601, Ukraine;
tel.: 380 44–235–14–2. *E-mail:* biotech@biochem.kiev.ua; *Web-site:* www.biotechnology.kiev.ua

According to the resolution of the Presidium of the the National Academy of Sciences of Ukraine from 27.05.2009 №1-05 / 2 as amended on 25.04.2013 number 463 Biotechnologia Acta has been included in High Attestation Certification Commission list of Ukraine for publishing dissertations on specialties "Biochemistry" and "Biotechnology".

Tel.: 380-44-235-14-72; **E-mail:** biotech@biochem.kiev.ua; **Web-site:** www.biotechnology.kiev.ua

Certificate of registration of print media КВ series №19650-9450ПР on 01.30.2013

Literary editor — H. **Shevchenko**; Computer-aided makeup — O. **Melezhyk**
Authorized for printing 30.12.2015, Format — 210×297. Paper 115 g/m^2
Gaqrn. SchoolBookC. Print — digital. Sheets 13,68. An edition of 100 copies. Order 6.6.
Make-up page is done in Palladin Institute of Biochemistry of the National Academy of Sciences of Ukraine.
Print — O. **Moskalenko** FOP

NATIONAL ACADEMY OF SCIENCES OF UKRAINE
Palladin Institute of Biochemistry

BIOTECHNOLOGIA ACTA

Scientific journal

Bimonthly

Vol. 8, No 6, 2015

CONTENTS

EXPERIMENTAL ARTICLES

ЗМІСТ

ЕКСПЕРИМЕНТАЛЬНІ СТАТТІ

СОДЕРЖАНИЕ

ЭКСПЕРИМЕНТАЛЬНЫЕ СТАТЬИ

EXPERIMENTAL ARTICLES

UDK 577.112:616 doi: 10.15407/biotech8.06.009

OVEREXPRESSION OF DOMINANT-NEGATIVE IRE1 ENZYME IN H1299-shE6AP CELLS INCREASES HEAT SHOCK ELEMENT-DEPENDENT TRANSCRIPTION

D. O. Tsymbal
O. H. Minchenko

Palladin Institute of Biochemistry
of the National Academy of Sciences of Ukraine, Kyiv

E-mail: dariiabova@gmail.com

Received 12.10.2015

To investigate IRE1-dependent branch of endoplasmic reticulum stress pathway in various cancer cells we created cDNA-constructs for expression of dominant-negative inositol-requiring enzyme 1 IRE1 and cytosolic domain of IRE1 fused on a C-terminus with c-Myc and 6xHis tags. The non-small-cell lung carcinoma cells H1299-shE6AP were transfected with these constructs. Using anti-c-Myc antibodies we demonstrated effective, dose-dependent expression of dominant-negative and cytosolic IRE1 proteins. In order to investigate IRE1-mediated, heat shock element-dependent transcription, the cells were further transfected with a reporter construct containing heat shock element. We observed that overexpression of dnIRE1 in H1299-shE6AP cells led to significant induction of heat shock element-dependent transcription. This observation may reflect the induction of heat shock genes, which contribute to cellular adaptation to inhibition of native IRE1, a key sensory-signaling enzyme of endoplasmic reticulum stress pathway, which suppresses cancer cell proliferative capacities and alternates the expression of numerous genes, including many transcription factors.

Key words: endoplasmic reticulum stress, IRE1 enzyme, recombinant protein expression, heat shock element, luciferase reporter assay.

Endoplasmic reticulum (ER) stress signaling pathway is activated as an adaptive response to accumulation of misfolded proteins in its lumen, which might be caused by a handful of factors including increase in protein synthesis, oxidative stress, perturbations of calcium homeostasis, etc. [1, 2]. In mammals three transmembrane stress sensors, namely PERK (double stranded RNA activated protein kinase, PRK-like ER kinase, IRE1/ERN1 (inositol-requiring enzyme 1, endoplasmic reticulum to nucleus signaling 1) and ATF6 (activating transcription factor 6) are responsible for downstream signaling during endoplasmic reticulum stress [3, 4]. Among those IRE1 is a dominant sensory-signaling enzyme, conserved through different groups of organisms including green plants and yeast [5]. IRE1 protein consists of a sensory domain, which is localized in the lumen, a transmembrane part and a cytoplasmic domain with two distinct enzymatic activities: kinase and endoribonuclease [4]. The main function of a kinase domain is IRE1 autophosphorylation, which in turn leads to its dimerization and subsequent activation of endoribonuclease. Activated IRE1 endoribonuclease performs a unique cytosolic splicing of transcription factor XBP1 (X-box binding protein 1) mRNA, as well as specific degradation of a subset of mRNAs [6–8]. Taken together these enzymatic activities contribute to stress alleviation and restoration of cellular homeostasis [5, 8, 9].

For glioma and lung adenocarcinoma it was shown that IRE1 knockdown results in suppression of tumor growth due to alterations in expression of numerous pro- and anti-angiogenic genes, tumor suppressors, cyclins and transcription factors [10–16]. IRE1 is considered to be a promising target for new chemotherapeutic agents, especially in case of aggressive cancers, such as glioma, where surgery still remains a poor therapeutic option [17].

One of the approaches used to inhibit IRE1 function in living cell is a dominant-negative cDNA-constructs strategy, based on the mammalian expression vector systems, such as pcDNA3.1 [4, 10, 11]. In this case, a plasmid DNA, used for transfection, includes a modified cDNA sequence of IRE1 gene, which codes a protein lacking one of or both enzymatic activities [11, 18]. In U87 glioma cells, which express dominant-negative IRE1 (dnIRE1), the downregulation of its phosphorylated form was demonstrated along with an absence of transcription factor XBP1 (X-box binding protein 1) splicing, confirming the inhibition of both kinase and endoribonuclease activities of this bifunctional enzyme [18, 19]. Advantages of this method include the possibility of selection of clones with stable IRE1 knockdown and, in comparison to RNA interference, exclusion of possible off-target effects [11, 18, 20]. Still the detection of modified IRE1 forms, as well as purification of recombinant proteins depends on specific antibodies, which increases the complexity and cost of experimental procedures.

One of the most intriguing aspects of cancer cell biology is the cross-talk between different signaling pathways. For instance, a number of heat shock proteins are known to be involved in the ER stress response. When ER folding capacity is exceeded, molecules of chaperone BiP/GRP78 dissociate from sensory domains of IRE1, PERK and ATF6, which leads to their activation [21]. It was shown, that stressful conditions result in increased BiP/GRP78 expression in glioma cells regardless of IRE1-XBP1 branch of ER stress [14]. Activation of transcription factor ATF6 results in increased expression of ER chaperones GRP78 and GRP94 [21]. In contrast, induction of two HSP40 (heat shock protein-40)-like proteins Erdj4 and $p58^{IPK}$ upon ER stress seems to be mostly XBP1-dependent [22]. Along with other regulatory elements, such as XBP1 of ATF6 binding sites, promoters of *HSP* genes contain the so-called heat shock elements (HSE), various arrays of inverted repeats of the pentameric sequence nGAAn which are responsible for binding of heat shock transcription factors under conditions of thermal stress [23]. Up to date, it was largely unknown for mammalian cells whether disruption of certain branches of ER stress pathway results in compensatory induction of heat shock response.

The aim of this work was creation of improved cDNA-constructs of IRE1 with C-terminal c-Myc and 6xHis tags for investigation of the IRE1-dependent branch of endoplasmic reticulum stress pathway. Using original dnIRE1 expression construct in combination with HSE-containing luciferase reporter we studied the effect of dnIRE1 overexpression on the HSE-dependent transcription in a subline of non-small cell lung carcinoma H1299-shE6AP [24]. It was shown, that overexpression of dominant-negative IRE1 led to significant induction of HSE-dependent transcription.

Materials and Methods

Creation of genetic constructs pcDNA4+dnIRE1 and pcDNA4+cytIRE1

Genetic constructs pcDNA4+dnIRE1 and pcDNA4+cytIRE1 were based on the vector pcDNA4-Myc/His-A (Invitrogen, USA). The vector was linearized simultaneously with two restriction enzymes HindIII and XbaI (NEB, USA). Coding sequence of dominant-negative IRE1 (dnIRE1) was obtained via PCR with forward 5′-GAGAAGCTTCCTCGCCATGCCGG-3′ and reverse 5′-GACTCTAGAGTCTTG-TTCCAGGGAG-3′primers, which include recognition sites for HindIII and XbaI restriction enzymes, respectively. Coding sequence of cytoplasmic domain of IRE1 (cytIRE1) was obtained via PCR with forward 5′-CATAAGCTTTCCCCTGAGCATGCAT-3′ primer with HindIII recognition site and reverse 5′-CTTCTAGAGAGGGCGTCTGGAG-3′ primer with XbaI recognition site. Introduction of restriction enzyme recognition sites into primer sequences was done in order to enable sticky end directional cloning. As a PCR template we used a construct with a full length IRE1 cDNA sequence in pcDNA3.1 vector (kindly provided by prof. M. Moenner, University of Bordeaux-1, France). Obtained fragments were ligated into a linearized vector using T4 DNA ligase (NEB, USA) according to manufacturer's instructions. DH5α *E. coli* cells were heat-shock transformed with pcDNA4+dnIRE1 and pcDNA4+cytIRE1 constructs and subsequently plated on a solid LB medium with 100 μg/mL ampicillin. Nucleotide sequence of created constructs was determined by GATC Biotech (Germany) using T7 and BGH standard sequencing primers.

Cell culture

H1299-shE6AP cells (kindly provided by prof. Martin Scheffner, University of Konstanz, Germany, described in [24]) were cultured in DMEM (Gibco, USA) with 10% FBS at 37 °C, 5% CO_2.

Transfection

For transient expression of dnIRE1 and cytIRE1 H1299-shE6AP cells that reached > 90% confluence were transfected with different combinations of plasmid DNA by lipofection using Lipofectamine 2000 (Invitrogen, USA) according to manufacturer's instructions. Transfection was performed in 6-well polystyrene plates (Greiner bio-one, Germany). For analytical expression of dnIRE1 cells were transfected with plasmid DNA in following combinations: 100 ng pcDNA4+dnIRE1, 300 ng β-galactosidase expression construct [24] 400 ng pcDNA4-Myc/His-A vector (Invitrogen, USA); 500 ng pcDNA4+dnIRE1, 300 ng β-galactosidase expression construct. For analytical expression of cytIRE1 cells were transfected with plasmid DNA in following combinations: 500 ng pcDNA4+cytIRE1, 300 ng β-galactosidase expression construct, 1 500 ng pcDNA4-Myc/His-A vector, 1 000 ng pcDNA4+cytIRE1, 300 ng β-galactosidase expression construct, 1 000 ng pcDNA4-Myc/His-A vector, 2 000 ng pcDNA4+cytIRE1, 300 ng β-galactosidase expression construct.

As a control cells were transfected with 500 ng vector pcDNA4-Myc/His-A together with 300 ng β-galactosidase expression construct.

For luciferase reporter assay cells were transfected with 500 ng pcDNA4+dnIRE1, 1 000 ng 3xHSE-luc construct (kindly provided by prof. Martin Scheffner, University of Konstanz, Germany), 300 ng β-galactosidase expression construct. Control cells were transfected with 500 ng pcDNA4-Myc/His-A vector, 1 000 ng 3xHSE-luc-construct, 300 ng β-galactosidase expression construct.

Cell lysis and β-galactosidase assay

Cell lysis was performed 24 hours after transfection in TNN buffer (100 mM Tris-HCl, 100 mM NaCl, 1% NP-40, 1 mM Pefabloc, 1 μg/mL Aprotinin/Leupeptin, 1 mM DTT, pH 8.0). In order to determine the β-galactosidase activity 5 μl of lysate was mixed with 5 μl ortho-nitrophenyl-β-galactoside (4 mg/ml in 100mM Na_2HPO_4, pH 7.0) and 120 μl buffer Z (100 mM Na_2HPO_4, 10 mM KCl, 1 mM $MgSO_4$, 50 mM β-mercaptoethanol, pH 7.0) and incubated at 37 °C for 10 min. Measurements were performed at Wallac 1420 multilabel counter (PerkinElmer, USA) at wave length of 405 nm. Obtained values were used for calculation of relative transfection efficiency.

Western blot

Cell lysates were normalized with regard to relative transfection efficiency. Protein transfer to PVDF membrane (Millipore, Germany) was performed with wet electroblotter (Bio-Rad, USA) for 90 min at 60 V. After the transfer membrane was incubated in 5% milk powder for 48 hours at 4 °C. Anti-c-Myc mouse monoclonal antibodies (Abcam, UK) in 1:1 000 dilutions were used for detection of recombinant proteins. Blots were developed using WesternBright ECL (Advansta, USA) Signal detection was performed in the imaging system LAS-3000 (Fujifilm, Japan).

Luciferase reporter assay

Luciferase activity in lysates was measured using Luciferase Assay system kit (Promega, USA) on Wallac 1420 multilabel counter (PerkinElmer, USA). Measurement results were normalized according to relative transfection efficiency. For statistical analysis of obtained data we performed one sample T-test.

Results and Discussion

Genetic constructs pcDNA4+dnIRE1 and pcDNA4+cytIRE1

Creation of an appropriate dominant-negative form of IRE1 requires a construction of its truncated cDNA sequence, which would code intact N-terminal signal peptide (residues 1-18), sensory (residues 18-443) and transmembrane (residues 444-464) domains, but would lack the full sequences of kinase (residues 571-831) and endoribonuclease (residues 837-963) parts (Fig. 1, *A*). To the contrary, for expression of cytosolic domain of IRE1 protein must be truncated from N-terminus for at least 464 residues. At the same time, for expression of C-terminally tagged proteins it is necessary to maintain the open reading frame and avoid formation of stop codons during the cloning. A 1690 bp long fragment coding a dominant-negative IRE1, which corresponds to amino acid residues 1 to 537 of native IRE1, was obtained via PCR and subsequently digested with restriction enzymes HindIII and XbaI (Fig. 1, *B*). Respective fragment was ligated into pcDNA4-Myc/His-A vector. Similar approach was used to obtain a coding sequence of cytosolic domain of IRE1. A 1557 long PCR product, which corresponds to amino acid residues 488 to 977 of a full length IRE1 was restriction digested and ligated into vector (Fig. 1, *C*).

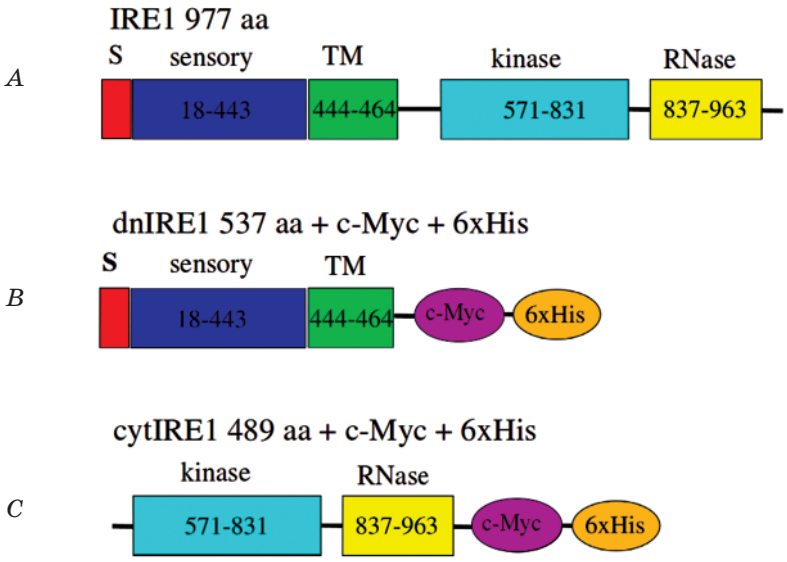

Fig. 1. **Schematic representation of expected protein products:**
A — domain structure of native IRE1;
B — dominant-negative form of IRE1 (dnIRE1) with C-terminal c-Myc and 6xHis tags;
C — cytosolic domain of IRE1 (cytIRE1) with C-terminal c-Myc and 6xHis tags.
S — N-terminal signal peptide, *TM* — transmembrane region, RNase — endoribonuclease

Sequencing results have shown that the sequences of the fragments were as expected and open reading frames remained intact, thus fusing the desired IRE1 parts with C-terminal tags.

Analytical expression of IRE1 cytosolic domain and dominant-negative IRE1 in H1299-shE6AP cells

In order to determine, whether the created constructs are suitable for expression of desired protein products, we transfected H1299-shE6AP cells with different amounts of pcDNA4+dnIRE1 and pcDNA4+cytIRE1 plasmids and performed the Western blot analysis with anti-c-Myc antibody. Our data show, that dominant-negative IRE1 is expressed as a protein product of expected size (Fig. 2). For both dnIRE1 and cytIRE1 the amount of protein depends on the quantity of plasmid, used for transfection (Fig. 2, Fig. 3). Surprisingly, in case of cytIRE1 two fragments of similar size were detected (Fig. 3).

Interestingly, a similar picture was earlier observed by different authors, who also utilized different cloning strategies. For instance, two bands were detected by Wang and co-authors after expressing a cytoplasmic domain of murine IRE1, fused N-terminally with GAL4 and C-terminally tagged with c-Myc epitope [25]. However, they did not attempt to explain their observation. Uemura and co-authors expressed a C-terminally HA-tagged cytoplasmic domain of IRE1 (residues 469-977) and observed two distinct protein products on the blot [26]. The authors suggest that the bands represent an autophosphorylated and non-phosphorylated forms of IRE1 cytoplasmic domain, supporting their suggestion by the fact, that a kinase-dead cytoplasmic part of IRE1 forms a single band on the blot. Moreover, they demonstrate that the resulting recombinant protein is able to catalyze the XBP1 mRNA splicing [26]. Thus, we can assume that pcDNA4+cytIRE1 construct is suitable for expression of a catalytically active cytoplasmic domain of IRE1. Notably, no second band was observed in case of dnIRE1, providing additional evidence for its dominant-negative character (Fig. 2).

Overexpression of dominant-negative IRE1 influences HSE-mediated transcription in H1299-shE6AP cells

Previously, it was shown that in yeast a constitutive activation of heat shock response (HSR) by overexpression of Hsf1 (heat shock factor 1) is able to rescue growth in IRE1 knockout cells [27]. Moreover, it was demonstrated that in IRE1-deficient yeast cells heat shock response is activated by ER stress, while in wild-type IRE1 cells no ER stress-mediated activation of HSR was observed [27]. In this study we aimed to test, whether overexpression of dnIRE1 alone, with no additional stress induction is sufficient for activation of HSE-dependent transcription in mammalian cells. For this we used an HSE-containing luciferase reporter construct

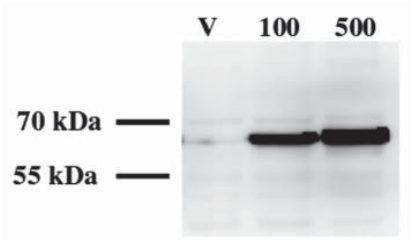

Fig. 2. **Western blot analysis of dnIRE1 expression in H1299-shE6AP cells:**
V — cells transfected with empty vector pcDNA-4mycHis4; 100 — cells transfected with 100 ng pcDNA4+dnIRE1; 500 — cells transfected with 500 ng pcDNA4+dnIRE1

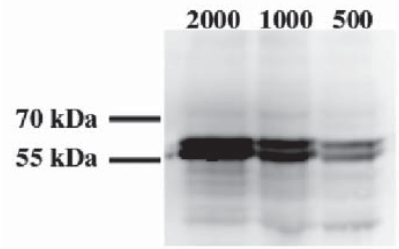

Fig. 3. **Western blot analysis of cytIRE1 expression in H1299-shE6AP cells:**
2000 — cells transfected with 2000 ng pcDNA4+cytIRE1; 1000 — cells transfected with 1000 ng pcDNA4+cytIRE1; 500 — cells transfected with 500 ng pcDNA4+cytIRE1

(3xHSE-luc) (Fig. 4). H1299-shE6AP cells were co-transfected with pcDNA4+dnIRE1, 3xHSE-luc and β-galactosidase expression construct. Luciferase activity was measured in cell lysates and normalized according to relative transfection efficiency. We found that overexpression of dominant-negative IRE1 led to more than two-fold increase in HSE-mediated transcription (Fig. 5). These results suggest that inhibition of IRE1 function may lead to heat-shock independent activation of HSR pathway in mammalian cells, which in turn may contribute to restoration of cellular homeostasis.

Overall, as a result of this study we created original expressing constructs for dominant-negative IRE1 and cytoplasmic part of IRE1. The respective recombinant proteins possess C-terminal c-Myc and 6xHis tags, which make their detection easier, and also provide an option for effective affinity purification. Despite promising indirect evidence, the enzymatic activity of cytIRE1 is still to be tested. We were first to demonstrate that overexpression of dominant-negative IRE1 alone with no additional thermal or ER stress leads to activation of HSE-dependent transcription in H1299-shE6AP cells. This might reflect a cellular adaptive response to inhibition of IRE1 activity. An interaction between two pathways: endoplasmic reticulum stress and heat shock response in cancer cells is an interesting and therapeutically relevant topic, which requires further attention.

Fig. 4. **Schematic representations of 3xHSE-luc reporter construct:**
A — general scheme; *B* — nucleotide sequence of the region containing heat shock response elements (3xHSE — single elements underlined, inverted repeats marked in red)

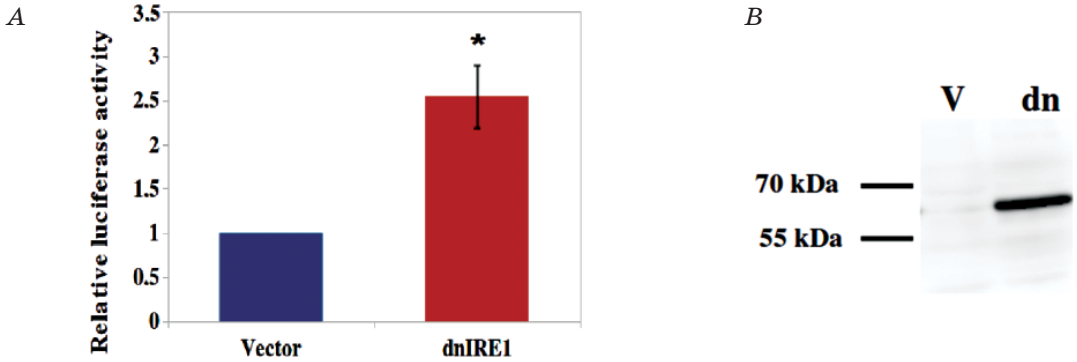

Fig. 5. **Effect of dominant-negative IRE1 overexpression on HSE-mediated transcription in H1299-shE6AP cells:**
A — relative luciferase activity, * — $P < 0.05$; $n = 4$; *B* — Western blot analysis of dnIRE1 expression:
V — cells transfected with empty vector pcDNA4-Myc/His-A; dn — cells transfected with pcDNA4+dnIRE1

REFERENCES

1. *Moenner M., Pluquet O., Bouchecareilh M., Chevet E.* Integrated endoplasmic reticulum stress responses in cancer. *Cancer Res.* 2007, 67 (22), 10631–10634.
2. *Wang S., Kaufman R. J.* The impact of the unfolded protein response on human disease. *J. Cell Biol.* 2012, 197 (7), 857–867.
3. *Marciniak S. J., Ron D.* Endoplasmic reticulum stress signaling in disease. *Physiol. Rev.* 2006, 86 (4), 1133–1149.
4. *Minchenko O. H., Kharkova A. P., Bakalets T. V., Kryvdiuk I. V.* Endoplasmic reticulum stress, its sensor and signalling systems and the role in regulation of gene expression at malignant tumor growth and hypoxia. *Ukr. Biokhim. Zh.* 2013, 85 (5), 5–16. (In Ukrainian).
5. *Chen Y., Brandizzi F.* IRE1: ER stress sensor and cell fate executor. *Trends in Cell Biol.* 2013, 23 (11), 547–555.
6. *Korennykh A. V., Egea P. F., Korostelev A. A., Finer-Moore J., Zhang C., Shokat K. M., Stroud R. M., Walter P.* The unfolded protein response signals through high-order assembly of Ire1. *Nature*. 2009, 457 (7230), 687–693.
7. *Oikawa D., Tokuda M., Hosoda A., Iwawaki T.* Identification of a consensus element recognized and cleaved by IRE1α. *Nucl. Acids Res.* 2010, 38 (18), 6265–6273.
8. *Maurel M., Chevet E., Tavernier J., Gerlo S.* Getting RIDD of RNA: IRE1 in cell fate aregulation. *Trends Biochem. Sci.* 2014, 39 (5), 245–254.
9. *Acosta-Alvear D., Zhou Y., Blais A., Tsikitis M., Lents N. H., Arias C., Lennon C. J., Kluger Y., Dynlacht B. D.* XBP1 controls diverse cell type- and condition-specific transcriptional regulatory networks. *Mol. Cell.* 2014, 27 (1), 53–66.
10. *Auf G., Jabouille A., Guerit S., Pineau R., Delugin M., Bouchecareilh M., Magnin N., Favereaux A., Maitre M., Gaiser T., von Deimling A., Czabanka M., Vajkoczy P., Chevet E., Bikfalvi A., Moenner M.* Inositol-requiring enzyme 1alpha is a key regulator of angiogenesis and invasion in malignant glioma. *Proc. Natl. Acad. Sci. USA.* 2010, 107 (35), 15553–15558.
11. *Drogat B., Auguste P., Nguyen D. T., Bouchecareilh M., Pineau R., Nalbantoglu J., Kaufman R. J., Chevet E., Bikfalvi A., Moenner M.* IRE1 signaling is essential for ischemia-induced vascular endothelial growth factor-A expression and contributes to angiogenesis and tumor growth in vivo. *Cancer Res.* 2007, 67 (14), 6700–6707.
12. *Drogat B., Bouchecareilh M., North S., Petibois C., Deleris G., Chevet E., Bikfalvi A., Moenner M.* Acute L-glutamine deprivation compromises VEGF-A up-regulation in A549/8 human carcinoma cells. *J. Cell. Physiol.* 2007, 212 (2), 463–472.
13. *Minchenko D. O., Karbovskyi L. L., Danilovskyi S. V., Moenner M., Minchenko O. H.* Effect of hypoxia and glutamine or glucose deprivation on the expression of retinoblastoma and retinoblastoma-related genes in IRE1 knockdown glioma U87 cell line. *Am. J. Mol. Biol.* 2012, 2 (1), 142–152.
14. *Minchenko O. H., Tsymbal D. O., Minchenko D. O., Moenner M., Kovalevska O. V., Lypova N. M.* Inhibition of kinase and endoribonuclease activity of IRE1/IRE1α affects expression of proliferation-related genes in U87 glioma cells. *Endoplasm. Reticul. Stress Dis.* 2015, 2 (1), 18–29.
15. *Minchenko O. H., Tsymbal D. O., Minchenko D. O., Kovalevska O. V., Karbovskyi L. L. Bikfalvi A.* Inhibition of IRE1 signaling enzyme affects hypoxic regulation of the expression of *E2F8*, *EPAS1*, *HOXC6*, *ATF3*, *TBX3* and *FOXF1* genes in U87 glioma cells. *Ukr. Biochem. J.* 2015, 87 (2), 76–87.
16. *Minchenko O. H., Tsymbal D. O., Minchenko D. O.* IRE-1alpha signaling as a key target for suppression of tumor growth. *Single Cell Biol*. 2015, 4(3), 118.
17. *Jiang D., Niwa M., Koong A. C.* Targeting the IRE1–XBP1 branch of the unfolded protein response in human diseases. *Semin. Cancer Biol.* 2015, V. 33, P. 48–56.
18. *Auf G., Jabouille A., Delugin M., Guerit S., Pineau R., North S., Platonova N., Maitre M., Favereaux A., Vajkoczy P., Seno M., Bikfalvi A., Minchenko D., Minchenko O., Moenner M.* High epiregulin expression in human U87 glioma cells relies on IRE1α and promotes autocrine growth through EGF receptor. *BMC Cancer*. 2013, 13(1), 597.
19. *Minchenko D. O., Kubajchuk K. I., Ratushna O. O., Komisarenko S. V., Minchenko O. H.* The vascular endothelial growth factor genes expression in glioma U87 cells is dependent from IRE1 signaling enzyme function. *Adv. Biol. Chem.* 2012, 2 (2), 198–206.
20. *Jackson A., Linsley P. S.* Recognizing and avoiding siRNA off-target effects for target identification and therapeutic application. *Nat. Rev. Drug Discov.* 2010, 9 (1), 57–67.
21. *J ger R., Bertrand M. J. M., Gorman A. M., Vandenabeele P., Samali A.* The unfolded protein response at the crossroads of cellular life and death during endoplasmic reticulum stress. *Biol. Cell*. 2012, 104 (5), 259–270.
22. *Lee A-H., Iwakoshi N. N., Glimcher L. H.* XBP-1 regulates a subset of endoplasmic reticulum resident chaperone genes in the unfolded protein response. *Mol. Cell. Biol.* 2003, 23 (21), 7448–7459.
23. *Morimoto R. I., Sarge K. D., Abravaya K.* Transcriptional regulation of heat shock

genes. A paradigm for inducible genomic responses. *J. Biol. Chem.* 1992, 267 (31), 21987–21990.
24. *K hnle S., Mothes B., Matentzoglu K., Scheffner M.* Role of the ubiquitin ligase E6AP/UBE3A in controlling levels of the synaptic protein Arc. *Proc. Natl. Acad. Sci. USA.* 2013, 110 (22), 8888–8893.
25. *Wang X., Harding H. P., Zhang Y., Jolicoeur E. M., Kuroda M., Ron D.* Cloning of mammalian Ire1 reveals diversity in the ER stress response. *EMBO J.* 1998, 17 (19), 5708–5717.
26. *Uemura A., Oku M., Mori K., Yoshida H.* Unconventional splicing of XBP1 mRNA occurs in the cytoplasm during the mammalian unfolded protein response. *J. Cell Sci.* 2009, 122 (16), 2877–2886.
27. *Liu Y., Chang A.* Heat shock response relieves ER stress. *EMBO J.* 2008, 27 (7), 1049–1059.

НАДЕКСПРЕСІЯ ДОМІНАНТ-НЕГАТИВНОЇ ФОРМИ ЕНЗИМУ IRE1 У СУБЛІНІЇ КЛІТИН H1299-shE6AP ПОСИЛЮЄ ТРАНСКРИПЦІЮ, ЩО ЗАЛЕЖИТЬ ВІД ЕЛЕМЕНТУ ТЕПЛОВОГО ШОКУ

Д. О. Цимбал, О. Г. Мінченко

Інститут біохімії ім. О. В. Палладіна
НАН України, Київ

E-mail: dariiabova@gmail.com

Метою роботи було дослідження функції IRE1-залежної гілки сигнального шляху стресу ендоплазматичного ретикулуму в різних пухлинних клітинах. Для цього було створено кДНК-конструкції для експресії домінант-негативної форми ензиму IRE1 — dnIRE1 та цитозольного домену IRE1, злитих на С-кінці із с-Мус епітопом та 6xHis. Цими конструкціями було трансфіковано клітини недрібноклітинної карциноми легень сублінії H1299-shE6AP і за допомогою анти-с-Мус антитіл показано ефективну дозозалежну експресію протеїнів домінант-негативної форми та цитозольного домену IRE1. Для дослідження опосередкованої IRE1-транскрипції, залежної від елементу теплового шоку, клітини були повторно трансфіковані люциферазним репортером, який включав елемент теплового шоку. Встановлено, що надекспресія dnIRE1 у клітинах сублінії H1299-shE6AP призводить до вираженого індукування транскрипції, залежної від елементу теплового шоку. Це може свідчити про посилення експресії генів теплового шоку, які відіграють важливу роль в адаптації цих клітин до пригнічення активності нативного IRE1, ключового сенсорно-сигнального ензиму стресу ендоплазматичного ретикулуму, що знижує здатність пухлинних клітин до проліферації та модифікує експресію численних генів, включаючи велику кількість транскрипційних факторів.

Ключові слова: стрес ендоплазматичного ретикулуму, ензим IRE1, експресія рекомбінантних протеїнів, елемент теплового шоку, метод люциферазного репортера.

СВЕРХЭКСПРЕССИЯ ДОМИНАНТ-НЕГАТИВНОЙ ФОРМЫ ЭНЗИМА IRE1 В СУБЛИНИИ КЛЕТОК H1299-shE6AP УСИЛИВАЕТ ТРАНСКРИПЦИЮ, ЗАВИСЯЩУЮ ОТ ЭЛЕМЕНТА ТЕПЛОВОГО ШОКА

Д. А. Цымбал, А. Г. Минченко

Институт биохимии им. О. В. Палладина
НАН Украины, Киев

E-mail: dariiabova@gmail.com

Целью работы было исследование функции IRE1-зависимой ветви сигнального пути стресса эндоплазматического ретикулума в разных опухолевых клетках. Для этого были созданы кДНК-конструкции для экспрессии доминант-негативной формы энзима IRE1 и цитозольного домена IRE1, сшитых на С-конце с с-Мус эпитопом и 6xHis. Этими конструкциями были трансфицированы клетки немелкоклеточной карциномы легких сублинии H1299-shE6AP и с помощью анти-с-Мус антител показана эффективная дозозависимая экспрессия протеинов доминант-негативной формы и цитозольного домена IRE1. Для исследования опосредованной IRE1-транскрипции, зависимой от элемента теплового шока, клетки были повторно трансфицированы люциферазным репортером, включающим элемент теплового шока. Установлено, что сверхэкспрессия dnIRE1 в клетках сублинии H1299-shE6AP приводит к выраженной индукции транскрипции, зависимой от элемента теплового шока. Это может свидетельствовать об усилении экспрессии генов теплового шока, играющих важную роль в адаптации клеток к подавлению активности нативного IRE1, ключевого сенсорно-сигнального энзима стресса эндоплазматического ретикулума, который снижает способность опухолевых клеток к пролиферации и модифицирует экспрессию многочисленных генов, включая большое количество транскрипционных факторов.

Ключевые слова: стресс эндоплазматического ретикулума, энзим IRE1, экспрессия рекомбинантных протеинов, элемент теплового шока, метод люциферазного репортера.

UDK 543.6 + 577.15 + 543.555 + 544.475 doi: 10.15407/biotech8.06.016

INVESTIGATION AND OPTIMIZATION OF REACTIVATION OF UREASE BIOSENSOR FOR HEAVY METALS INHIBITION ANALYSIS

Budnikov S. R.[1, 2]
Soldatkin O. O.[1, 2]
Kukla A. L.[3]
Khomenko I. I.[1, 4]
Dzyadevych S. V.[1, 2]
Soldatkin O. P.[1, 2]

[1]Institute of Molecular Biology and Genetics of the National Academy of Sciences of Ukraine, Kyiv
[2]Taras Shevchenko National University of Kyiv, Ukraine
[3]Lashkaryov Institute of Semiconductor Physics of the National Academy of Sciences of Ukraine, Kyiv
[4]Centre of Intellectual Property and Technology Transfer of the National Academy of Sciences of Ukraine, Kyiv

E-mail: dzyad@yahoo.com

Received 14.09.2015

Research was aimed at the optimization of the urease biosensor for analysis of heavy metals and determining the opportunities of its reactivation. A differential pair of gold interdigitated electrodes deposited on a ceramic substrate was used as the conductometric transducer. As a bioselective membrane served urease, coimmobilized with bovine serum albumin by glutaraldehyde cross-linking on the surface of conductometric transducer. 1.0 mM urea was selected as an optimal substrate concentration for the inhibition analysis of heavy metals. The biosensor was tested for its sensitivity to different heavy metals, the calibration curves were plotted. The proposed biosensor was shown to have high reproducibility of signals prior and after inhibition, the measurement error was less than 3%. It was proved a possibility of reactivation of the bioselective membrane after urease irreversible inhibition by heavy metals, using the ethylenediamine tetraacetic acid solution. The optimum conditions of reactivation, i.e. the dependence of its level on time and concentration of heavy metals, were determined. The additional stage, post-inhibition reactivation, was shown to increase significantly the selectivity of biosensor determination of heavy metals.

Key words: conductometric transducer, biosensor, urease, heavy metals, inhibition analysis, enzyme reactivation.

At present, one of the most acute environmental problems is the contamination with waste products [1]. Among the various pollutants, heavy metals and their compounds are notable by abundance, high toxicity, ability to accumulate in living organisms [2]. They are widely used in manufacture, therefore, despite the clean-up, the content of heavy metals in industrial wastewater is rather high.

They also enter the environment with sewage, smoke and dust from industrial enterprises. Many metals form stable organic compounds, high solubility of which facilitates the migration of heavy metals in natural waters. More than 40 chemical elements are referred to as heavy metals, but significantly fewer number should be controlled taking into account toxicity, persistence, abundance, an ability to accumulate in the environment [3, 4].

In the aquatic environment, microparticles of heavy metals are present as solutions, suspensions and colloids. Free hydrated ions, simple inorganic and organic complexes are soluble [5–9]. Currently, there are many methods, which are widely used for the determination of heavy metals, such as atomic absorption spectrometry, plasma mass spectrometry, etc. However, these methods utilize sophisticated appliances and are unsuitable in the field [10]. Electrochemical biosensor methods in general are more reasonable in the field because they do not require complex equipment [11–13].

Biosensor determination of heavy metal ions is based on their inhibition effect on enzymes. For example, ions of copper, cadmium, mercury, zinc are effective inhibitors of the urease activity in the urea hydrolysis. An important stage in the running of urease biosensor is a procedure of its reactivation after inhibition by heavy metal ions. An exposure of the inhibited biosensor in

buffer solution for a long time does not restore the enzymatic activity of its biomembranes whereas EDTA solution acts as efficient reactivator [14].

Materials and Methods

Materials

In the work, the enzyme urease from soya beans with activity of 66 U/mg was used (Fluka, Germany). Bovine serum albumin (BSA, fraction V), 50% aqueous solution of glutaraldehyde (GA) and urea were from Sigma-Aldrich Chemie (Germany).

The compounds for the preparation of buffers, inhibitors, reactivator and other inorganic compounds used in the work were of domestic production and had a chemical purity grade.

Conductometric transducers

Conductometric transducers were produced in Lashkaryov Institute of Semiconductor Physics (Kyiv, Ukraine) in accordance with our recommendations. They consist of the sital substrate (fused Al_2O_3) 5 × 30 mm in size with a pair of gold interdigitated electrodes. The 0.1 μ thick titanium sublayer is used for better adhesion of metal to the substrate. More information on the transducers used is in the previous paper [15].

Scheme of experimental setup for conductometric measurements

The changes in conductivity of near-electrode layer of conductometric transducer were determined by the conductometric measuring unit. The differential mode of measurement was used to increase the sensor sensitivity and minimize noise caused by nonspecific effects. The scheme and function of this conductometric setup have been described earlier [16, 17].

Preparation of bioselective elements

To prepare working urease-based bioselective membranes, the solution containing 5% of urease, 5% of BSA and 10% of glycerol in 20 mM phosphate buffer, pH 6.5, was used. The mixture for the reference membrane was prepared in the same way, but no enzyme was taken, only BSA of the final concentration equivalent to the amount of protein in the membrane, i.e. 10%. The solutions prepared were deposited onto the transducer working parts by micropipettes to cover completely the working electrode surface. The transducers with deposited membranes were incubated in saturated glutaraldehyde (GA) vapor for 25 min and dried for 5 min in air at room temperature. Then the biosensors were washed for 6 min in the working buffer to remove excess unbound GA and other components of the membrane (changing the buffer every 2 min).

Methods of measurement

Measurements were carried out at room temperature in an open cell filled with 5 mM phosphate buffer, pH 6.5, with constant stirring. The specified substrate concentration in the working cell was obtained by adding the aliquots of substrates stock solutions. For inhibition analysis, the responses to substrate were evaluated before inhibition, then the biosensor was incubated for 20 min in a solution of heavy metal ions of different concentrations and washed from excess inhibitor, and the response to substrate was re-assessed. In this way, a level of the enzyme inhibition, which corresponds to the concentration of heavy metal ions in the sample, was determined. Reactivation of the inhibited bioselective elements was performed by incubation in 10 mM EDTA solution for 30 min. Then they were washed from excess reactivator, and the response to the substrate was measured again.

All experiments were conducted in 3–5 series. Non-specific changes in the output signal associated with electrical noise and fluctuations in environmental temperature and pH were avoided due to use of a differential mode of measurements. In the statistical analysis of the results obtained, the values of arithmetic mean and its standard deviation were calculated; the data were considered significant at $P < 0.05$.

Results and Discussion

Study of main analytical characteristics of biosensor in direct substrate determination

The biosensor operation is underlain by the enzymatic reaction in the membrane containing urease deposited on the surface of conductometric transducer:

$$H_2N\text{-}CO\text{-}NH_2 + 2H_2O + H^+ \xrightarrow{\text{Urease}} 2NH_4^+ + HCO_3^-.$$

In the course of the reaction, protons are absorbed, which leads to changes in pH and generation of additional ions (NH_4^+ and HCO_3^-) in the working membrane [18]. This changes the solution conductivity, which is registered by the conductometric transducer.

In inhibition analysis, first it was necessary to determine an optimal concentration of urea as a substrate, i.e. to choose the urea concentration, at which the biosensor sensitivity to heavy metal ions is maximal. It is known that at irreversible inhibition the largest biosensor sensitivity to toxins can be reached if the substrate concentrations are within the range of biosensor saturation with the substrate when each enzyme molecule is involved in the conversion of this substrate. The graph of dependence of biosensor responses on the urea concentration in solution (Fig. 1) shows that above 1.0 mM complete biosensor saturation with the substrate is observed. Therefore, in further experiments on inhibition analysis 1.0 mM substrate was used.

It was necessary to confirm that a decrease in the biosensor response to the substrate after its incubation in a solution of heavy metals occurs due to the inhibition of bioselective element, but not because of the measurement error. Therefore, at the next stage of work the biosensor operational stability and reproducibility of its signal were tested. For this, the biosensor responses to the same substrate concentration were measured with an 12.5 min interval over one working day. The biosensor was characterized by relatively high signal reproducibility, standard deviation 2.93%.

Research on sensitivity of developed biosensors to heavy metal ions

Heavy metal ions can inhibit the biological activity of urease through the interaction with sulfhydryl groups of the enzyme active site:

$$\text{Enz-Ser-OH} + \text{Me}^{+} \rightarrow \text{Enz-Ser-O-Me} + \text{H}^{+}.$$

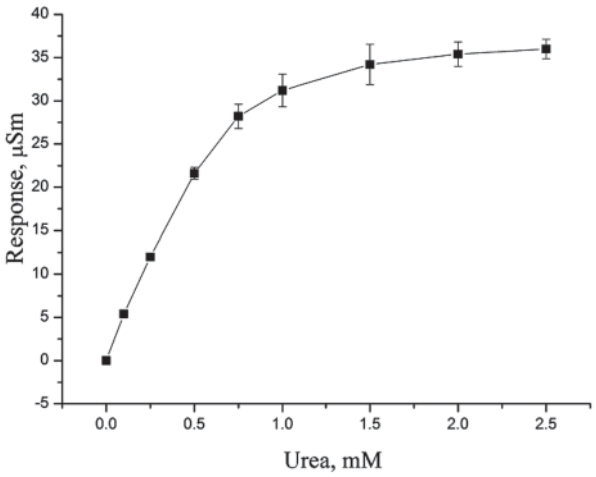

Fig. 1. **Dependence of biosensor response from urea concentration in solution.** Measurement was performed in 5 mM phosphate buffer, pH 6.5

The enzyme inhibition by heavy metal ions causes a decrease in the amount of ions of ammonium and bicarbonate formed as a result of enzymatic reaction of the substrate conversion, and thus — a decrease of the biosensor response [19–21].

Using selected optimal concentration of urea, it was investigated the level of inhibition of urease biosensor by various heavy metals of the same concentration (Fig. 2). Initially, the solutions of nitrates of divalent metals zinc, copper, mercury and cadmium of the same concentration (100 μM) were taken, so, the concentration of all ions was also equal. The results showed that inhibition depends on the kind of ion and its ability to inhibit the enzyme described by the inhibition constant [22, 23].

Next, sensitivity of the developed biosensor to different concentrations of heavy metals ions was studied taking copper ions as an example. The calibration curve of the residual activity of urease-based bioselective element after inhibition (Fig. 3) showed its strong dependence on the concentration of copper ions in the measurment environment.

The stability of the biosensor inhibition after its incubation in the solution by heavy metal ions was also investigated (Fig. 4). For this, the responses of a number of biosensors to copper ions of the same concentration were measured after incubation under identical conditions. It was shown that the developed biosensors were characterized by relatively high signal reproducibility after inhibition with standard deviation of 2.6%.

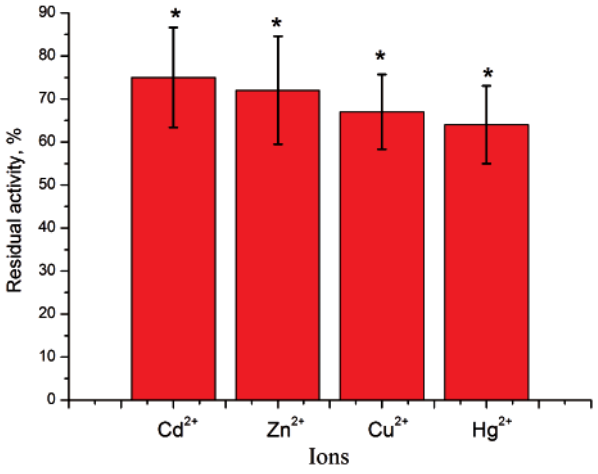

Fig. 2. **Residual activity of urease biosensor after inhibition by different heavy metal ions. Ions concentration — 100 μM.** Measurement was performed in 5 mM phosphate buffer, pH 6.5; * $P < 0.05$ in comparison with initial activity of biosensor

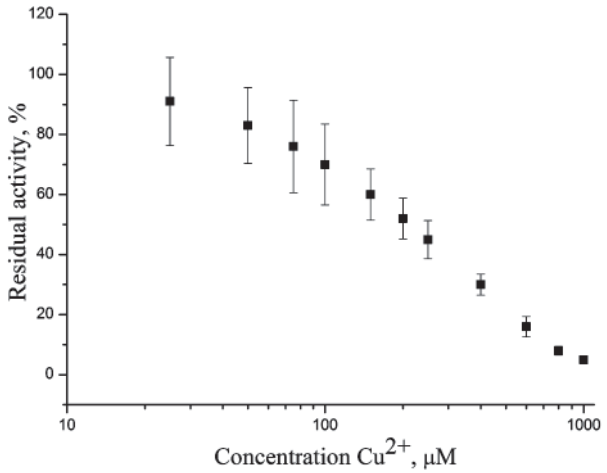

Fig. 3. **Residual activity of urease biosensor after inhibition by Cu^{2+} ions with different concentrations. Inhibition time — 20 minutes.**
Measurement was performed in 5 mM phosphate buffer, pH 6.5

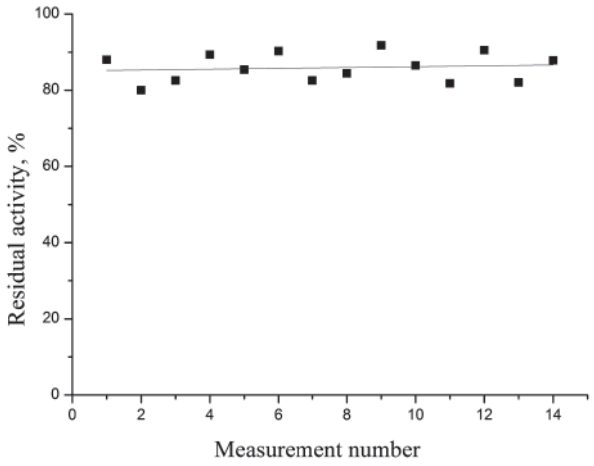

Fig. 4. **Reproducibility of urease biosensor after inhibitory analysis. Inhibitor concentration — 50 μM Cu^{2+}. Inhibition time — 20 minutes.**
Measurement was performed in 5 mM phosphate buffer, pH 6.5

Research and optimization of conditions of biosensor reactivation using EDTA

The urease inhibition by heavy metal ions is known to be irreversible, which is a cause of inefficiency of urease-based biosensors due to its one-time usage. Therefore, it was proposed to use a stage of biosensor reactivation for its repetitive employ, namely, to explore the possibility of reactivation of the developed biosensor after its inactivation by heavy metal ions. The initial urease activity after inhibition can be recovered by the reactivator EDTA, which displaces the heavy metal ion bound to serine residue in the enzyme. Thus the enzyme is reactivated, i.e. its ability to interact with the substrate is restored [14, 24].

$$\text{Enz-Ser-OMe} + \text{EDTA} \rightarrow \text{Enz-Ser-OH} + \text{EDT[Me]}$$

The reactivation efficiency depends strongly on the time of reactivation, reactivator concentration, and other parameters. Therefore, the conditions of reactivation by EDTA should be first optimized. For this purpose, it was chosen an optimal time of biosensor incubation in the reactivator solution, which corresponds to the highest possible level of recovery of the enzyme membrane activity after inhibition. The optimal time of reactivation by 10 mM EDTA was 30 min.

It was also studied an efficiency of reactivation of urease biosensor after its inhibition during constant time (30 min) in the solution of copper ions of different concentrations. Fig. 5 shows that reactivation under selected optimum conditions provided complete restoration of the enzymatic activity of membrane inhibited in the solution of copper nitrate of concentrations up to 400 μM.

Determination of number of cycles of reactivation of urease-based biosensor

At the next stage, the possibility of multiple reactivation of the developed biosensor was estimated with a purpose of its repetitive application for the inhibition analysis of heavy metal ions. In this case the biosensor can be used several times when working with irreversible inhibitors.

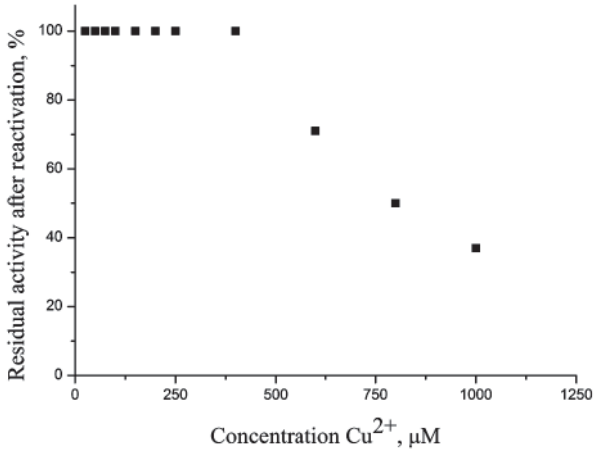

Fig. 5. **Dependence of biosensor reactivation level after inhibition by Cu^{2+} ions with different concentrations.**
Measurement was performed in 5 mM phosphate buffer, pH 6.5

The experimental results are shown in Fig. 6. First, the basic responses to urea were received (the first column). Next, the biosensors were incubated in a copper ions solution to obtain a certain residual activity of the enzyme (the second column). Further step was the biosensor reactivation in EDTA solution up to restoration of the urease activity to its original level (the third column). This procedure described was repeated until the bioselective membrane activity was completely restored.

The next cycles of inhibition and reactivation did not lead to complete restoration of the enzyme activity, but the sensitivity of biosensor was sufficient to reuse it for the analysis of heavy metal ions in the solution.

In the work, the urease-based biosensor is optimized for determination of heavy metal ions. The biosensor sensitivity was tested, the calibration curves were plotted for direct urea determination and for inhibition analysis of heavy metal ions. The developed biosensor was characterized by high signal reproducibility at determination of both substrate and inhibitor. The possibility of biosensor reactivation after inhibition by heavy metal ions was proved. The optimum conditions of the process of reactivation using EDTA were selected.

It was established that the initial level of enzyme inhibition affects the capability of biosensor to be reactivated. It is shown that application of the reactivation stage allows repetitive usage of urease-based biosensors for inhibition analysis of heavy metal ions, which indicates the suitability of the method for multiple application.

The authors are grateful for financial support from the National Academy of Sciences of Ukraine in the frame of complex scientific and technical program “Sensor devices for medical-environmental and industrial-technological needs: metrological support and pilot exploitation”.

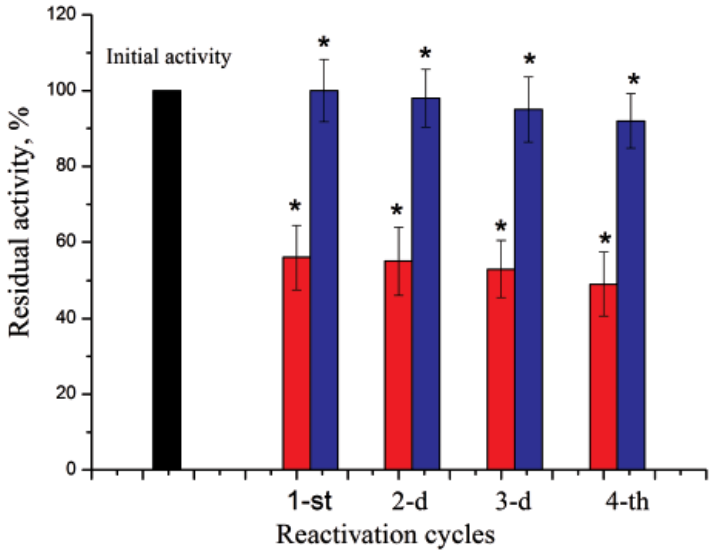

Fig. 6. **Reproducibility application of urease based conductometric biosensor after inhibition by copper ions and reactivation by EDTA. Inhibition time in copper (II) nitrate solution (150 μM) — 20 min, reactivation time in EDTA solution (10 mM) — 30 min.**
Measurement was performed in 5 mM phosphate buffer, pH 6.5; * $P < 0.05$ in comparison with initial activity of biosensor

REFERENCES

1. *Korobkin V. I., Peredelskiy L. V.* Ecology. 12-th ed., add. and rec. *Rostov n/D: Feniks.* 2007, 602 p. (In Russian).
2. *Evdokimova G.A.* Microbiological activity of soils contaminated by heavy metals. *Pochvovedenie.* 1982, V. 6, P. 125–132. (In Russian)
3. *Alekseev Yu. V.* Heavy metals in soils and plants. *Leningrad: Agropromizdat.* 1987, 142 p. (In Russian)
4. *Vetoshkin A. G.* Processes and mechanisms of hydrosphere protection. *Penza: Izd-vo Penz. Gos. Un-ta.* 2004, 188 p. (In Russian).
5. *Kabata-Pendias A.* Soil–plant transfer of trace elements — an environmental issue. *Geoderma.* 2004, 122, 143–149. doi:10.1016/j.geoderma.2004.01.004.
6. *Song J., Zhao F. J., Luo Y. M., McGrath S. P., Zhang H.* Copper uptake by Elsholtzia splendens and Silene vulgaris and assessment of copper phytoavailability in contaminated soils. *Environmental Pollution.* 2004, V. 128, P. 307–315. doi:10.1016/j.envpol.2003.09.019
7. *Semenova A. D.* Guidance for chemical analysis of surface waters. *Leningrad: Gidrometeoizdat.* 1977, 541 p. (In Russian)
8. *Yatsenko V.* Determining the characteristics of water pollutants by neural sensors and pattern recognition methods. *Journal of Chromatography A.* 1996, V. 722, P. 233–243. doi: 10.1016/0021-9673(95)00571-4.
9. *Lee S-M., Lee W-Y.* Determination of Heavy Metal Ions Using Conductometric Biosensor Based on Sol-Gel-Immobilized Urease. *Bull. Korean Chem. Soc.* 2002, 23(8), 1169-1171.
10. *Anderson J. L., Bowden E. F., Pickup P. G.* Dynamic electrochemistry: methodology and application. *Anal. Chem.* 1996, 68(12), 379–444. doi: 10.1021/a1960015y.
11. *Tran-Minh C.* Immobilized enzyme probes for determining inhibitors. *Ion-Selective Electrode Rev.* 1985, V. 7, P. 41–75.
12. *Krajewska B.* Urease Immobilized on Chitosan Membrane. Inactivation by Heavy Metal Ions. *J. Chem. Tech. Biotechnol.* 1991, 52(2), 157–162. doi: 10.1002/jctb.280520203.
13. *Krajewska B., Zdarta J., Jesinowski T.* Enzyme immobilization by adsorption: a review. *J. Adsorption.* 2014, 20(5), 801–821. doi: 10.1007/s10450-014-9623-y.
14. *Zhylyak G. A., Dzyadevich S. V., Korpan Y. I., Soldatkin A. P., El'skaya A. V.* Application of urease conductometric biosensor for heavy-metal ion determination. *Sensors and Acuators B.* 1995, V. 24–25, P. 145–148. doi:10.1016/0925-4005(95)85031-7.
15. *Dziadevych S. V., Soldatkin O. P.* Scientific and technologic foundations for miniature electrochemical biosensors development. *Kyiv: Naukova dumka.* 2006, 255 p. (In Ukrainian).
16. *Schuvailo O. M., Danyleyko L. V., Arkhypova V. M., Dzyadevych S. V., El'skaya A. V., Cespuglio R., Soldatkin A. P.* Development of microbiosensors based on carbon fibres for in vivo determination of glucose, acetylcholine and choline. *Biopolym. Cell.* 2002, 18(6), 489–495. (In Russian).
17. *Soldatkin O. O., Kucherenko I. S., Pyeshkova V. M., Kukla A. L., Jaffrezic-Renault N., El'skaya A. V., Dzyadevych S. V., Soldatkin A. P.* Novel conductometric biosensor based on three-enzyme system for selective determination of heavy metal ions. *Bioelectrochemistry.* 2012, V. 83, P. 25–30. doi:10.1016/j.bioelechem.2011.08.001.
18. *Soldatkin O. O., Kucherenko I. S., Marchenko S. V., Kasap B. O., Akata B., Soldatkin A. P., Dzyadevych S. V.* Application of enzyme/zeolite sensor for urea analysis in serum. *Materials Science and Engineering: C,* 2014, V. 42, P. 155–160. doi: 10.1016/j.msec.2014.05.028.
19. *Kukla A. L., Soldatkin O. O., Pavluchenko A. S., Kucherenko I. S., Peshkova V. M., Arkhypova V. N., Dzyadevych S. V.,* Toxicity analysis of real water samples of different origin with ISFET multibiosensor. *Biochemistry and Biophysics.* 2014, 2(1), 7–12.
20. *Gabrovska K., Godjevargova T.* Optimum immobilization of urease on modified acrylonitrile copolymer membranes: Inactivation by heavy metal ions. *Journal of Molecular Catalysis B: Enzymatic,* 2009, 60(1–2), 69–75. doi:10.1016/j.molcatb.2009.03.018.
21. *Zaborska W., Krajewska B., Olech Z.* Heavy Metal Ions Inhibition of Jack Bean Urease: Potential for Rapid Contaminant Probing. *Journal of Enzyme Inhibition and Medicinal Chemistry.* 2004, 19 (1), 65–69. doi: 10.1080/14756360310001650 23.
22. *Zaborska W., Krajewska B., Leszko M., Olech Z.* Inhibition of urease by Ni^{2+} ions: Analysis of reaction progress curves. *Journal of Molecular Catalysis B: Enzymatic.* 2001, 13(4–6), 103–108. doi:10.1016/S1381-1177(00)00234-4.
23. *Krajewska B., Zaborska W., Chudy M.* Multi-step analysis of Hg^{2+} ion inhibition of jack bean urease. *Journal of Inorganic Biochemistry.* 2004, 98(6), 1160–1168. doi:10.1016/j.jinorgbio.2004.03.014.
24. *Smolińska B., Cedzyńska K.* EDTA and urease effects on Hg accumulation by *Lepidium sativum. Chemosphere.* 2007, 69(9), 1388–1395. doi:10.1016/j.chemosphere.2007.05.003.

ДОСЛІДЖЕННЯ ТА ОПТИМІЗАЦІЯ РЕАКТИВАЦІЇ УРЕАЗНОГО БІОСЕНСОРА ЗА ІНГІБІТОРНОГО АНАЛІЗУ ІОНІВ ВАЖКИХ МЕТАЛІВ

Будніков С. Р.[1, 2]
Солдаткін О. О.[1, 2]
Кукла О. Л.[3]
Хоменко І. І.[1, 4]
Дзядевич С. В.[1, 2]
Солдаткін О. П.[1, 2]

[1]Інститут молекулярної біології і генетики НАН України, Київ
[2]Київський національний університет імені Тараса Шевченка, Україна
[3]Інститут фізики напівпровідників ім. В. Є. Лашкарьова НАН України, Київ
[4]Центр інтелектуальної власності та передачі технологій НАН України, Київ

Метою роботи було визначення умов оптимізації роботи уреазного біосенсора під час аналізу важких металів та можливості його реактивації. Як кондуктометричний перетворювач використовували диференційну пару золотих гребінчастих електродів, нанесених на керамічну підкладку. Роль біоселективної мембрани відігравала уреаза, коіммобілізована з бичачим сироватковим альбуміном за допомогою поперечного зшивання глутаровим альдегідом на поверхні кондуктометричного перетворювача. Для інгібіторного аналізу іонів важких металів підібрано оптимальну концентрацію субстрату — 1,0 мМ сечовини. Перевірено чутливість біосенсора до різних іонів важких металів та побудовано калібрувальні криві. Показано, що запропонований біосенсор характеризувався високою відтворюваністю сигналів до та після процесу інгібування з похибкою вимірювання менше 3%. Доведено можливість реактивації біоселективної мембрани розчином етилендіамінтетраоцтової кислоти після незворотного інгібування уреази важкими металами. Підібрано оптимальні умови реактивації біосенсорів, зокрема залежність рівня реактивації від часу та концентрації іонів важких металів у розчині. Встановлено, що, використовуючи додатковий етап реактивації біосенсорів після інгібування, можна значно підвищити селективність процедури біосенсорного визначення іонів важких металів.

Ключові слова: кондуктометричний перетворювач, біосенсор, уреаза, важкі метали, інгібіторний аналіз, реактивація ензиму.

ИССЛЕДОВАНИЕ И ОПТИМИЗАЦИЯ РЕАКТИВАЦИИ УРЕАЗНОГО БИОСЕНСОРА ПРИ ИНГИБИТОРНОМ АНАЛИЗЕ ИОНОВ ТЯЖЕЛЫХ МЕТАЛЛОВ

Будников С. Р.[1, 2]
Солдаткин А. А.[1, 2]
Кукла А. Л.[3]
Хоменко И. И.[1, 4]
Дзядевич С. В.[1, 2]
Солдаткин О. П.[1, 2]

[1]Институт молекулярной биологии и генетики НАН Украины, Киев
[2]Киевский национальный университет имени Тараса Шевченко, Украина
[3]Институт физики полупроводников им. В. Е. Лашкарева НАН Украины, Киев
[4]Центр интеллектуальной собственности и передачи технологий НАН Украины, Киев

Целью работы было определение условий оптимизации работы уреазного биосенсора при анализе тяжелых металлов и возможности его реактивации. Как кондуктометрический преобразователь использовалась дифференциальная пара золотых гребенчатых электродов, нанесенных на керамическую подложку. Роль биоселективной мембраны играла уреаза, коиммобилизованная с бычьим сывороточным альбумином с помощью поперечной сшивки гутаровым альдегидом на поверхности кондуктометрического преобразователя. Подобрана оптимальная концентрация субстрата для ингибиторного анализа ионов тяжелых металлов — 1,0 мМ мочевины. Проверена чувствительность биосенсора к разным ионам тяжелых металлов и построены калибровочные кривые. Показано, что предложенный биосенсор характеризовался высокой воспроизводимостью сигналов до и после ингибирования с погрешностью измерения менее 3%. Доказана возможность реактивации биоселективных мембран раствором этилендиаминтетрауксусной кислоты после необратимого ингибирования уреазы тяжелыми металлами. Подобраны оптимальные условия реактивации биосенсоров, в частности зависимость уровня реактивации от времени и концентрации ионов тяжелых металлов в растворе. Установлено, что, используя дополнительный этап реактивации биосенсоров после ингибирования, можно значительно повысить селективность процедуры биосенсорного определения ионов тяжелых металлов.

Ключевые слова: кондуктометрический преобразователь, биосенсор, уреаза, тяжелые металлы, ингибиторный анализ, реактивация энзима.

UDC 759.873.088.5:661.185 **doi: 10.15407/biotech8.06.023**

INTENSIFICATION OF SURFACTANTS SYNTHESIS UNDER *Nocardia vaccinii* IMV B-7405 CULTIVATION ON A MIXTURE OF GLUCOSE AND GLYCEROL

T. Pirog [1, 2]
T. Shevchuk[1]
K. Beregova[2]
N. Kudrya[2]

[1] Zabolotny Institute of Microbiology and Virology of the National Academy of Sciences of Ukraine, Kiyv
[2] National University of Food Technologies, Ukraine, Kiyv

E-mail: tapirog@nuft.edu.ua

Received 16.11.2015

The purpose of this study was to establish optimal molar glycerol to glucose ratio for enhanced biosurfactant synthesis by the cultivation of *Nocardia vaccinii* IMV B-7405 on a mixture of energetically nonequivalent substrates (glucose and glycerol).

Based on theoretical calculations of the energy requirements for biomass production and the synthesis of surface-active trehalose monomycolates on the energy-deficient substrate (glycerol), the concentration of the energy-excessive substrate (glucose), which increased the efficiency of the substrate carbon conversion to biosurfactant, was determined. It was found that the synthesis of extracellular biosurfactant on a mixture of glucose and glycerol at molar ratio of 1.0:2.5 increased 2.0–2.3-fold compared to that on corresponding monosubstrates.

The increased level of biosurfactant on the mixed substrate is determined by intensification of surface-active trehalose monomycolate synthesis, confirmed by 1.2–5.7-fold increase in activity of the enzymes involved in their biosynthesis (trehalose phosphate synthase, phosphoenolpyruvate-carboxykinase, phosphoenolpyruvate-synthetase) compared to cultivation on monosubstrates glucose and glycerol. The results indicate the feasibility of using a mixture of energetically nonequivalent substrates for enhancing the synthesis of secondary metabolites, as well as possibility of achieving the high efficiency of these mixed substrates if they are properly chosen and the molar ratio of their concentrations are correctly determined.

Key words: *Nocardia vaccinii* IMB B-7405, biosurfactant, energetically nonequivalent substrates.

Literature data and results of own studies indicate the prospects of the use of a mixture of growth and non-growth substrate for the intensification of the microorganism growth and the synthesis of metabolites valuable for practical use. It has been shown by the example of microbial exopolysaccharide ethapolan and biosurfactants (BS) such as *Rhodococcus erythropolis* IMV Ac-5017 and *Acinetobacter calcoaceticus* IMV B-7241 [1–4]. This approach allowed avoiding inefficient loss of carbon and energy that occur when using monosubstrates, as well as improving the efficiency of substrate carbon conversion to products of microbial synthesis.

It was shown the possibility of using mixed growth substrates (*n*-hexadecane, glycerol, ethanol, glucose) to intensify the synthesis of surfactants by *Nocardia vaccinii* IMV B-7405, at that, the highest values were observed for a mixture of glucose and glycerol [5]. However, to attain the maximum efficiency of carbon conversion to the final product, the determining the optimal for its synthesis molar ratio of monosubstrate concentrations in the mixture is necessary, which in turn requires the theoretical calculations of the energy requirements for the biomass production and BS synthesis on the energy-deficient substrate followed by determining the concentration of energy-excessive substrate which compensate for the energy expenditure [1–4]. To implement these theoretical calculations, understanding of the metabolic pathways of relevant monosubstrate synthesis is important.

It was revealed in our previous work [6] that glucose in *N. vaccinii* IMV B-7405 was assimilated in the pentose phosphate cycle, and the catabolism of glycerol to dihydroxyacetone phosphate (glycolysis intermediate) could

proceed via both the glycerol-3-phosphate and the dihydroxyacetone pathway.

The aim of this work was to determine the optimal molar ratio of glucose to glycerol for the intensification of BS synthesis by *N. vaccinii* IMV B-7405 on a mixture of these substrates.

Materials and Methods

Nocardia vaccinii K-8 strain registered in the Depository of microorganisms of Institute of Microbiology and Virology of the National Academy of Sciences of Ukraine under the number IMV B-7405 was used in the study. *N. vaccinii* IMV B-7405 strain was grown in liquid mineral medium composed of (g/l): $NaNO_3$ — 0.5, $MgSO_4 \cdot 7H_2O$ — 0.1, $CaCl_2 \cdot 2H_2O$ — 0.1, KH_2PO_4 — 0.1, $FeSO_4 \cdot 7H_2O$ — 0.001, yeast autolysate — 0.5 **(vol/vol)**. Glucose 0.75%, glycerol 0.6% (vol/vol) as well as mixtures of 0.5% glucose and glycerol (0.2; 0.4; 0.5; 0.6 and 0.8% vol/vol) in molar ratios of 1:1; 1:2; 1:2.5; 1:3 and 1:4 respectively were used as the carbon and energy sources.

The mid-exponential-phase culture grown in the medium of the indicated above composition was used as the inoculum. Glucose (0.5%), glycerol (0.5% vol/vol) and a mixture of glucose (0.25%) and glycerol (0.25% vol/vol) were used as the carbon and energy sources for the inoculum preparation.

The amount of inoculum (10^4–10^5 cell/ml) was 5% of the medium volume. Cultivation was performed in 750 ml flasks with 100 ml of medium on a shaker (220 rpm) at 28–30 °C for 24–120 h.

Amount of the extracellular BS was determined after their extraction from the cultural liquid supernatant by chloroform/methanol (2:1) mixture using the modified method [7]. To obtain the supernatant, the culture liquid was centrifuged at 5000 g for 20 min.

Considering that *N. vaccinii* IMV B-7405 strain synthesizes complex of polar and non-polar lipids [6] and a reported method of BS extraction [7] allows to extract mainly non-polar lipids, we modified the classic Folch mixture by introducing into it 1N HCl (chloroform : methanol : water = 4:3:2). This mixture allows most efficient extraction of both polar and non-polar lipids.

The supernatant (25 ml) was placed into cylindrical separatory funnel (100 ml), 1N HCl was added to achieve pH 4.0–4.5 (about 5 ml), the funnel was closed with a ground stopper and stirred for 3 min, and then the chloroform-methanol (2:1) mixture (15 ml) was added and again stirred for 5 min (lipid extraction). The resulting mixture was left in separatory funnel for phase separation, thereafter the bottom fraction was poured off (the organic extract 1) and the aqueous phase was re-extracted. At the re-extraction, 1N HCl to achieve pH 4.0–4.5 (about 5 ml), chloroform-methanol (2:1) mixture (15 ml) were added to the aqueous phase and lipids were extracted for 5 min. After phase separation, the bottom fraction was poured off (the organic extract 2). At the third stage, chloroform-methanol (2:1) mixture (25ml) was added to the aqueous phase and extraction was performed as described above (the organic extract 3). The extracts 1–3 were combined and evaporated on a rotary evaporator IR-1M2 at 50 °C and absolute pressure 0.4 atm up to constant mass.

To determine the emulsification index (E_{24}, %), sunflower oil (5 ml) (emulsified substrate) was added to culture liquid (5 ml) and the mixture was stirred for 2 min. Thereafter the measurement of the emulsification index was determined after 24 h as of the ratio of the emulsion layer height to the total height of the liquid in the tube and it was expressed in percent.

Preparation of cell-free extracts and determination of the activity of enzymes involved in glucose and glycerol catabolism, anaplerotic pathways and BS biosynthesis were performed as described in [6]. The activity of glucose-6-phosphate dehydrogenase (EC 1.1.1.49) was measured by detecting $NADP^+$ reduction at 340 nm using glucose-6-phosphate as an electron donor. Dihydroxyacetone kinase activity (EC 2.7.1.29) was determined on dihydroxyacetonephosphate formation which was assayed by spectrophotometry measuring the oxidation of $NADH^+$ in the coupled reaction with glycerol-3-phosphate dehydrogenase. The activity of isocitrate lyase (EC 4.1.3.1) was estimated by measuring the rate of phenylhydrazone glyoxylate formation at 324 nm, the activity of phosphoenolpyruvate (PEP) synthetase (EC 2.7.9.2) — by measuring the rate of pyruvate formation which was detected through NADH oxidation at 340 nm in the coupled reaction with lactate dehydrogenase, the activity of PEP-carboxykinase (EC 4.1.1.49) — by assessing the PEP and pyruvate formation during NADH oxidation, and the activity of glutamate dehydrogenase (EC 1.4.1.4) — by measuring the glutamate formation at NADPH oxidation at 340 nm, the activity of PEP carboxylase (EC 4.1.1.31) — by measuring

NADH oxidation at 340 nm, the activity of trehalose-phosphate synthase (EC 2.4.1.15) — by measuring uridine diphosphate formation which was determined by the NADH oxidation at 340 nm in coupled reactions with pyruvate kinase and lactate dehydrogenase.

NAD^+, $NADP^+$, uridine-5'-diphosphate-glucose (Fluka, Switzerland), lactate dehydrogenase, isocitrate (Serva, Germany) were used for enzyme assays. Others reagents were Sigma, USA.

Enzyme activity was expressed in nmol of product formed per 1 min and calculated per 1 mg of protein. Protein concentration in cell-free extracts was determined by Bradford assay [8]. Enzyme activity assessment was performed at 28–30 °C (optimal temperature for the *N. vaccinii* IMV B-7405 growth).

All experiments were performed in 3 replicates, the number of parallel determination in the experiment was 3-5. Statistical processing of the obtained data was performed as previously described [3]. The differences between average means were considered significant at $P < 0.05$.

Results and Discussion

It was previously shown [1–4] that the auxiliary substrate concept, proposed by Babel [9] to increase the biomass yield, can serve as theoretical basis for studies on the enhanced synthesis of secondary metabolites on mixture of several substrates. According to "energy-based classification" (on which concept is based), all substrates are divided into energy-excessive and energy-deficient [10]. According to this classification, phosphoglyceric acid (PGA) is a central carbon precursor (key intermediate) for the synthesis of all cellular components. The energy needed for the synthesis of cellular components from this precursor, is a constant value and found to be 1 mol of ATP per 10.5 g of dry biomass [10]. Substrates are classified as energy-excessive if the amount of ATP as well as reducing equivalents, generated on the pathway from the substrate to PGA, is sufficient for the biomass synthesis. Substrates, which must be partly oxidized to CO_2 to produce the energy required for the synthesis of cellular components, are classified as energy-deficient. Knowledge of the metabolic pathways of carbon substrate conversion into key intermediate (PGA) of biomass synthesis enables to determine the substrate "energy value".

According to the "energy-based classification" by Babel [10], glycerol is always energy-deficient substrate, whilst glucose may be, depending on catabolism pathway, either energy-deficient (glycolysis, the Entner-Doudoroff pathway) or energy-excessive (pentose phosphate pathway) substrate.

Previously it was found that *N. vaccinii* IMV B-7405 synthesizes complex of neutral, glyco- and aminolipids, at that, glycolipids were presented as trehalose mycolates [11]. Enzymatic studies [9] confirmed the ability of *N. vaccinii* IMV B-7405 to synthesize surface active glyco- and aminolipids, as evidenced by the high activity of enzymes of gluconeogenesis (PEP-carboxykinase and PEP-synthetase) and $NADP^+$-dependent glutamate dehydrogenase as well as trehalose-phosphate synthase — a key enzyme of the trehalose mycolates biosynthesis.

Calculation of the glucose/glycerol concentrations ratio for N. vaccinii I*MV B-7405 cultivation on their mixture*. The calculation of the optimal glucose/glycerol ratio was based on the following assumptions: 1) trehalose mycolates are the main BS components; 2) catabolism of glucose is performed via the pentose phosphate pathway; 3) glycerol is involved in metabolism through dihydroxyacetone with the participation of pyrroloquinoline quinine- and nitroso-N,N-dimethylaniline-dependent alcohol dehydrogenases and dihydroxyacetone kinase; 4) glucose is used primarily as an energy source, and for the synthesis of biomass and trehalose mycolates carbon of glycerol is used; 5) the mycolic acid in the trehalose mycolates is 3-hydroxy-2-dodecanoyl-docosanoic acid containing 34 carbon atoms (similar to *Rhodococcus erytropolis* trehalose lipids [12]); 6) P/O ratio is 2.

A possible scheme for the synthesis of trehalose monomycolate from glycerol is shown in Fig. 1. This scheme is based on our following studies of glycerol metabolism in the IMV B-7405 strain [6]:

1. *Assimilation of this substrate through dihydroxyacetone*. It was found [6] that glycerol catabolism to dihydroxyacetonephosphate (glycolysis intermediate) may be performed in two ways: through glycerol-3-phosphate and through dihydroxyacetone. Since the dihydroxyacetone kinase activity was higher than glycerol kinase activity (732 and 244 nmol/min^{-1}·mg^{-1} protein, respectively), exactly this pathway of glycerol catabolism is indicated in Fig. 1.

2. *Peculiarities of the central metabolism* (enzyme activities of tricarboxylic acid cycle, including the succinate formation in the alternative 2-oxoglutarate synthase reaction, gluconeogenesis reaction).

It should be noted, according to [6], that both gluconeogenesis enzymes (PEP-carboxykinase and PEP-synthetase) function in the *N. vaccinii* IMV B-7405 cells. Since the PEP-synthetase activity was higher than PEP-carboxykinase activity (1071 and 820 nmol/min^{-1}·mg^{-1} protein, respectively), exactly this reaction is shown in Fig. 1.

3. *Biosynthesis of surface-active trehalose mycolates* (formation of trehalose-6-phosphate in the trehalose-phosphate synthase reaction).

Based on data [12], the formation of mycolic acid via 3-hydroxy-2-dodecanoyl docosanoic acid and the synthesis of trehalose-6-mycolate from trehalose-6-phosphate and mycolic acid are shown in Fig. 1.

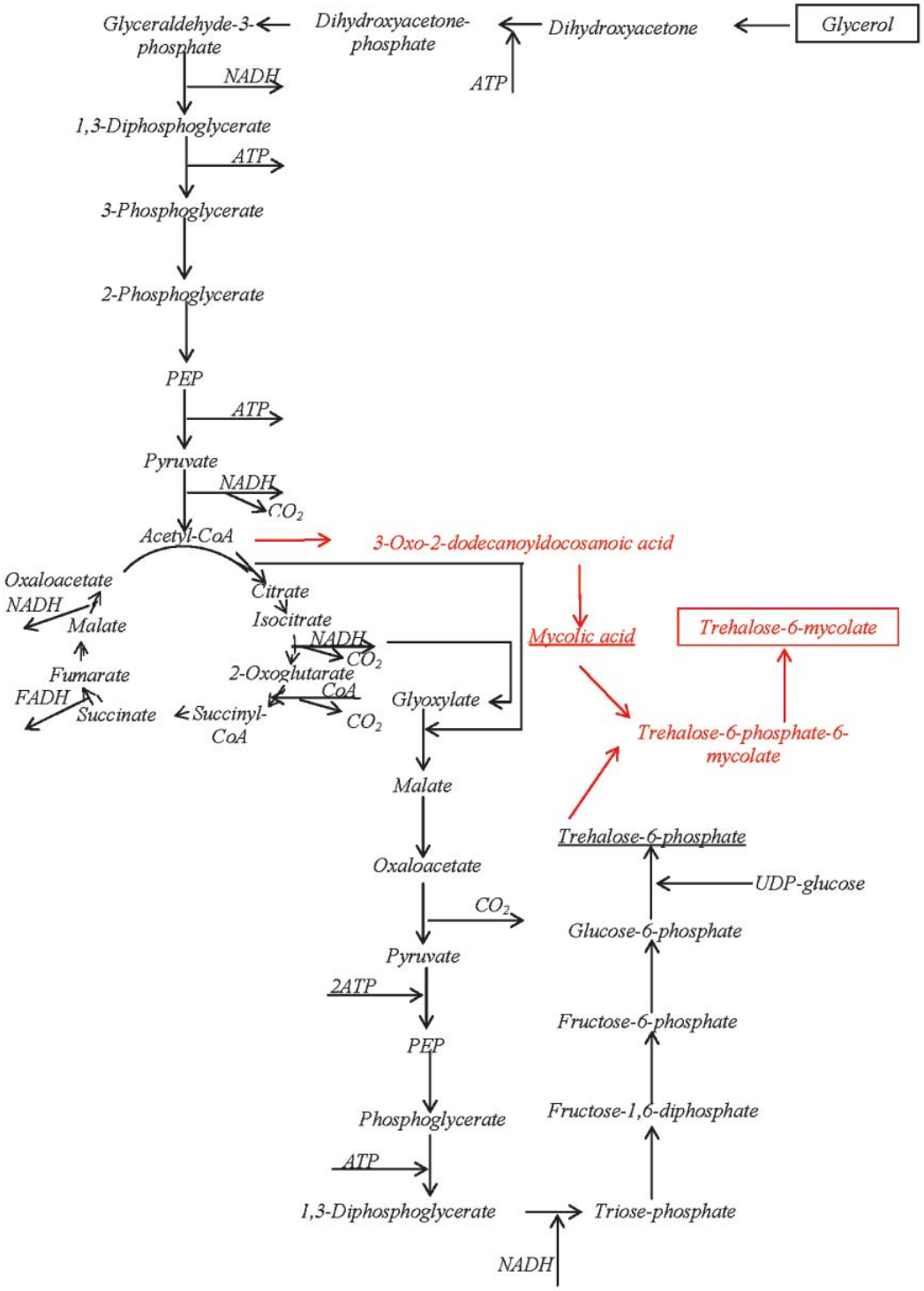

Fig. 1. **A proposed scheme for the biosynthesis of trehalose monomycolates from glycerol in *N. vaccinii* IMV B-7405.** The data from [12] are marked by red.

Energy consumption during the trehalose phosphate synthesis. As can be seen from the scheme, 8 mol of glycerol are required for the synthesis of one molecule of trehalose phosphate (4 mol to produce glyoxylate and 4 mol for the synthesis of acetyl-CoA, which reacts with glyoxylate to form malate). Thus, 8 mol of ATP are consumed during the formation of glycerol-3-phosphate from glycerol, 8 mol of ATP — in the formation of PEP from pyruvate, 4 mol of ATP — in the synthesis of 1,3-diphosphoglycerate from phosphoglyceric acid (PGA) and 8 (4 NADH) — during conversion of 1,3-diphosphoglycerate into triose phosphate. Hence, energy consumption is 28 mol of ATP. In addition, one mol of ATP is consumed during the formation of nucleoside-diphosphate-saccharide (glucose-6-phosphate → UDP-glucose) necessary for the synthesis of trehalose-6-phosphate. Hence, the energy consumption during synthesis of trehalose-6-phosphate from glycerol is 30 mol of ATP.

Energy consumption during the synthesis of mycolic acid. Considering the pathway of biosynthesis of fatty acids from acetyl-CoA described in [1], it can be calculated that for the producing of 3-hydroxy-2-dodecanoyl docosanoic acid containing 34 carbon atoms, 17 mol of acetyl-CoA are required, for the synthesis of which from glycerol, 17 mol of ATP is used. Given the number of cycles (16) in the synthesis of mycolic acids from acetyl-CoA, the energy consumption is 16 + 17 = 33 mol of ATP.

ATP generation during the synthesis of trehalose monomycolate from glycerol.

Energy is generated at the formation of acetyl-CoA:

$$\text{Glycerol} \rightarrow \text{Acetyl CoA} + \text{ATP} + 2\text{NADH}. \quad (1)$$

Since 17 mol of acetyl-CoA for mycolic acid synthesis and 8 mol of acetyl-CoA are required for trehalose phosphate synthesis, the equation (1) can be represented as:

$$25\ \text{Glycerol} \rightarrow 25\ \text{Acetyl-CoA} + 25\ \text{ATP} + 50\ \text{NADH}, \quad (2)$$

From equation (2), given P/O=2, it follows that during the formation of trehalose monomycolate from glycerol 25 + 100 = 125 mol of ATP are generated, or 5 mol of ATP per mole of glycerol. The total energy consumption during the synthesis of trehalose phosphate and mycolic acid from glycerol is 30 + 33 = 63 mol of ATP, or 2.52 mol of ATP per mol of utilized glycerol.

Thus, the energy generated during the trehalose monomycolate formation is 5–2.52 = 2.48 mol ATP / mol of utilized glycerol.

The energy consumption during the biomass synthesis. Synthesis of biomass from phosphoglyceric acid, a key intermediate of synthesis of cellular components, can be represented as follows [10]:

$$4\ \text{PGA} + NH_3 + 29\ \text{ATP} + 5.5\ \text{NAD(P)H} \rightarrow (C_4H_8O_2N)_3 \quad (3),$$

where $(C_4H_8O_2N)_3$ is a formula of mole of the biomass.

Total conversion reactions of glycerol and glucose in PGA are [8]:

$$\text{Glycerol} \rightarrow \text{PGA} + \text{NAD(P)H}; \quad (4)$$

$$\text{Glucose} \rightarrow \text{PGA} + 7\ \text{NAD(P)H} + 3CO_2. \quad (5)$$

For P/O = 2 equations (4) and (5) can be presented as:

$$\text{Glycerol} \rightarrow \text{PGA} + 2\ \text{ATP}; \quad (6)$$

$$\text{Glucose} \rightarrow \text{PGA} + 14\ \text{ATP}. \quad 7)$$

Considering the equation of biomass synthesis from PGA (equation (3) and the glycerol catabolism to PGA equation (equation (6), it can be calculated that the ATP amount required for biomass synthesis (per mol of glycerol) is 8 mol of ATP. In our opinion, this energy can be obtained from glucose. Given that 2.48 mol of ATP / mol of glycerol is generated during the synthesis of trehalosemonomycolate from glycerol, 8 — 2.48 = 5.52 mol ATP should be obtained at the expense of glucose. The equation (7) implies that 0.394 mol of glucose is needed for this amount of energy. Consequently, the glucose/glycerol molar ratio in the medium should be 0.394:1 or 1:2.5.

Effect of molar ratio of glucose/glycerol concentrations on BS synthesis. In the next step, BS synthesis by *N. vaccinii* IMV B-7405 at various molar ratios of glucose and glycerol concentrations in a mixture was studied (Fig. 2). As it can be seen (Fig. 2), the highest rates of BS synthesis were observed at molar ratio of monosubstrates 1:2.5–1,4, i.e. closest to the theoretical one.

Further experiments showed that in the cells of *N. vaccinii* IMV B-7405 strain grown on a mixture of glucose and glycerol (1:2.5), the enzymes of both substrates catabolism functioned simultaneously. Thus, the activity of $NADP^+$-dependent glucose-6-phosphate

Table 1. **Characteristics of BS synthesis under cultivation of *N. vaccinii* IMV B-7405 on glucose, glycerol and their mixture**

Substrate concentration,%	BS, g/l	E24,%
Glucose, 0.5+ Glycerol, 0.5	3.0±0.15*	55±2.8**
Glucose, 0.75	1.3±0.06	51±2.5
Glycerol, 0.6	1.5±0.07	53±2.6

Notes. The concentration of glycerol is given in% (vol/vol). The molar ratio of glucose/glycerol concentrations is 1:2.5 (Table 1 and 2). Mixed and monosubstrates are equimolar for carbon. Under cultivation on glucose and glycerol, the inoculum was grown on respective monosubstrates (0.5%), for the mixed substrate — on mixture of glucose (0.25%) and glycerol (0.25%). The concentration of biomass in all cases was the same 0.8–0.9 g/l.

* — $P < 0.05$ relative to control (BS concentration on the monosubstrates).

** — $P < 0.05$ relative to control (emulsification index on the monosubstrates).

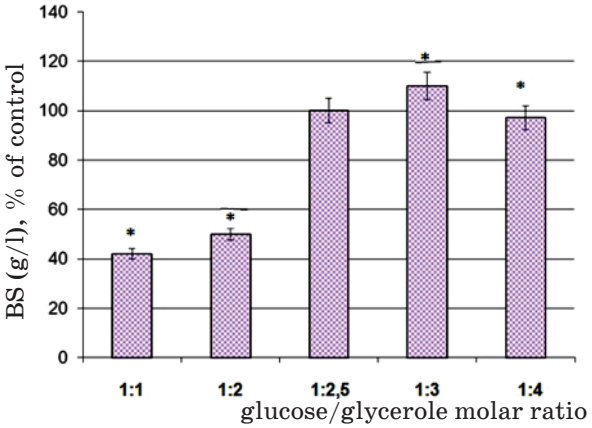

Fig. 2. **Effect of molar ratio of glycerol/glucose concentrations in the cultivation medium of *N. vaccinii* IMV B-7405 on BS synthesis:** *Hereinafter: *— $P < 0.05$* relative to the control (BS concentration at the theoretically calculated glucose/glycerol molar ratio 1:2.5). The inoculum was grown on a mixture of glucose (0.25%) and glycerol (0.25%, vol/vol)

dehydrogenase (one of enzymes of the pentose phosphate pathway) and dihydroxyacetone kinase (the key enzyme of the dihydroxyacetone pathway of glycerol assimilation) was was 400–450 nmol/min^{-1}·mg^{-1} protein). These data indicated the mixotrophic nature of the *N. vaccinii* IMV B-7405 growth on a mixture of glucose and glycerol.

Characteristics of BS synthesis by *N. vaccinii* IMV B-7405 on glucose and glycerol mixture (molar ratio 1:2.5), as well as on monosubstrates equimolar for carbon concentrations shown in Table 1. The concentration of extracellular biosurfactants obtained on the mixture of glucose and glycerol was 2-2.3 times higher than ones synthesized on monosubstrates and emulsification index of the culture liquid did not substantially change (51–55%).

These data may indicate that cultivation of IMV B-7405 strain on the mixed substrate is accompanied by enhanced synthesis of metabolites with surfactant properties. To test this assumption the activity of enzymes of the surfactants biosynthesis was determined (Table 2).

The data presented in the Table 2 have shown that under cultivation IMV B-7405 on the glucose and glycerol mixture, the activity of PEP-carboxylase (enzyme of anaplerotic reaction that replenishes the pool of C_4-dicarboxylic acids — precursors of gluconeogenesis) was 1.3-1.4 fold higher, and the activity of key enzymes of gluconeogenesis (PEP-carboxykinase and PEP-synthetase) was 1.2-5.7-fold higher than that under cultivation on monosubstrates. These data, as well as the higher activity of trehalose-phosphate synthase on mixed substrate (69 against 38–39 nmol/min^{-1}·mg^{-1} protein on glucose and glycerol) indicated an increase in the surface-active trehalosemycolate synthesis under such conditions. Enhanced synthesis of exactly glycolipids on a mixture of glucose and glycerol was also evidenced by almost the same (394–427 nmol/ min^{-1}·mg^{-1} protein) activity of $NADP^+$-dependent glutamate dehydrogenase, the enzyme of surface-active aminolipid biosynthesis, on both mixed and monosubstrates. It should be noted that under cultivation of IMV B-7405 strain on either glycerol or mixture of glucose and glycerol, activity of isocitrate lyase (one of the key enzymes of the glyoxylate cycle functioning in microorganisms growing on non-carbohydrate substrates) was not detected.

Thus, both, the data presented in Table 2 and the results of growth experiments (Table 1) have confirmed the enhanced synthesis of surface-active metabolites under cultivation of *N. vaccinii* IMV B-7405 on a mixed substrate.

Table 2. **The activity of enzymes of BS biosynthesis and anaplerotic pathways under *N. vaccinii* IMV V-7405 cultivation on the mono- and mixed substrates**

Enzyme	Activity (nmol/min·mg protein) in the cell-free extracts, obtained from cells grown on:		
	glycerol	glucose	mixture of glycerol and glucose
PEP-carboxylase	714±35	218±10	1250±62*
PEP-synthetase	1042±52	623±31	1290±64*
$NADP^+$-dependent glutamate dehydrogenase	394±19	427±21	417±20*
PEP-carboxylase	714±35	803±40	1036±51*
Isocitrate lyase	0	0	0
Trehalose-phosphate synthase	39±2	38±2	69±3*

Notes. Enzyme activity was determined in the cell-free extracts obtained from the cells in early exponential growth phase. * — $P < 0.05$ relative to control (enzyme activity in the cells grown on the monosubstrates).

We reviewed in [4] the literature data (mainly 2005–2010) on the application of the mixture of substrates for intensification of technologies of microbial synthesis of practically valuable products of fermentation (ethanol, lactic acid, butanediol), the primary (amino acid, *n*-hydroxybenzoate, triglycerides) and secondary (lovastatin, surfactants) metabolites as well as biodegradation of xenobiotics of aromatic nature (benzene, cresols, phenols, toluene) and pesticides (dimethoate).

Following this review, a little new information on the microbial synthesis of industrial products, including microbial surfactant mixtures on growth substrates was published. For example, in [13] the possibility of enhancing the synthesis of 1,3-propanediol by *Klebsiella pneumoniae* ME-303 on the mixture of xylose and glycerol was shown. It was found that under cultivation of ME-303 strain in a fermenter on a medium containing 30 g/l glycerol and 8 g/l xylose, the concentration of 1,3-propanediol was 13.2 g/l and was only 9.4% higher than under cultivation on monosubstrate glycerol.

Study of biomass production and polyols (mannitol and arabitol) synthesis by *Yarrowia lipolytica* on glycerol, glucose and mixture of these subsrtates (10 g/l) showed that cultivation of yeast on mixed substrate was accompanied by an increase in growth rate, levels of biomass, but not the amount of alcohol [14].

Formation of sophorolipids by strain *Starmerella* (*Candida*) *bombicola* ATCC 22214 on a mixture of glycerol (15%) and sunflower oil (10%), and a mixture in which the purified glycerol was replaced with glycerol-containing waste products of commercial fats lyposis was studied in [15]. It was found that regardless of the glycerol source in mixture, concentration of synthesized surfactant was almost the same (6.36–6.61 g/l).

Yeast *Cyberlindnera samutprakarnensis* $JP52^T$ when grown on a mixture of glucose (2%) and palm oil (2%, vol/vol) synthesized 1.89 g/l BS [16]. Interestingly, BS synthesis was not observed under cultivation of JP52T strain on palm oil, on monosubstrate glucose concentration of surfactant was only 0.03 g/l.

In [17], synthesis of mannosylerythritol lipid BS by *Pseudozyma hubeiensis* Y10BS025 on mixtures of several substrates was studied. It was established that cultivation of Y10BS025 strain on a mixture of glucose and glycerol at ratio 75:25 with addition of soybean oil (8%, vol/vol), accompanied by synthesis of 115 g/l BS, that higher than if olive oil was added (65 g/l).

In studies [15–17] (and other aforementioned publications), monosubstrates and their concentrations in the mixture were established empirically. It is noteworthy that the substrates were used in extremely high (sometimes 100 g/l) concentrations. In this case, the enhancement of the BS synthesis on the mixture of growth substrates compared to the cultivation on monosubstrates was not indicative, since the main criterion of efficiency of mixed substrates was the maximal carbon conversion into final product.

In previous researches [1–4] and in this study, to provide the highest carbon conversion

of the two energetically unequal substrates into microbial products (surfactants), we performed a theoretical calculation of optimal molar ratio of monosubstrate concentrations in the mixture that allowed increasing the concentration of the final product by several times in comparison with that on monosubstrates.

The theoretical calculation of the energy required for the synthesis of trehalose mycolates *R. erythropolis* IMV Ac-5017 and *A. calcoaceticus* IMV B-7241 on a mixture of energy-excessive hexadecane and energy-deficient glycerol showed that the optimum molar ratio of substrates for BS synthesis found to be 1:7 [3, 4]. Under such cultivation conditions the BS synthesis was 2.6–3.5-fold higher compared to synthesis on hexadecane or glycerol. In present work it was found that amount of BS synthesized by *N. vaccinii* IMV B-7405 at molar ratio of glucose and glycerol concentration 1:2.5–1:4 as close to the theoretically calculated 1:2.5 was 2.0–2.3-fold higher than those obtained on monosubstartes.

Thus, the obtained results confirmed own previous results [1–4] that the use of the mixture of energetically unequal growth substrates is rational for the increase of the synthesis of secondary metabolites and indicated that the high efficiency of these mixed substrates can be achieved by both the correct choice of substrates and the correct determination of the molar ratio of their concentrations.

REFERENCES

1. *Pirog T. P., Kovalenko M. A., Kuz'minskaya Yu. V.* Intensification of exopolysaccharide synthesis by *Acinetobacter* sp. on an ethanol–glucose mixture: aspects related to biochemistry and bioenergetics. *Microbiology*. 2003, 72 (3), 305–312.
2. *Pidhorskyy V., Iutinska G., Pirog T.* Intensification of microbial synthesis technologies. *Kyiv: Nauk. dumka*. 2010, 327 p. (In Ukrainian).
3. *Pirog T. P., Konon A. D., Shevchuk T. A., Bilets I. V.* Intensification of biosurfactant synthesis by *Acinetobacter calcoaceticus* IMV B-7241 on a hexadecane–glycerol mixture. *Microbiology*. 2012, 81 (5), 565–572.
4. *Pirog T. P., Shulyakova M. A., Shevchuk T. A.* Mixed substrates in environment and biotechnological processes. *Biotechnol. acta*. 2013, 6 (6), 28–44. doi: 10.15407/biotech6.06.028. (In Ukrainian).
5. *Kudrya N., Pirog T.* The specifics of surfactants synthesis during *Nocardia vaccinii* IMV B-7405 cultivation on mixed substrates. *Ukrainian food journal*. 2013, 2 (2), 203–209. (In Ukrainian).
6. *Pirog T., Shevchuk T., Beregova K., Kudrya N.* Peculiarities of glucose and glycerol metabolism in *Nocardia vaccinii* IMB B-7405 — producer of biosurfactants. *Ukr. Biochem. J.* 2015, 87 (2), 66–75. (In Ukrainian).
7. *Bligh E. G., Dyer W. J.* A rapid method for total lipid extraction and purification. *Can. J. Biochem. Physiol.* 1959, 37 (8), 911–917.
8. *Bradford M.* A rapid sensitive method for the quantitation of microgram quantities of protein utilizing the principle of protein-dye binding. *Anal. Biochem.* 1976, 72 (3), 248–254.
9. *Babel W.* Bewertung von substraten fur das mikrobielle wachstum auf der grundlage ihres kohlenstoff/energie-verhaltnisses. *Z. Allg. Mikrobiol*. 1979, 19 (9), 671–677.
10. *Babel W., Muller R. H.* Mixed substrate utilization in microorganisms: Biochemical aspects and energetic. *J. Gen. Microbiol.* 1985, 131 (1), 39–45.
11. *Pirog T., Gritsenko N., Khomyak D., Konon A., Antonuk S.* Optimization of synthesis of biosurfactants of *Nocardia vaccinii* K-8 under bioconversion of biodiesel production waste. *Mikrobiol. Zh*. 2011, 73 (4), 15–24. (In Russian).
12. *Rosenberg E., Ron E.Z.* High- and low-molecular-mass microbial surfactants. *Appl. Microbiol. Biotechnol.* 1999, 52 (2), 154–162.
13. *Jin P., Lu S., Huang H., Luo F., Li S.* Enhanced reducing equivalent generation for 1,3-propanediol production through cofermentation of glycerol and xylose by *Klebsiella pneumonia*. *Appl. Biochem. Biotechnol*. 2011, 165 (7–8), 1532–1542.
14. *Workman M., Holt P., Thykaer J.* Comparing cellular performance of *Yarrowia lipolytica* during growth on glucose and glycerol in submerged cultivations. *AMB Express*. 2013, 3:58. doi: 10.1186/2191-0855-3-58.
15. *Wadekar S. D., Kale S. B., Lali A. M., Bhowmick D. N., Pratap A. P.* Utilization of sweetwater as a cost-effective carbon source for sophorolipids production by *Starmerella bombicola* (ATCC 22214). *Prep. Biochem. Biotechnol*. 2012, 42 (2), 125–142. doi: 10.1080/10826068.2011.577883.
16. *Poomtien J., Thaniyavarn J., Pinphanichakarn P., Jindamorakot S., Morikawa M.* Production and characterization of a biosurfactant from *Cyberlindnera samutprakarnensis* JP52^T. *Biosci. Biotechnol. Biochem*. 2013, 77 (12), 2362–2370.
17. *Sari M., Kanti A., Artika I. M., Kusharyoto W.* Identification of *Pseudozyma hubeiensis* Y10BS025 as a potent producer of glycolipid biosurfactant mannosylerythritol lipids. *Amer. J. Biochem. Biotechnol*. 2013, 9 (4), 430–437.

ІНТЕНСИФІКАЦІЯ СИНТЕЗУ ПОВЕРХНЕВО-АКТИВНИХ РЕЧОВИН ЗА КУЛЬТИВУВАННЯ *Nocardia vaccinii* IMB B-7405 НА СУМІШІ ГЛЮКОЗИ ТА ГЛІЦЕРОЛУ

Т. П. Пирог[1, 2]
Т. А. Шевчук[1]
К. А. Берегова[2]
Н. В. Кудря[2]

[1]Інститут мікробіології та вірусології ім. Д. К. Заболотного НАН України, Київ
[2]Національний університет харчових технологій, Київ, Україна

E-mail: tapirog@nuft.edu.ua

Метою роботи було визначення оптимального молярного співвідношення глюкози та гліцеролу для інтенсифікації синтезу поверхнево-активних речовин *N. vaccinii* IMB B-7405 на суміші енергетично нерівноцінних субстратів (глюкози і гліцеролу).

На основі теоретичних розрахунків енергетичних потреб синтезу поверхнево-активних трегалозомономіколатів та біомаси на енергетично дефіцитному субстраті (гліцерол) встановлено концентрацію енергетично надлишкової глюкози, що дає змогу підвищити ефективність конверсії вуглецю використовуваних субстратів у поверхнево-активні речовини. За молярного співвідношення концентрацій глюкози та гліцеролу 1,0:2,5 кількість синтезованих позаклітинних поверхнево-активних речовин була у 2,0–2,3 раза більша, ніж на відповідних моносубстратах.

Підвищення концентрації поверхнево-активних речовин на змішаному субстраті зумовлено збільшенням синтезу поверхнево-активних трегалозоміколатів, про що свідчило зростання в 1,2–5,7 раза активності ензимів їх біосинтезу (трегалозофосфатсинтази, фосфоенолпіруваткарбоксикінази, фосфоенолпіруватсинтетази) порівняно з культивуванням на моносубстратах глюкозі та гліцеролі. Отримані результати свідчать про доцільність використання суміші енергетично нерівноцінних ростових субстратів для підвищення синтезу вторинних метаболітів, а також про те, що високої ефективності таких змішаних субстратів може бути досягнено як за правильного вибору субстратів, так і коректного визначення молярного співвідношення їх концентрацій.

Ключові слова: *Nocardia vaccinii* IMB B-7405, поверхнево-активні речовини, енергетично нерівноцінні субстрати.

ИНТЕНСИФИКАЦИЯ СИНТЕЗА ПОВЕРХНОСТНО-АКТИВНЫХ ВЕЩЕСТВ ПРИ КУЛЬТИВИРОВАНИИ *Nocardia vaccinii* IMB B-7405 НА СМЕСИ ГЛЮКОЗЫ И ГЛИЦЕРОЛА

Т. П. Пирог[1, 2]
Т. А. Шевчук[1]
К. А. Береговая[2]
Н. В. Кудря[2]

[1]Институт микробиологии и вирусологии им. Д. К. Заболотного НАН Украины, Киев
[2]Национальный университет пищевых технологий, Киев

E-mail: tapirog@nuft.edu.ua

Целью работы было определение оптимального молярного соотношения глюкозы и глицерола для интенсификации синтеза поверхностно-активных веществ *N. vaccinii* IMB B-7405 на смеси энергетически неравноценных субстратов (глюкозы и глицерола).

На основе теоретических расчетов энергетических потребностей синтеза поверхностно-активных трегалозомономиколатов и биомассы на энергетически дефицитном субстрате (глицерол) установлена концентрация энергетически избыточной глюкозы, позволяет повысить эффективность конверсии углерода используемых субстратов в поверхностно-активные вещества. При молярном соотношении концентраций глюкозы и глицерола 1,0:2,5 количество синтезируемых внеклеточных поверхностно-активных веществ было в 2,0–2,3 раза больше, чем на соответствующих моносубстратах.

Повышение концентрации поверхностно-активных веществ на смешанном субстрате обусловлено увеличением синтеза поверхностно-активных трегалозомиколатов, о чем свидетельствовало возрастание в 1,2–5,7 раза активности энзимов их биосинтеза (трегалозофосфатсинтазы, фосфоенолпируваткарбоксикиназы, фосфоенолпируватсинтетазы) по сравнению с культивированием на моносубстратах глюкозе и глицероле. Полученные результаты свидетельствуют о целесообразности использования смеси энергетически неравноценных ростовых субстратов для повышения синтеза вторичных метаболитов, а также о том, что высокая эффективность таких смешанных субстратов может быть достигнута как при правильном выборе субстратов, так и корректном определении молярного соотношения их концентраций.

Ключевые слова: *Nocardia vaccinii* IMB B-7405, поверхностно-активные вещества, энергетически неравноценные субстраты.

UDK 612.115.3:577.114 doi: 10.15407/biotech8.06.032

PREPARATION OF CHITOSAN WITH HIGH BLOOD CLOTTING ACTIVITY AND ITS HEMOSTATIC POTENTIAL ASSESSMENT

M. D. Lootsik[1]
R. O. Bilyy[1, 2]
M. M. Lutsyk[2]
R. S. Stoika[1]

[1]Institute of Cell Biology of the National Academy of Sciences of Ukraine, Lviv

[2]Danylo Halytsky Lviv National Medical University, Ukraine

E-mail: lootsik@cellbiol.lviv.ua

Received 21.10.2015

The aim of research was the evaluation of blood clotting activity and hemostatic effect of chitosan specimens using developed set of laboratory tests and preparation of chitosan with high blood clotting activity. Chitosan specimens were powdered to the particle size less than 0.25 mm and characterized by *in vitro* tests including determination of coagulation time of heparinized blood, bulk density of material, swelling of particles in water and Tris-buffered saline, pH 7.4, as well as *in vivo* tests based on estimation of efficacy in controlling hemorrhage from wounds in mice and rats. Using of the developed tests it was revealed that available chitosan specimens (reagent grade, dietary supplements, samples prepared in laboratory) are hemostatically inactive as compared with Celox preparation. We developed a method of activation of above mentioned chitosan specimens to active hemostatic preparations. Some characteristics of chitosan that are significant for blood clotting activity are described. It was demonstrated that high molecular weight chitosan specimens are more effective as hemostatic agents comparing with low molecular weight chitosan specimens.

Key words: chitosan, Celox, hemostatic effect, laboratory tests *in vitro* and *in vivo*.

In a great number of hemostatic agents implicated in different field of medicine, the hemostatic materials based on chitosan are the most effective in stemming acute hemorrhages, especially severe ones, and are of the first order significance in the emergency and military medicine [1, 2]. Methods of chitin and chitosan isolation and purification from different sources have been described in numerous patents and papers [3–9]. Nevertheless, there is a problem in verification of the hemostatic or hemocoagulating activity of chitosan specimens purchased from different commercial sources or prepared in laboratory according to described methods. We found that chitosan as a chemical reagent or dietary supplement did not exhibit hemocoagulating or blood clotting activity. Thus, monitoring of such activity is necessary when using chitosan samples of commercial origin or samples prepared in laboratory for obtaining high quality hemostatic material whose characteristics are comparable with that of known commercial hemostatic agent Celox. Several tests for measuring hemostatic activity of chitosan preparations were proposed. They include determination of whole blood clotting time and plasma recalcification time [10], involvement of platelets (aggregation, deposition and release of ATP and other factors involved in blood clotting) [11], determination of the duration of bleeding time from pricked finger tip using chitosan soaked bandage [12], flocculation of 0.5% solution of bentonite [13], stemming of hemorrhage in a swine after groin injury with transection of the femoral vessels [14]. The last one is considered to be the most decisive, however, screening process is rather inconvenient and expensive, and the duration of bleeding time from pricked finger tip [12] is rather subjective and not suitable for the repeated performance.

In our studies, commercial chitosan specimens, as well as laboratory prepared specimens and the original Celox (Medtrade Products, UK) used as a positive control of the hemostatic agent were tested when developing different laboratory tests *in vitro* and *in vivo* that permit predicting distinct chitosan sample to be a potent hemostatic agent in clinics conditions. The *in vitro* tests included: a) clotting of blood in the presence of heparin;

b) swelling of chitosan particles in water and in saline; c) bulk density of powder (g/cm^3). While the *in vivo* tests included estimation of the efficacy of studied material in controlling of hemorrhage from wound in mice or rats.

The aim of this study was to compare properties and hemostatic activity of selected specimens of chitosan and Celox by using a developed set of tests and to elaborate the method of chitosan activation for obtaining the product possessing high blood clotting activity.

Material and Methods

The following chitosan specimens were investigated: 1) low molecular weight chitosan from crab shells (Aldrich, gift of Dr. Zaichenko O. S., Lviv National Polytechnic University); 2) chitosan Tyanshi, a dietary supplement (www.tiens.in.ua) [15]; 3) chitosan purchased from Organica (Health Products Inc., Canada) that is a dietary supplement for management of blood cholesterol level; 4) chitosan prepared in our laboratory from chitin of crab shells (obtained as described in [16]. The last preparation was subjected to hydrolysis in 40% NaOH (110 °C for 5 hours with further washing from alkali, dehydration with ethanol and drying), as described in [17]. In order to obtain reproducible results, studied material were grinded to a powder with particle size less than 0.25 mm using porcelain mortar and sieve of 60 mesh.

The obtained chitosan specimens were characterized by determination of the molecular weight and degree of deacetylation. Molecular weight was defined by the viscometry method, as described in [18]. Viscosity was measured at 25 °C with a viscometer of Ubbelohde type VPZh-4 (ВПЖ-4, Soyuznauchpribor, USSR) with capillar diameter = 0.56 mm. Measurements of chitosan solutions in a mixture of 0.17 M acetic acid:0.2 M NaCl (1:2) were conducted.

A degree of deacetylation of chitosan specimens was determined by the potentiometric titration based on measuring a capacity of ion exchange sorbents, as described below. Chitosan specimen was converted to base (OH^-) form by adjustment of 0.5% solution in 3% acetic acid to pH 8.5–9.0 with 10% ammonium hydroxide. Precipitated substance was collected by centrifugation (10 min at 2,000 rpm), washed with water and ethanol, and dried by evaporation on a glass surface. Otherwise, precipitate could be harvested on a glass (Schott) filter, washed with water, ethanol and dried. Dry material was powdered and stored in the dessicator over $CaCl_2$.

100 mg of chitosan base was dissolved in 10 ml of 0.1 N HCl. The dissolving of high molecular weight chitosan was proceeded slowly, for 2–4 hours under stirring. Then solution was titrated with 0.1 N NaOH using glass electrode in pH meter EB-74 (EV-74, Grodno, Belaruss). The titration curves were constructed (Fig. 1) from which the equivalent value of free HCl titrated to pH 2.5 was determined. That pH value was accepted on a basis of titration of 10 ml 0.1 N HCl. A degree of deacetylation was determined by comparison with chitosan samples of known deacetylation

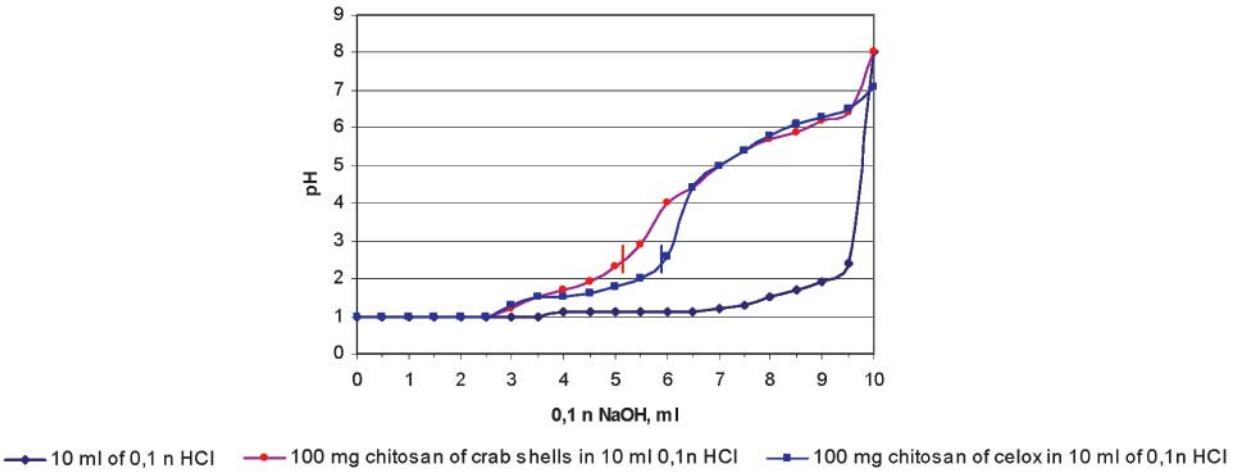

Fig. 1. **Determination of chitosan deacetylation degree as measured by the potentiometric titration:**
vertical bars on titration curves denote points which were accepted as the end of free HCl titration

level, as indicated in the accompanying certificates.

The mEq of HCl bound to chitosan base can be calculated as a difference between 1 mEq HCl (10 ml of 0.1 N HCl) and quantity of mEq titrated to pH 2.5. The obtained value was recalculated to 1 g of chitosan specimen from which the number of mEq of glucosamine in 1 g of chitosan was calculated. It was determined that 1 g of chitosan with 100% degree of deacetylation contained 6.17 mEq of glucosamine residues (considering 162 mg as 1 mEq of glucosamine residue, 1000 mg/162 = 6.17 mEq of glucosamine residues per 1 g).

Bulk density of chitosan preparations was measured in small glass tubes (inner diameter 4–5 mm, volume 0.6 ml) graduated in 0.1 ml scale. Chitosan powder was introduced into tube and its mass was measured by weighting with ±0.1 mg accuracy. Then powder was packed by striking the bottom of the tube on table surface up to the constant level, and then the volume was registered. Bulk density value of specimen was presented as g/cm^3. When the amount of tested material was sufficient, the size of the tube can be choice arbitrary, e.g. standard glass conic centrifuge tube. The material under investigation was not altered and can be reutilized in further experiments.

Swelling of chitosan in water media was determined in small tubes, like ones described above. 0.5 ml of distilled water or Tris-buffered saline (TBS, pH 7.4), was introduced into a tube, and 5 mg of tested powder was poured over the liquid. The behavior of particles was observed for 1 min and checked if they are retained on the surface or drawn to the bottom. Thereafter, the content was mixed with a small hook made from glass capillary, the tube was placed vertically and a result was registered after 1 hour (volume of sediment, dissolution of particles, viscosity of mixture). Finally, the condition of mixture (complete or partial dissolution of chitosan particles and volume of sediment, if present) were registered after 12 hours.

For *blood clotting test*, 2 ml of blood were withdrawn from the peripheral vein of human volunteers after their written agree into a plastic tube containing 0.2 ml of heparin (2 mg/ml in TBS). Analysis was performed in a flat bottom glass tubes, 8×35 mm. 0.2 ml of fresh heparinized blood was introduced into a tube, 7 mg of tested chitosan powder was added, and content was mixed with a glass hook. Time of clot formation was registered by a stop watch. Blood clotting was manifested as disappearance of liquid state of blood layer, i.e. no changing of its shape during bending of the tube or putting it bottom up.

Experiments in vivo were conducted on mice and rats taking into account the approval of the BioEthics Committee at Danylo Halytsky Lviv National Medical University (Protocol N 3 dated by 2015.03.16). Animal treatment was conducted in compliance with recommendations of *The European Community Council Directive*, 24 November 1986 (86/609/EEC).

Mouse was immobilized by its placing in a special small "house", the tail of animal hanging from it freely. Bleeding was evoked by cutting off 10 mm of tail end with a sharp razor blade. Bandage was applied upon the wound, which was prepared as follows. A peace of double sheet gauze (2×2 cm size) was moistened with 10% propylene glycol solution, an excess of liquid was blotted with filter paper and 10 mg of chitosan powder was spread over the gauze surface. After drying during 15–30 min, the gauze was folded to 1×1 cm square like a filter paper funnel and stored in the closed Eppendorf tube. Just before use, additional 3–5 mg of chitosan powder was introduced into this funnel. In control, bandage was loaded with inert powder, e.g. starch. Bandage was attached to the wound by fingers for 5 min, and then it was fixed with a peace of plaster. After 10–15 min, mouse was released into a cage and observed in about 1 hour. Bandage was left further for 12–24 hours in a place of application until spontaneous detachment. The level of blood loss was evaluated semi-quantitatively by measuring hemoglobin washed out from the bandage with water.

Similar experiment on rats was conducted under general anesthesia with diethyl ether. Bandage (double sheet gauze) was of bigger size (3×3 cm) than in the case of mouse, and respectively more chitosan powder (22 + 5 mg added *ex tempore*) was used.

Results and Discussion

It was revealed that commercial preparations of chitosan (produced as chemical reagent or dietary supplement), as well as that obtained in our laboratory by using known methods, did not exhibit hemocoagulating effect towards the heparinized blood, while Celox preparation possessed such activity. When using the test of chitosan swelling in water, we revealed that inactive chitosan particles differ from Celox by a lack of swelling and solubility in

water. After application upon water column in a tube, chitosan particles rapidly fall down to the tube bottom and form small white sediment. Similar behavior was observed when acetate and succinate salts of chitosan were used. On the contrary, Celox particles were hydrated immediately with a formation of very viscous substance that did not sediment. Thereafter, Celox particles were slowly dissolved. It was suggested that a lack of swelling depended upon structure of the particles which ought to be similar to dry gel, and also depended on conditions of chitosan precipitation and desiccation at final steps of preparation. It was found that precipitation of chitosan acetate with ethanol at concentration < 50% in pH interval of 5.9–7.0 provides gel-like structure of chitosan particles that saved their swelling property. Desiccation of gel by free evaporation on flat surface of glass sheet was another revealed feature of chitosan particles. Taking into account these observations, we developed a method of chitosan activation necessary for obtaining of highly active hemocoagulating agent.

Activation of commercial and reagent grade chitosan samples to obtain blood clotting agent. Chitosan sample was dissolved in 3% acetic acid (final concentration 0.75–1.5%) under constant mechanical stirring overnight. Dissolving proceeds slowly, and diversity in denoted concentration value is due to viscosity of solution depending on the molecular weight of chitosan sample. The insoluble material, if occur, was withdrawn by centrifugation (20 min, 2,000 g). Clear chitosan solution was treated with ammonia by bubbling NH_3 gas at constant stirring until pH 8.5–9.0 is achieved, at which chitosan precipitates like cheese flakes. The precipitate was collected by filtration through a synthetic cloth that was dense enough in order to retain sediment, and then it was washed with a small volume of distilled water. The obtained material was suspended in water and treated in Potter-Elvehjem homogenizer to a uniform slurry, thereafter it was solubilized by a stepwise addition of 10% solution of the acetic acid at intensive stirring. Dissolution began at pH 6.5 and was completed at pH 5.8, giving a viscous mass. In order to destroy clumps, it was necessary to use homogenization of the mass with whatever versatile mode, and Potter-Elvehjem homogenizer was the best. pH of the obtained mixture must be 5.9–6.0, and it might be corrected with 10% solutions of acetic acid or ammonium hydroxide. Mixture was left overnight for equilibration, thereafter, ethanol was added under constant stirring up to final concentration of alcohol 25 ± 2%. Mixture was centrifuged for 15 min at 2,000 g, and sediment denoted "chitosan fraction 1" was saved. Clear supernatant was adjusted to pH 6.7 with small volume of 10% NH_4OH which induced massive precipitation of chitosan. The sediment was collected by 10 min centrifugation at 1,500 g and denoted as "chitosan fraction 2". In case of turbid supernatant, it was treated with additional quantity of ammonium hydroxide to reach pH 7.2, and small sediment, if occurred, was collected by centrifugation. Material of fractions 1 and 2 was spread in a thin layer on glass sheets and dried by spontaneous evaporation. Dry material was collected, grinded to powder that was thereafter fractionated by sieving. Fraction with particle size < 0.25 mm corresponding to 60 mesh were collected. The yield of final product was 90%. Samples were stored in the dessicator over anhydrous $CaCl_2$. Characteristics of specific chitosan specimens before and after activation are presented in Table 1.

Average molecular weight of studied chitosan samples was determined by the viscometry. The experimental data obtained for chitosan of crab shells soluble in 1% acetic acid are presented in Table 2 and Fig. 2. An intrinsic viscosity ($[\eta] = \eta_{sp}$ at C = 0) was estimated graphically and corresponded to 560 ml/g (Fig. 2). Average molecular weight of the exemplified chitosan was calculated according to Staudinger formula: $\log [\eta] = \lg K + a \log M$, where constant values in used system were:

$K = 1.8 \times 10^{-3}$, a = 0.93

$\log 560 = \log 0{,}0018 + 0.93 \log M$

$2.748 = -2.745 + 0.93 \log M$

$\log M = 5.493 / 0.93 = 5.906$

M = 805378, approx. 800 KDa.

Average molecular weight and degree of deacetylation values of studied chitosan specimens in comparison with their coagulating activity are shown in Table 3.

Obtained data show that the molecular weight of chitosan is very important for its blood clotting activity. High molecular weight chitosan preparations exhibit faster clot formation. It is suggested that chitosan obtained in our laboratory from crab shells

Table 1. **Characteristics of different chitosan specimens**

Type of chitosan specimen	Characteristics				
	Bulk density (g/cm^3)	Swelling/ solubility in water*	pH of suspension/ solution	Swelling/ solubility in TBS*	Heparinized blood clotting time**
Aldrich	0.59	Sediment 0.04 ml	5.0	Sediment 0.03 ml	No clot formation
Aldrich activated	0.26	Dissolved, viscous solution	5.0	Dissolved, viscous solution	60–120 s
Tyanshi	0.33	Sediment 0.05 ml	5.5	Sediment 0.03 ml	No clot formation
Tyanshi activated	0.27–0.43	Dissolved, moderately viscous	5.5	Dissolved, moderately viscous	2.5–3 min
Organica	0.55	Sediment 0.05 ml	5.7	Sediment 0.03 ml	No clot formation
Organica activated	0.38	Dissolved partially, sediment 0.10 ml	5.5	Sediment 0.07ml	3.5–4 min
Home prepared	0.59	Sediment 0.10 ml	5.0	0.06 ml	No clot formation
Home prepared activated	0.17–0.40	Dissolved partially, highly viscous	5.5	Dissolved partially, highly viscous	45–90 s
Celox	0.56	Dissolved partially, highly viscous	4.7	Dissolved partially, highly viscous	60–90 s

Notes. * — 5 mg of chitosan sample were introduced into 0.5 ml of water or TBS;
** — 7 mg of chitosan sample were added to 0.2 ml of heparinized blood.

Table 2. **Results of viscosity measurement of chitosan isolated from crab shells**

Solution	Concentration ($\times 10^{-3}$ g/ml)	Time (s)	η_r	η_{sp}	η_{sp}/C (ml/g)
So	0.00	87.2	1.000	0.000	0
S1	1.00	154.4	1.769	0.769	769
S2	0.78	135.9	1.557	0.557	502
S3	0.60	122.3	1.401	0.401	494
S4	0.47	114.0	1.306	0.306	490
S5	0.33	105.2	1.205	0.205	470

Notes. $\eta_r = T_{solution} / T_{solvent}$; $\eta_{sp} = \eta_r - 1$.

Table 3. **Effect of molecular weight and degree of deacetylation upon hemocoagulating efficacy of activated chitosan specimens**

Type of chitosan	Molecular weight (KDa)	Degree of deacetylation	Clotting time of heparinized blood
Organica	150	98%	3.5–4.0 min
Tyanshi	600	98%	2.0–3.0 min
Chitosan from crab shells	800	95%	45–90 s
Celox	500	95%	45–90 s

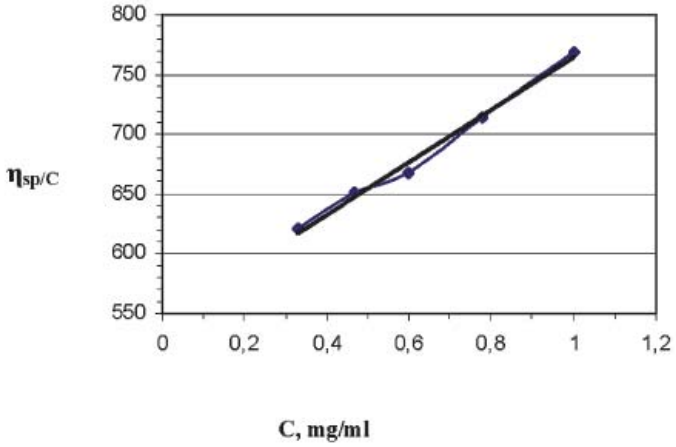

Fig. 2. **Graphical determination of intrinsic viscosity of chitosan solution on basis of relation between η_{sp}/C and concentration of chitosan solution**

exhibits high hemocoagulating activity due to the presence of high molecular weight (more then million Daltons) fractions that do not dissolve completely in 1% acetic acid and need more concentrated acetic acid for complete dissolution. Similar property was observed for Celox, while chitosans of other origin (Tyanshi and Organica) were readily dissolved in 1% acetic acid. Species specificity and mode of preparation also have an influence upon biological activity of product, as can be deduced from comparison of Tyanshi and Celox specimens.

For preparing chitosan with effective antihemorrhagic action, it is necessary to have a set of tests for monitoring process of chitosan purification and controlling quality of final product. Among different tests mentioned in the "Introduction", only the coagulation of bentonite particles [13] may be considered as a convenient screening procedure. In this investigation, we have developed several tests and indices that permit evaluating blood clotting and hemostatic activity of used chitosan preparations. They are easy enough and do not require special reagents and instruments (see below).

Clotting of the heparinized blood is the most important *in vitro* test witnessing a sufficient hemostatic activity of chitosan sample. This indicator of Celox is well known [2], but it was not applied for evaluating blood clotting activity of chitosan samples. We consider that this blood coagulation test at validation of chitosan preparations must not exceed 90 s. If the coagulation time of tested chitosan sample is 5–12 min, that means low hemostatic activity and such chitosan is not acceptable for practical application. The use of Ca-chelating anticoagulants (EDTA, sodium citrate, oxalate) for blood stabilization is not recommended, since chitosan samples themselves may contain Ca cations and, thus, can induce blood coagulation beside chitosan's action.

Interesting data were obtained when coagulation of the defibrinated blood by active chitosan and Celox was compared. It is known that defibrination causes elimination of fibrin and most of pool of blood platelets. Thus, the absoption of blood plasma, drastic increase of viscosity due to swelling of chitosan particles and binding of blood cells on the positively charged chitosan leading to appearance of the pseudoclot might be of primary significance in the mechanism of chitosan-induced blood clotting. Activation of blood platelets [12] may be involved in the coagulation process at later stages and play a role in stabilization of the clot.

Swelling of chitosan powder in water is the next important indicator of chitosan's hemostatic activity. The particles of chitosan's active samples are retained on the surface of water column after introduction into the tube, and after mixing, they swell rapidly and form viscous jelly-like medium that becomes optically homogenous after later dissolution of material. In case of using inactive chitosan samples, the particles rapidly fall down on the bottom of the tube and, thus, do not cause medium viscosity. The swelling of chitosan powder in water correlates closely with its hemocoagulating/ hemostatic activity.

pH of chitosan solution/suspension in water is also important, and it is advisable that it is close to neutral, since an excessive acidity will irritate tissues underlying a wound. Celox provides pH 4.5–4.8, our preparations show pH 5.0–5.4. Although in buffered saline (pH 7.3) swelling of chitosan particles is less than in water, Celox and hemostatic chitosan samples are well swollen and dissolve gradually in the TBS producing highly viscous solution (phosphates must be omitted as they induce precipitation of chitosan). While inactive chitosan samples swell weakly that is in one half of their swelling capability in water.

Bulk density is another useful index of chitosan samples, since it reflects a porosity of material. Lower value of density corresponds to higher porosity and subsequently higher surface of particles available for contact and their higher coagulation efficacy. Besides, equal quantity of lighter powder of chitosan permits covering bigger area of injury than its dense powder. Bulk density does not correlate with blood clotting activity. Some commercial chitosan samples having low bulk density (e. g. 0.33 g/cm^3) show no blood clotting activity, while Celox with bulk density of 0.56 g/cm^3 is a highly active hemostatic agent.

Chitosan obtained by us differs from Celox specifically by its lower bulk density that corresponds to a higher porosity.That is a useful property since it permits covering bigger areas of tissue lesion with less quantity of material (chitosan). Lower bulk density of chitosan samples was achieved by using special conditions of precipitation and dessication. It was found that treatment of chitosan sediment with high concentration of ethanol or aceton leads to an increase in bulk density and, subsequently, to a decrease of porosity of gel particles, probably due to marked dehydration and tighter package of chitosan's polysaccharide chains.

Thus, chitosan preparations obtained in this study could be used as a starting material for production different chitosan-based materials of the biomedical implication, first of all, as hemostatic bandage and wound dressing. Now-a-day, it is proved that Celox used as bandage is more convenient and pfererable in field conditions than Celox used as powder [2]. Chitosan powder can be used for impregnation of gauze since its particles are highly sensitive to moisture and firmly attach to wet cotton fibers and threads.

In general chitosan is highly perspective material especially in biomedical aspects [19–28]. Ukraine has a potential and it is desirable the own industrial production of chitin and chitosan for making them accessible to a broader community of reserchers and inventors.

Method of activation of chitosan specimens to a products with high blood clotting activity was developed. It is based on a proposed set of laboratory tests *in vitro* and *in vivo* for characterization of hemocoagulating/hemostatic effect of the sample. It was shown that high molecular weight chitosans exhibit higher hemocoagulating activity than those with low molecular weight. The first ones are preferable for preparation of hemostatic agents. Biological activity of chitosan is also dependent upon its species specificity and method of preparation.

REFERENCES

1. *Achneck H. E., Bantayehu Sileshi, Jamiolkowski R. N., Albala D. M., Shapiro M. L., Lawson J. H.* A comprehensive review of topical hemostatic agents: efficacy and recommendations for use. *Ann. Surg.* 2010, 251 (2), 217–228.
2. Hemostatic material «Celox». A comphensive manual from SURV24. http://www.surv24.ru/blogs/2014/11/21/. (In Russian).
3. *Kuzin B. A., Babievsky C. K., Prokhorenkova G. K., Kuzin A. B.* Method of obtaining of chitosan. *R. F. Patent Ru 2 067 588*. October 10, 1996. (In Russian).
4. *Kasjanov G. I., Kvasenkov O. I., Nikolayev A. I., Kasjanova E. E.* Method of obtaining of chitosan. *R. F. Patent Ru 2 116 314*. July 27, 1998. (In Russian).
5. *Ivanov A. V., Gartman O. R., Tsvetkova A. V., Poltoratskaya E. B.* Method of obtaining of chitosan. *R. F. Patent Ru 2 117 673*. August 12, 1998. (In Russian).
6. *Bannikov V. V., L'vovich F. I., Frayman D. B.* Method of obtaining of chitosan. *R. F. Patent Ru 2 073 017*. February 10, 1997. (In Russian).
7. *Solodovnik T. V., Unrod V. I.* Method of obtaining of chitosan. *Ukraine Patent UA 33 765*. Fubruary 15, 2001. (In Ukrainian).
8. *Gartman O. R., Vorobyova V. M.* Technology and properties of chitosan from Hammarus crayfish. *Fundamental investigations.* 2013, N 5–6, P. 1188–1192. (In Russian).
9. *Nemtsev S. V., Zuyeva O. U., Hismatullin M. R., Albulin A. I., Varlamov V. P.* Obtaining of chitin and chitosan from honey bees. *Applied biochem microbiol*. 2004, 40 (1), 46–50. (In Russian).
10. *Janvikul W., Uppanan P., Thavornyutikarn B., Krewraing J., Prateepasen R. In vitro* comparative hemostatic studies of chitin, chitosan and their derivatives. *J. Appl. Polym. Sci.* 2006, 102 (1), 445–451. doi: 10.1002/app.24192.
11. *Okamoto Y., Yano R., Miyatake K., Tomohiro I., Shigemasa Y., Minami S.* Effects of chitin and chitosan on blood coagulation. *Carbohydr. Polym.* 2003, 53 (3), 337–342. doi: 10.1016/S0144- 8617(03)00076-6.
12. *Sanandam M., Salunkhe A., Shejale K., Patil D.* Chitosan bandage for faster blood clotting and wound healing. (Determination of the duration of bleeding from pricked finger tip using chitosan soaked bandage). *Int. J. Adv. Biotechnol. Res.* 2013, 4 (1), 47–50.
13. *Hardy C., Johnson E. L., Luksch P.* Hemostatic material. *U. S. Patent US 7 981 872*. July 19, 2011.
14. *Littlejohn L. E., Devlin J. J., Kircher S. S., Lueken R., Melia M. R., Johnson A. S.* Control of hemorrhage in a swine model of penetrating trauma, i.e. groin injury with transection of the femoral vessels. *Acad. Emerg. Med.* 2011, 18 (4), 340–350. doi: 10.111/j.1553-2712.2011.01036.x.
15. http://tiens.in.ua/products/kapsuly-s-hitozanom-tyanshi.
16. *Lazurievsky G. V., Terentieva I. V., Shamshurin A. A.* Practical exercises in chemistry of natural compounds. *Moskva: Vysshaya shkola*. 1966, P. 88–91. (In Russian).
17. *Skriabin K. G., Vikhoreva G. A., Varlamov V. P.* Chitin and Chitosan. Production, properties and usage. *Moskva: Nauka*. 2002, 368 p. (In Russian).
18. *Costa C. N., Teixeira V. G., Delpech M. C., Souza J. V., Costa M. A.* Viscometric studies of chitosan solutions in acetic acid/sodium acetate and acetic acid/sodium chloride. *Carbohydr. polym*. 2015, V. 133, P. 245–250. doi: 10.1016/j.carbpol. 2015.06.094.
19. *Felse P. A., Panda T.* Studies on application of chitin and its derivatives. *Biopr. Engin*. 1999, V. 20, P. 505–512.
20. *Majeti N., V Ravi Kumar.* A review of chitin and chitosan applications. *React. Funct. Polym*. 2000, 45 (1), 1–27.
21. *Hiroshi Sashiwa, Sei-ichi Aiba*. Chemically modified chitin and chitosan as biomaterials. Review article. *Progr. Polym. Sci*. 2004, 29 (9), 887–908.
22. *Rinaudo M*. Chitin and chitosan: properties and applications. *Progr. Polym. Sci*. 2006, 31 (7), 603–632. doi: 10.1016/j. progpolymsci.2006.06.001.
23. *Tikhonov V., Stepnova E., Lopez-Llorka L., Gerasimenko D., Avdienko I., Varlamov V.* Bactericidal and antifungal activities of low molecular weight chitosan derivatives. *Carbohydr. Polym*. 2006, 64 (1), 66–72.
24. *Dasha M., Chiellinia F., Ottenbriteb R. M., Chiellinia E*. Chitosan — a versatile semi-synthetic polymer in biomedical applications. *Progr. Polym. Sci*. 2011, 36 (8), 981–1014.
25. *Jayakumar R. Prabaharan, Sudheesh Kumar P. T., Nair S. V., Tamura H*. Biomaterials based on chitin and chitosan in wound dressing applications. *Biotechnol. Adv*. 2011, 29 (3), 322–337.
26. *Pogorielov M. V., Kornienko V. V., Tkachenko Yu. A., Oleshko O. M.* Materials to treat the skin defects: chitosan derivatives and perspectives for their application (literature review). *J. Clin. Experiment. Med. Res.* 2013, 1 (3), 275–284. (In Ukrainian).
27. *Xiaosong Li, Min Min, Nan Du, Ying Gu, Tomas Hode, Mark Naylor, Dianjuo Chen, Nordquist R. E., Wei R. Chen.* Chitin, chitosan, and glycated chitosan regulate immune responces: the novel adjuvants for cancer vaccine. *Clin. Developm. Immunol.* 2013, Article ID 387023, 8 p. http://dx.doi.org10.1155/2013/387023.
28. *Smith A., Perelman M., Hinchcliffe M*. Chitosan: a promising safe and immune enhancing adjuvant for intranasal vaccines. *Hum. Vaccin. Immunother.* 2014, 10 (3), 797–807.

ОТРИМАННЯ ХІТОЗАНУ З ВИСОКОЮ ГЕМОКОАГУЛЯЦІЙНОЮ АКТИВНІСТЮ ТА ОЦІНКА ЙОГО ГЕМОСТАТИЧНОЇ АКТИВНОСТІ

М. Д. Луцик[1]
Р. О. Білий[1, 2]
М. М. Луцик[2]
Р. С. Стойка[1]

[1]Інститут біології клітини НАН України, Львів
[2]Львівський національний медичний університет ім. Данила Галицького, Україна

E-mail: lootsik@cellbiol.lviv.ua

Метою роботи було вивчення гемостатичної дії різних препаратів хітозану за допомогою розроблених лабораторних тестів для визначення його гемокоагуляційної активності. Із застосуванням тестів *in vitro* зразки хітозану (порошки з розміром частинок менше 0,25 мм) характеризували за такими показниками: час коагуляції гепаринізованої крові, насипна щільність порошку, ступінь набухання частинок порошку у воді та в трис-забуференому фізрозчині, pH 7,4. У разі застосування тестів *in vivo* визначали ефективність зупинки кровотечі з рани у лабораторних мишей або щурів. За допомогою запропонованих тестів виявлено, що зразки хітозану, доступні як комерційні реагенти, харчові добавки або отримані в лабораторії, не виявляють гемокоагуляційної активності порівняно з препаратом Целокс. Розроблено метод активації хітозану й отримання препаратів з гемокоагуляційною активністю на рівні препарату Целокс. Розглядаються властивості хітозану, суттєві для виявлення його гемокоагуляційної дії. Показано, що препарати високомолекулярного хітозану мають вищу гемокоагуляційну активність порівняно з низькомолекулярним і є більш придатними для одержання гемостатичних засобів.

Ключові слова: хітозан, Целокс, гемостатична активність, лабораторні тести *in vitro* та *in vivo*.

ПОЛУЧЕНИЕ ХИТОЗАНА С ВЫСОКОЙ ГЕМОКОАГУЛИРУЮЩЕЙ АКТИВНОСТЬЮ И ОЦЕНКА ЕГО ГЕМОСТАТИЧЕСКОЙ АКТИВНОСТИ

М. Д. Луцик[1]
Р. А. Билый[1, 2]
М. М. Луцик[2]
Р. С. Стойка[1]

[1]Институт биологии клетки НАН Украины, Львов
[2]Львовский национальный медицинский университет им. Данила Галицкого, Украина

E-mail: lootsik@cellbiol.lviv.ua

Целью работы было изучение гемостатического действия различных препаратов хитозана с помощью разработанных лабораторных тестов для определения его кровосвертывающей активности. С использованием тестов *in vitro* образцы хитозана (порошки с размером частиц менее 0,25 мм) характеризовали по следующим показателям: время свертывания гепаринизированной крови, насыпная плотность порошка, степень набухания частиц порошка в воде и в трис-забуференном физрастворе, pH 7,4. С применением тестов *in vivo* определяли эффективность остановки кровотечения из раны у лабораторных мышей или крыс. С помощью предложенных тестов установлено, что образцы хитозана, доступные как коммерческие реагенты, пищевые добавки или полученные в лабораторных условиях, не проявляют гемостатической активности при сравнении с препаратом Целокс. Разработан метод активирования образцов хитозана и получения препаратов с гемостатической активностью на уровне препарата Целокс. Рассматриваются свойства хитозана, существенные для проявления его кровосвертывающего действия. Показано, что препараты высокомолекулярного хитозана проявляют более высокую гемокоагулирующую активность по сравнению с низкомолекулярным и более предпочтительны для получения гемостатических средств.

Ключевые слова: хитозан, Целокс, гемостатическая активность, лабораторные тесты *in vitro* и *in vivo*.

UDC 577.15 (088.8) **doi: 10.15407/biotech8.06.041**

ISOLATION AND PURIFICATION OF LYSOZYME FROM THE HEN EGG WHITE

S. S. Dekina[1, 2]
I. I. Romanovska[1]
A. M. Ovsepyan[1]
M. G. Bodyul[2]
V. A. Toptikov[3]

[1]Bogatsky Physico-Chemical Institute of the National Academy of Sciences of Ukraine, Odesa
[2]Odesa National Polytechnic University, Ukraine
[3]Mechnikov Odesa National University, Ukraine

E-mail: s.dekina@gmail.com

Received 05.10.2015

The aim of the research was the development of the method of lysozyme isolation from hen egg proteins. Lysozyme was isolated by differential heat denaturation of proteins with changing of the medium pH value, followed by neutralization, dialysis and additional purification by gel chromatography on Sephadex G-50. Activity was determined by bacteriolytic method (with *Micrococcus lysodeikticus* 4698 as a substrate). The enzyme purity and molecular mass were determined using SDS-electrophoresis and mass-spectrometry. The method of lysozyme isolation from hen egg proteins with the enzyme yield of 3.2 ± 0.2% and bacteriolytic activity of 22 025 ± 1 500 U/mg is modified. According to electrophoresis data, the isolated enzyme is characterized by high degree of purity (~95–98%) and is comparable with lysozyme of AppliChem company by main physical and chemical characteristics. The obtaining product is stored in a crystalline form at low temperature (–24 °C) for 9 months. The proposed method allows obtaining active and stable lysozyme with high purity from hen egg protein in laboratory conditions for the usage in biotechnology.

Key words: hen egg white, lysozyme.

Lysozyme (EC 3.2.1.17) is an enzyme of hydrolases class, it is also known as muramidase or N-acetylmuramoylhydrolase. Lysozyme is commercially important enzyme, and it is now widely used in biotechnology to extract intracellular bacterial components, in particular in the food industry as an antibacterial additive to increase the shelf life of products, as well as in medicine in the treatment of chronic septic states and purulent processes, burns, frost bytes, conjunctivitis, corneal erosion, stomatitis and other infectious diseases [1–3].

Lysozymes are widely distributed among eukaryotes and prokaryotes and can be classified into three main types: chicken (c-type), goose (g-type) and the type of invertebrates (i-type) [4, 5].

The lysozyme of c-type is most widespread; it occurs in most organisms including viruses, bacteria, plants, insects, reptiles, birds and mammals, and it is contained in a large amount in hen egg proteins.

Lysozyme is one of the first identified proteins (early 1900s). Initially, its isolation was carried out by salting out with ammonium sulfate, but the change in pH and high concentrations of salt affects the activity of the enzyme. The lysozyme isolated using ammonium sulfate was stable in acidic conditions, but only partly soluble in alkaline ones because of crystals formation [6].

In 1984 the ion exchange chromatography with carboxymethyl cellulose as a carrier was used for enzyme isolation; that was not effective in batch processes due to the small particle size and thus due to slow the flow velocity in column [7, 8].

In 2007 a group of Czech scientists offered to use the magnetic macroporous cation-exchange cellulose in isolation procedure [8]. The advantages of this process are one-stage and the purity of the obtained enzyme (more than 96%), and the main drawback is the high cost of the resin used.

Non-chromatographic methods were also used for lysozyme obtaining. Chang et al. suggested β-mercaptoethanol usage along with the other ingredients to lysozyme isolation [9]. However, this method is not widely used because of protein denaturation and β-mercaptoethanol toxicity, which limits

lysozyme usage in the food industry and medicine.

In 2006 Lu et al. suggested ultrafiltration usage to lysozyme isolation. The method allows the enzyme obtaining with purity and yield of 80%; however, it is applicable to lysozyme purification only in laboratory scale [10].

Since numerous methods for lysozyme isolation from hen egg proteins (lysozyme c), in particular chromatography, ultrafiltration, separation with reversed micelles, in two-phase systems, magnetic separation, metal-affinity precipitation, adsorption on plant waste etc., have several disadvantages, so the search, improvement and development of new methods for lysozyme obtaining are urgent tasks of biotechnology.

The aim of the research was to develop the method of lysozyme isolation from hen egg proteins.

Materials and Methods

Fresh hen eggs, *Micrococcus lysodeikticus* 4698 cells (Sigma-Aldrich, USA) and egg protein lysozyme as a standard sample (EC 3.2.1.17) (Mw 14.4 kDa, 20 000 units / mg, AppliChem, Belgium) were used.

Lysozyme activity was determined by bacteriolytic method [11]. The amount of enzyme which reduces the optical density of *Micrococcus lysodeikticus* 4698 cell suspension by 0.001 per 1 min was taken as the unit of its activity. Protein content was monitored by Hartree-Lowry method [12].

The enzyme was isolated according to Mickelson method in our modification [13]: thoroughly washed eggs were wiped with alcohol; protein was separated from the yolk extracting chalazae. The resulting protein was diluted five times in 0.5% solution of sodium chloride, acidified to pH 4.4–4.6 and boiled for 4 min for concomitant proteins coagulation. Then the mixture was neutralized to pH 7.0–7.2 with $NaCO_3$ and the supernatant containing lysozyme was separated by centrifugation (4000 g, 20 min, 4 °C). The supernatant was dialyzed 3 times against 50 volumes of distilled water at 4 °C. At each stage, the protein content and the hydrolytic enzyme activity were controlled. The resulting solution was concentrated by reverse dialysis with dry starch and subjected to gel chromatography on fine-grained Sephadex G-50 eluting with Tris-NaCl buffer (0.05 mol/dm^3 of tris (hydroxymethyl) aminomethane, 0.05 mol/dm^3 of NaCl, pH 8.2). Protein and hydrolytic activity were determined in eluates. The lysozyme containing fraction was subjected to repeated reverse dialysis with starch yielding transparent colorless plate crystals of the enzyme. The product was stored in a sealed package at –24 °C.

The resulting enzyme were analyzed by MALDI (matrix-assisted laser desorption/ionization) methods with mass spectrometer Autoflex II Bruker Daltonics Inc. [14, 15]. The results of mass spectrometric analysis were obtained at the Center for collective use at Chuiko Institute of Surface Chemistry of the National Academy of Sciences of Ukraine. SDS-electrophoresis in 10% polyacrylamide gel was carried out according to Laemmli system [16]. We used a set of molecular weight markers — Amersham, High-Range Rainbow Molekular Weight Markers (14 300–220 000), code RPN756. Markers: 1 — myosin (220 kDa); 2 — phosphorylase b (97 kDa); 3 — BSA (66 kDa); 4 — ovalbumin (45 kDa); 5 — carbonic anhydrase (30 kDa); 6 — trypsin inhibitor (20, 1 kDa); 7 — lysozyme (14.3 kDa).

The main physico-chemical and biochemical properties of the isolated enzyme compared with Sigma-Aldrich lysozyme, namely activity, protein content, pH optimum, thermal optimum, thermal stability, storage conditions were determined in accordance with [17].

Experimental data were subjected to statistical analysis in accordance with [18]. The confidence level of differences was evaluated at $n = 3$.

Results and Discussion

Most of the major pharmaceutical companies (Sigma-Aldrich Pharmaceuticals Inc., Applichem et al.) use hen egg white for lysozyme isolation. This raw material is available and contains about 3.4% of lysozyme which is considered as standard. Besides lysozyme, the main egg white proteins are ovalbumin (54%), ovotransferrin (12%), ovomucoid (11%) and ovomucin (3.5%) [19].

We have proposed a modification of Mickelson method of lysozyme isolation (Fig. 1), lie in:

– carrying out the five times (instead of 30-fold) protein dilution, followed by salting out the nondenaturated proteins with 5% solution of sodium carbonate;

– introduction of three additional stages of dialysis to remove low molecular weight contaminants;

– performing the step of reverse dialysis with dry starch to obtain the enzyme in crystalline form.

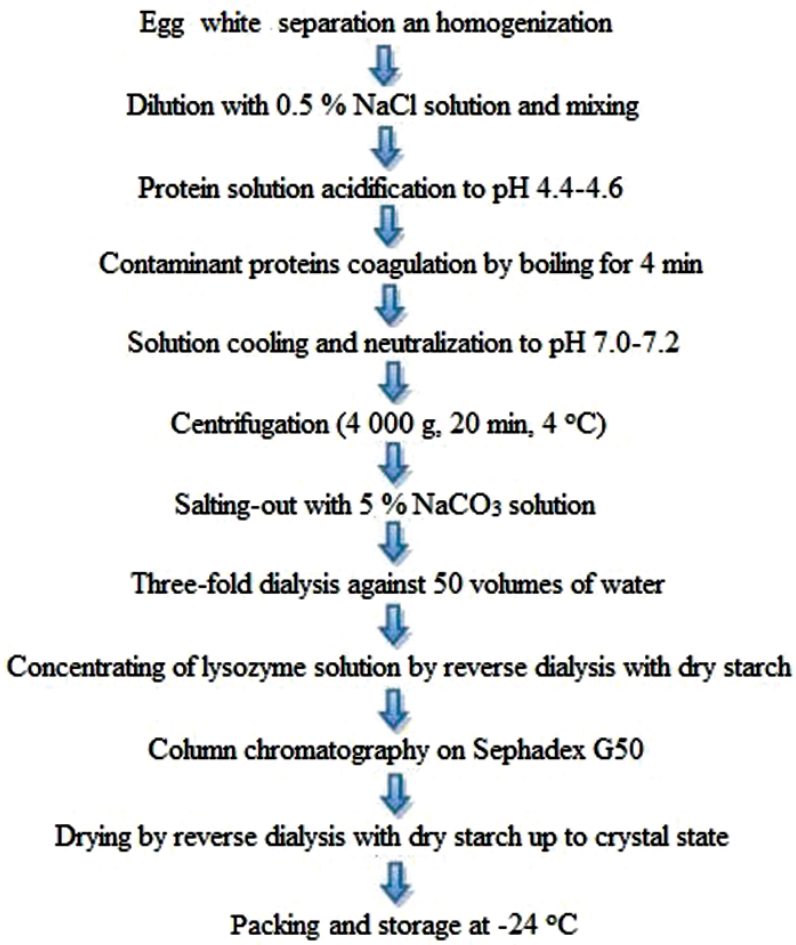

Fig. 1. **Diagram of lysozyme isolation from hen egg white**

The main advantages of the proposed method are ease of highly purified enzyme obtaining in the laboratory, economy, getting the product in crystalline form, high activity, and periods of storage comparable to commercial lysozyme of AppliChem firm.

The main results of the enzyme isolation are shown in Table 1. In the process of lysozyme isolation the volume and total protein content in egg, in the supernatant, after dialysis, and also the activity and yield of obtained lysozyme per 1 cm^3 of protein solution were determined.

It should be noted that after step of threefold dialysis against distilled water, partially purified enzyme containing, beside lysozyme, contaminants of other proteins is selected. Thus, in the mass spectrum (Fig. 2) peaks with a value of about 14 214 m/z (where m is mass of the particle, and z is its charge), 28 206 m/z, 56 682 m/z and 85 023 m/z are observed, this necessitates additional purification step.

The gel chromatography using Sephadex G-50 (Fig. 3) leads to the separation of partially purified lysozyme proteins to achieve a high degree of enzyme purity, as evidenced by the results of mass spectrometry.

MALDI spectrum of isolated enzyme showed the presence a single peak with m/z value of about 14 181 (Fig. 4) corresponding to the value of commercial lysozyme (Fig. 5). It should be noted that in the aqueous solution of a commercial enzyme, the associates formation is observed because it was lyophilized resulting in the formation of stable aggregates that are not fully degradable in solution.

According to the results of SDS-electrophoresis the most intensive band is in the molecular weight range of 12 to 17 kDa, and the purity of isolated lysozyme is 95–98% (Fig. 6).

As a result of isolating and purifying the colorless transparent plate crystals of the enzyme were obtained (Fig. 7).

The study of physical and chemical properties of commercial and isolated lysozyme

Table 1. **Parameters of lysozyme isolation**

Parameters, measurement units	Indices *, $M \pm m$
The amount of egg protein separated from one egg, cm^3	35,0 ± 5,5
Total egg protein, mg	5410,0 ± 380,6
Obtained crystalline lysozyme, mg	170,2 ± 3,0
Protein content in the isolated enzyme,%	100,0%
Hydrolytic activity of the obtained product, U/mg	22025 ± 1500
Yield of product,%	3,15 ± 0,16%

Note. Hereinafter * — $0.02 < P < 0.05$ compared with the control (commercial preparation) at $n = 3$.

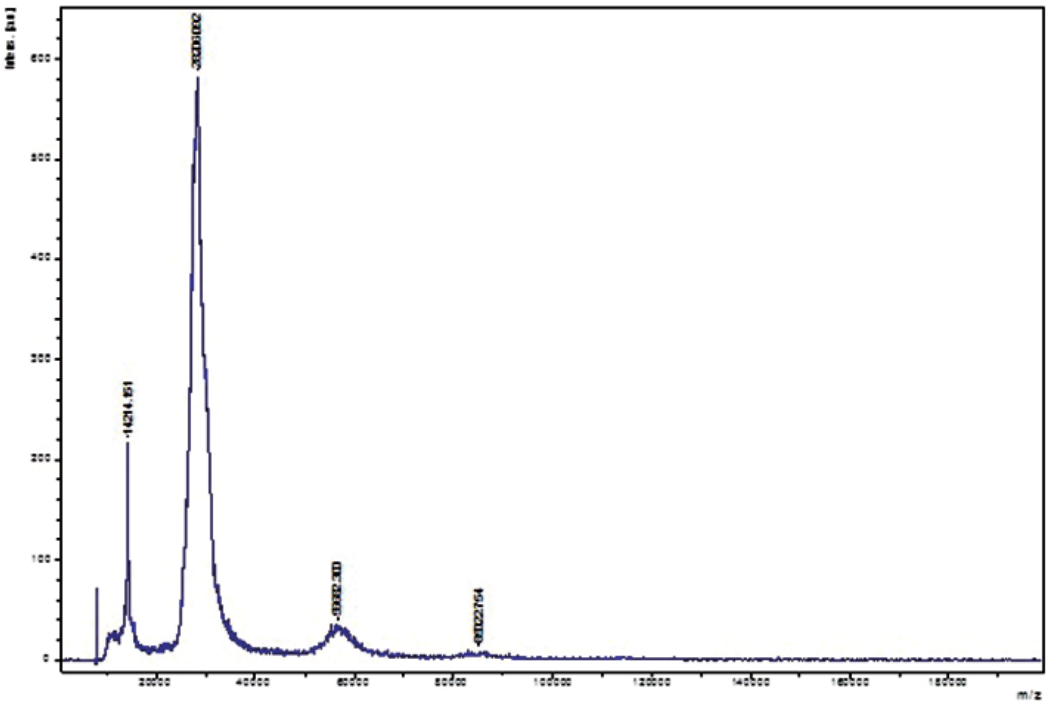

Fig. 2. **Mass spectrum of partially purified lysozyme after threefold dialysis step**
Hereinafter — results of a typical experiment

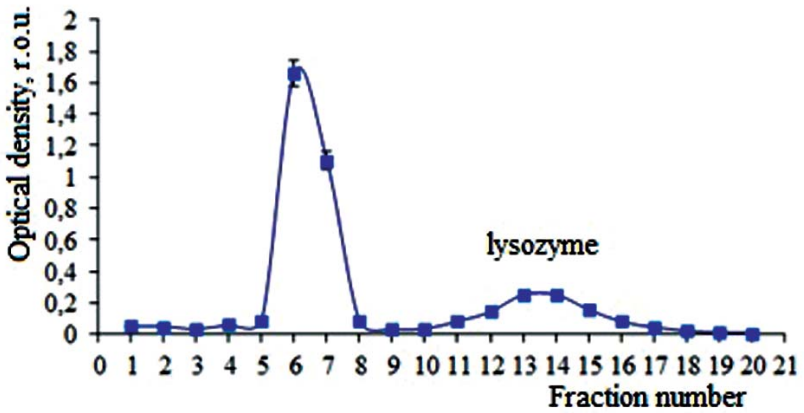

Fig. 3. **Chromatography of partially purified lysozyme on a column with Sephadex G-50 (0.05 mol/dm^3 of tris (hydroxymethyl) aminomethane, 0.05 mol/dm^3 of NaCl, pH 8.2)**

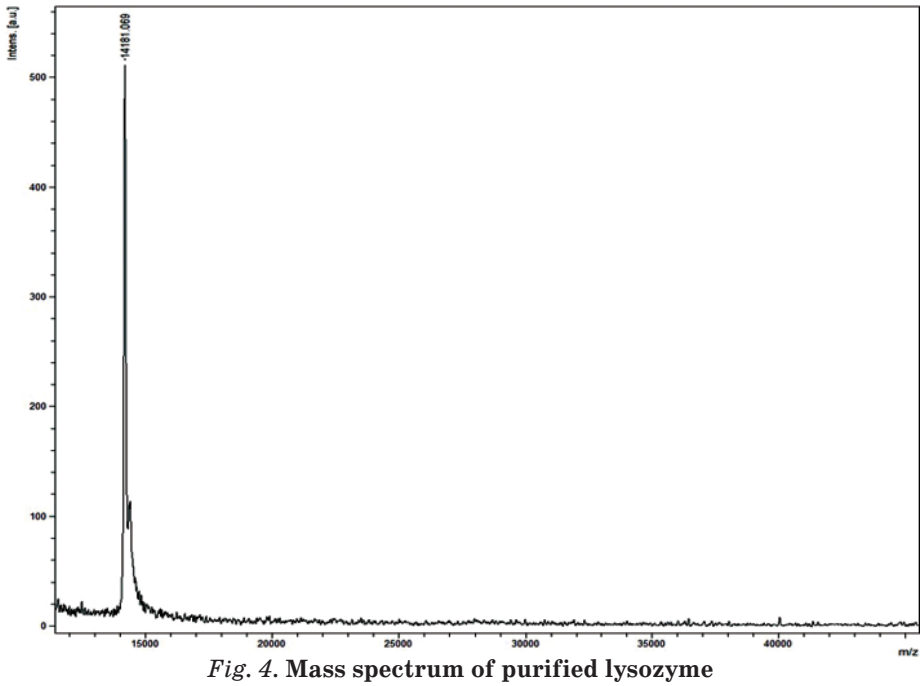

Fig. 4. **Mass spectrum of purified lysozyme**

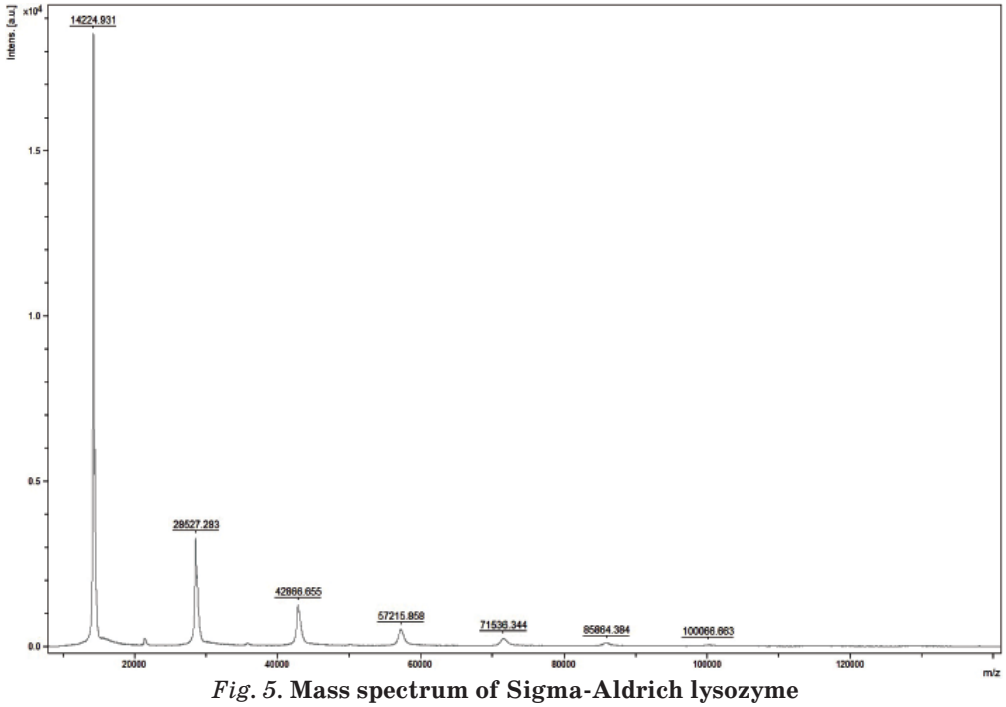

Fig. 5. **Mass spectrum of Sigma-Aldrich lysozyme**

shows the coincidence of bacteriolytic activity pH- and thermal optimum, similar storage periods and specific activity of the isolated enzyme (Table 2).

The resulting product retains the bacteriolytic activity for 9 months at a temperature of −24 °C. Isolated lysozyme shelf life increasing is possible using freeze-drying of the product.

Thus as a result of Michelson method modification [13], the lysozyme from hen egg protein in a yield of 3.2% and activity of 22 025 ± 1 500 U/mg is obtained. The purity of isolated enzyme (~ 95–98%) is confirmed by mass spectrometry and SDS-electrophoresis in a 10% PAAG.

The proposed method is economical and is available for implementation in the laboratory conditions; it allows obtaining a stable crystalline form of the active enzyme from hen egg proteins with a high degree of purity; and it is promising for the usage in biotechnology.

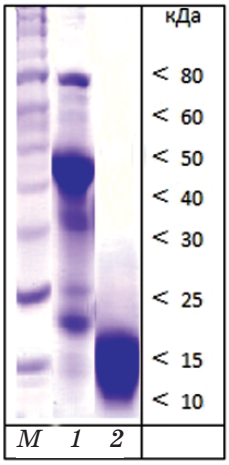

Fig. 6. **SDS-electrophoresis of lysozyme in 10% polyacrylamide gel:**
M — markers (15 µl); *1* — whole egg protein (5 µl in a slot); *2* — purified lysozyme (15 µl in a slot)

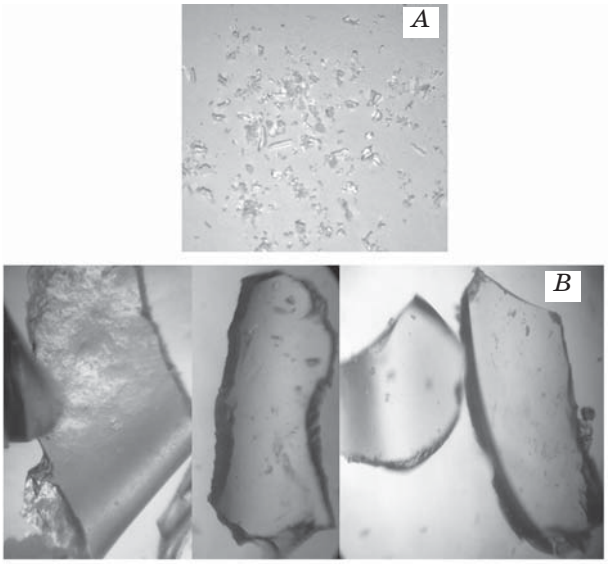

Fig. 7. **Microphotographs of isolated lysozyme:**
A ×8, *B* ×120

Table 2. **Characteristics of the isolated and commercial lysozyme main properties**

Properties	Lysozyme	
	AppliChem	Isolated
Specific activity, unit/mg, $M \pm m$	20 000 ± 5 000	22 025 ± 1 500*
pH-optimum	6.0	6.0
Thermal optimum, °C	55 °C	55 °C
The constants of thermal inactivation at 80 °C, min^{-1}	$5.2 \cdot 10^{-3}$	$4.7 \cdot 10^{-3}$
The shelf life of the enzyme at –24 °C, months	12	9*

REFERENCES

1. *Köse K., Denizli A.* Poly(hydroxyethyl methacrylate) based magnetic nanoparticles for lysozyme purification from chicken egg white. *Artif. Cell Blood Substit. Biotechnol.* 2013, V. 41, P. 13–20. doi: 10.3109/10731199. 2012.696067.
2. *Levitskiy A. P.* Lysozyme instead of antibiotics. *Odesa: KP OGT.* 2005, 74 p. (In Russian).
3. *Leśnierowski G., Cegielska-Radziejewska R.* Potential possibilities of production, modification and practical application of lysozyme. *Acta Sci. Pol. Technol. Aliment.* 2012, 11 (3), 223–230.
4. *Callewaert L., Michiels C. W.* Lysozymes in the animal kingdom. *J. Biosci.* 2010, V. 35, P. 127–160. doi: 10.1007/s12038-010-0015-5.
5. *Alderton G., Ward W. H., Fevold H. L.* Isolation of lysozyme from egg white. *J. Biol. Chem.* 1945, V. 157, P. 43–58.
6. *Abeyrathne N. S., Lee H. Y., Ahn D. U.* Sequential separation of lysozyme and ovalbumin from chicken egg white. *Korean J. Food Sci. An.* 2013, 33 (4), 501–507. doi: 10.5851/kosfa.2013.33.4.501.
7. *Strang R. H.* Purification of egg white lysozyme by ion exchange chromatography. *Biochem. Edu.* 1984, V. 12, P. 57–59.
8. *Safarik I., Sabatkova Z., Tokar O., Safarikova M.* Magnetic cation exchange isolation of lysozyme from native egg white. *Food Technol. Biotechnol.* 2007, 45 (4), 355–359.
9. *Chang H. M., Yan C. C., Chang Y. C.* Rapid separation of lysozyme from chicken egg white by reductants and thermal treatment. *J. Agric. Food Chem.* 2000, V. 48, P. 161–164. doi: 10.1021/jf9902797.
10. *Wana Y., Lub J., Cui Z.* Separation of lysozyme from chicken egg white using ultrafiltration. *Separ. Purif. Tech.* 2006, 48 (2), 133–142. doi:10.1016/j.seppur. 2005.07.003.
11. *Gorin G., Wang S. F., Papapavlou L.* Assay of lysozyme by its lytic action on *M. lysodeikticus* cells. *Anal. Biochem.* 1971, 39 (1), 113–127.
12. *Hartree E. F.* Determination of protein: a modification of the Lowry method, that gives a linear photometric response. *Anal. Biochem.* 1972, 48 (2), 422–427.

13. *Mickelson V. J., Anderson P. P., Kaulins U. Ya.* A method for isolating of lysozyme. *AS 1239147 USSR*. MKI 12 N 9/36. September 18, 1984. (In Russian).
14. *Binkley S. L., Ziegler C. J., Herrick R. S., Roger S.* Specific derivatization of lysozyme in aqueous solution with $Re(CO)_3(H_2O)_3^+$. *Rowlett. Chem. Commun*. 2010, V. 46, P. 1203–1205. doi: 10.1039/B923688K.
15. *Dekina S. S., Romanovska I. I., Gromovoy T. Y.* Influence of polymers on lysozyme molecules association processes. *Biopolymers and cells*. 2011, 27 (6), 442–445. (In Russian).
16. *Duhin S. S., Deryagin B. V.* Electrophoresis. *Moskva: Nauka*. 1976, 332 p. (In Russian).
17. *Dekina S. S., Romanovska I. I., Leonenko I. I., Yegorova A. V.* Mucoadhesive gel with immobilized lysozyme: preparation, properties. *Biotechnol. acta*. 2015, 8 (3), 104–109.
18. *Lapach S. N., Tschubenko A. V., Babich P. N.* Statistical methods in biomedical research using Excel. *Kyiv: Morion*. 2000, 320 p. (In Russian).
19. *Abeyrathne E. D., Lee H. Y., Ahn D. U.* Sequential separation of lysozyme, ovomucin, ovotransferrin, and ovalbumin from egg white. *Poult. Sci*. 2014, 93 (4), 1001–1009. doi: 10.3382/ps.2013-03403.

ВИДІЛЕННЯ Й ОЧИЩЕННЯ ЛІЗОЦИМУ З ПРОТЕЇНІВ КУРЯЧОГО ЯЙЦЯ

С. С. Декіна[1, 2], *І. І. Романовська*[1], *А. М. Овсепян*[1], *М. Г. Бодюл*[2], *В. А. Топтіков*[3]

[1]Фізико-хімічний інститут ім. О. В. Богатського НАН України, Одеса
[2]Одеський національний політехнічний університет, Україна
[3]Одеський національний університет ім. І. І. Мечникова, Україна

E-mail: s.dekina@gmail.com

Метою роботи було розроблення методу виділення лізоциму з протеїну курячого яйця. Лізоцим виділяли методом диференційної денатурації протеїнів шляхом нагрівання зі зміною pH середовища, наступною нейтралізацією, діалізом і доочищенням з використанням гель-хроматографії на Sephadex G-50. Активність визначали бактеріолітичним методом (субстрат — *Micrococcus lysodeikticus* 4698), чистоту ензиму і молекулярну масу — SDS-електрофорезом і мас-спектрометрією. Модифіковано метод виділення лізоциму із протеїну курячого яйця з виходом ензиму 3,2 ± 0,2% і бактеріолітичною активністю 22 025 ± 1 500 од/мг. Згідно з даними електрофорезу виділений ензим характеризується високим ступенем чистоти (~95–98%) і за основними фізико-хімічними характеристиками подібний до лізоциму фірми AppliChem. Одержаний продукт зберігається в кристалічному стані в умовах низьких температур (–24 °C) упродовж 9 міс. Запропонований спосіб виділення дає змогу одержувати в лабораторних умовах стабільний активний лізоцим із протеїну курячого яйця з високим ступенем чистоти для використання у біотехнології.

Ключові слова: протеїн курячих яєць, лізоцим.

ВЫДЕЛЕНИЕ И ОЧИСТКА ЛИЗОЦИМА ИЗ ПРОТЕИНОВ КУРИНОГО ЯЙЦА

С. С. Декина[1, 2], *И. И. Романовская*[1], *А. М. Овсепян*[1], *М. Г. Бодюл*[2], *В. А. Топтиков*[3]

[1]Физико-химический институт им. А. В. Богатского НАН Украины, Одесса
[2]Одесский национальный политехнический университет, Украина
[3]Одесский национальный университет им. И. И. Мечникова, Украина

E-mail: s.dekina@gmail.com

Целью работы была разработка метода выделения лизоцима из протеина куриного яйца. Лизоцим выделяли путем дифференциальной денатурации протеинов нагреванием с изменением pH среды, последующей нейтрализацией, диализом и доочисткой с использованием гель-хроматографии на Sephadex G-50. Активность определяли бактериолитическим методом (субстрат — *Micrococcus lysodeikticus* 4698), чистоту энзима и молекулярную массу — SDS-электрофорезом и масс-спектрометрически. Модифицирован метод выделения лизоцима из протеина куриного яйца с выходом энзима 3,2 ± 0,2% и бактериолитической активностью 22 025 ± 1 500 ед/мг. Согласно данным электрофореза выделенный энзим характеризуется высокой степенью чистоты (~95–98%) и по основным физико-химическим характеристикам сравним с лизоцимом фирмы AppliChem. Полученный продукт хранится в кристаллическом состоянии в условиях низких температур (–24 °C) на протяжении 9 мес. Предложенный способ выделения позволяет получать в лабораторных условиях стабильный активный лизоцим из протеина куриного яйца с высокой степенью чистоты для использования в биотехнологии.

Ключевые слова: протеин куриных яиц, лизоцим.

UDC 612.015:616.153.96:616.894 doi: 10.15407/biotech8.06.048

EFFECT OF CURCUMIN LIPOSOMAL FORM ON ANGIOTENSIN CONVERTING ACTIVITY, CYTOKINES AND COGNITIVE CHARACTERISTICS OF THE RATS WITH ALZHEIMER'S DISEASE MODEL

V. V. Sokolik[1]
S. M. Shulga[2]

[1]State Enterprise "Institute for Neurology, Psychiatry and Narcology of the National Academy of Medical Sciences of Ukraine", Kharkiv
[2]State Enterprise "Institute for Food Biotechnology and Genomics of the National Academy of Sciences of Ukraine", Kyiv

E-mail: Shulga5@i.ua

Recieved 12.10.2015

The purpose of the study was the investigation of curcumin liposome form effect on angiotensin-converting enzyme activity, cytokines and mnestic features of rats with experimental model of Alzheimer's disease. In the animals with intrahippocampal injection of Aβ42_Human, nasal therapy with curcumin liposome form was used. Cytokine concentration and angiotensin converting enzyme activity in brain regions (cerebral cortex and hippocampus) and in blood serum as well as indicators of conditioned avoidance response were registered. It was found that as a result of curcumin therapy the rats with Alzheimer's disease had suppressed cytokine and angiotensin converting enzyme activities and recovered mnestic indices. Nasal therapy with curcumin liposome form gave reduction of angiotensin-converting enzyme activity and anti-cytokine effect in the target regions of the brain (cerebral cortex and hippocampus), which helped the rats mnestic features and memory recovery.

Key words: curcumin, liposomes, β-amyloid peptide, cytokines, angiotensin converting enzyme.

The hitherto used approaches to treatment of dementia and amyloidosis in the case of Alzheimer's disease (AD) concentrated on suppression of β-amyloid peptide (Aβ) production and aggregation or on symptomatic therapy are ineffective [1–5], therefore correction of chronic inflammation provoked by amyloidosis will have positive effect. The mechanism by which Aβ causes the damage and death of neurons is generation of oxygen active forms in the course of own aggregation. At the same time neuron membranes lipids peroxidation is activated and ATPases function is deteriorated. As a result Aβ conduces to depolarization of synaptic membranes, excessive ingress of Ca^{2+} and mitochondrial insufficiency [6–8]. All these processes are concurrent with non-specific inflammatory reaction which is transformed into chronic form and induces synthesis of Aβ protein precursor (AβPP) and its processing pursuant to amyloidogenic scenario [9–11]. It is shown that the inflammatory process in case of AD is characterized by increased peripheral concentrations of anti-inflammatory cytokines and higher TGF-β levels in spinal cord liquid [12]. On the other side, cytokines, similar to Aβ, are mediators of inborn immunity [13, 14]. Their effect comes up through receptor activation of intracellular signals, which results in translocation of nuclear factor (NFκB) towards nucleus and activation of protein synthesis *de novo* [12]. In the end, the existing anti-cytokine therapy poorly represented itself for amyloidosis, except for anti-inflammatory effect of IL-10 [15]; although AD risk is lower in patients who take non-steroid anti-inflammatory preparations [16, 17]. Therefore we assumed that curcumin (CUA) with its anti-inflammatory properties may have essential therapeutic effect against Aβ-induced neurotoxicity and cognitive deficiency.

It is found that natural polyphenol CUA regulates NFκB, AP-1 transcription factors; suppresses expression of cyclooxygenase-2,

lipoxygenase, NO-synthase, matrix metalloproteinase-9, urokinase of plasminogen activator type, TNF, chemokines, cellular adhesion molecules and D1 cycline, inhibits expression of growth factor receptors and activity of JNK, protein tyrosine kinases as well as some other protein serine/threonine kinases [18, 19]. Curcumin also acts as inhibitor of DNA-methyltransferase therefore it is regarded as DNA hypomethylating agent. It establishes equilibrium between histone acetyltransferase and histone acetylase enzymes activity thus modulates expression of certain genes. At last CUA modulates activity of microRNA and their numerous target genes [20, 21]. Above-mentioned CUA effects are exhibited in its antioxidant, anti-inflammatory, anti-tumor and even anti-amyloidogenic properties [22–27]. The problem with curcumin usage, like with the other hydrophilic anions, lies only in the fact that it cannot enter the cell through plasmatic membrane on its own. Therefore it is reasonable to use nanocarriers, in particular, liposomes, as CUA carriers. Liposome advantages are obvious: prepared from natural phospholipids, they compared to other polymeric delivery systems, completely biodegrade in the body and are biocompatible [28].

β-Amyloid peptide aggregation process results in imbalance between its production and degradation. One of the systems, which maintain low Aβ level in tissues, are zinc metalloproteinases [29]. Angiotensin-converting enzyme (ACE) [EC 3.4.15.1], which is involved in regulation of arterial blood pressure, neuropeptide exchange, immune responses of the body is also among them [30]. This enzyme (chiefly its C-domain) separates C-terminal dipeptides from oligopeptides of various structures which have a free carboxyl group. But ACE interacts with Aβ exclusively by N-domain and decomposes Arg5–His6 or Asp7–Ser8 peptide bonds [30]. ACE is an integral membrane glycoprotein of the1st type which is released to blood circulation by zinc metalloesterase at the rate of 2% per hour therefore this enzyme functions both in bonded and dissolved forms. According to the conclusions of *ACE1* gene polymorphism and enzyme inhibitors studies it was found that ACE activity reduction is associated with AD risk and Aβ accumulation [31].

The purpose of the study was investigation of curcumin liposome form effect on ACE activity, cytokines and mnestic features of rats with experimental model of Alzheimer's disease.

Materials and Methods

The study involved 30 male rats of sexually mature age, with 200 to 250 g weight. All the animals were kept under controlled 12-hour light-darkness cycle with standard fodder for rodents and tap water. Experimental protocols were conducted in accordance with the rules of the European Convention for the Protection of Vertebrate Animals used for Experimental and Other Scientific Purposes (Strasbourg, 1986).

The rats were randomly distributed into 5 groups (6 animals in each). The reference group included intact animals; group 1 — the rats 1 month after intrahippocampal injection of Aβ42_Human (experimental model of AD); group 2 — sham operated animals; group 3 — the rats with AD experimental model which received daily nasal therapy with curcumin liposome form for 1 month, and group 4 — animals with AD experimental model which received daily nasal therapy with empty liposomes also for 1 month.

Beforehand, during 20 days conditioned avoidance response was formed in the rats on the basis of unconditioned reflex [32]. Infallible conditioned responses to metronome sound were considered as positive result. Apart from positive response portion (in %), the study registered duration of latent period of conditioned avoidance response in seconds. Animals from all groups were tested in the conditioned avoidance response parameters after AD experimental model formation in them and nasal therapy with curcumin liposome form or empty liposomes.

Aβ42_Human (Human Amyloid β Protein Fragment 1-42, Sigma-Aldrich), dissolved in bidistilled water was aggregated for 24 hours at 37 °C. Aβ42_Human large size rough conglomerates were dispersed by ultrasound and sterilized immediately before injection. The effect of 42_Human β-amyloid peptide was studied 1 month after its single injection in the dose of 15 nM Aβ42_Human to the hippocampus of the rats' brain. Solution volume was 10 mcl per animal. Stereotaxic coordinates of the left hippocampus were determined using the brain map of the rats [33], which corresponds to the distance from the intersection point of sagittal seam and bregma (zero point): distally — 2 mm, laterally — 2 mm and in depth — 3.5 mm. The stereotaxic operations in experimental animals were made under general anesthesia using intra-abdominal injections of thiopental (50 mg/kg of body weight).

To prepare liposomes with curcumin, lecithin/cholesterol was dissolved in the round-bottom flask at ratio 18:1 in 50% ethanol. After the lipid film was formed as a result of the solvent evaporation, 28.85 mM CUA in 5 ml of PBS buffer (10 mM Na_2HPO_4, 1.76 mM KH_2PO_4, 137 mM NaCl, 2.7 mM KCl, pH 7.4) was added and thoroughly mixed for suspension of liposomes with curcumin formation. The suspension of empty liposomes was prepared using the similar protocol but at the final stage PBS buffer without CUA was added. Both liposome suspensions were dissolved with PBS buffer to 0.7 g/l CUA immediately before nasal administration to the rats in the dose of 3.5 μg/animal. Daily nasal therapy of the rats with AD experimental model lasted for 1 month. Administration of liposome form curcumin by nasal method is determined by the fact that, unlike peripheral blood circulation, this is the shortest way to the target regions of the rat neocortex. It is known that after entering the body the dissolved curcumin is nearly unable to overcome the hematoencephalic barrier whereas its liposome form is actively and non-specifically entrapped by the formed elements of blood, which requires big doses of the preparation.

After the processing was finished the animals were decapitated. The assays of cerebral cortex and hippocampus were frozen and stored for further measurements. Blood was collected and centrifuged at 1000 g for 20 min. Serum was collected, frozen and stored. The tissues of hippocampus and fronto-coronal cortex were homogenized in Tris-buffer (50 mM Tris-HCl, 150 mM NaCl, pH 7.5), centrifuged at 14000 g for 5 min producing supernatant.

In the supernatant assays of hippocampus, cerebral cortex and blood serum cytokines were identified using ELISA method in accordance with the protocol Rat ELISA Kit Invitrogen BCM DIAGNOSTICS, USA for interleukine-6 (IL-6), interleukine-10 (IL-10) and tumor necrosis factor α (TNFα). Assay absorption was read out using GBG Stat FAX 2100 (USA) microplate analyzer at 450 nm with wavelength correction at 630 nm. The ELISA data were recalculated into general protein for nerve tissue or expressed in ng/l for blood serum. Concentration of general protein was quantitated by Lowry method [34].

ACE activity was determined by kinetic method [35]. As a substrate the short FAPGG peptide was used, from which by ACE action GG dipeptide was separated and transformed into hippuric acid. Reduction in assay absorption during 10 minute incubation at 37 °C was measured at 340 nm wavelength. Calculation was made using formula:

$$E_{ACE} = (\Delta A_{assay} / \Delta A_{hippuric\ acid\ calibrator}) \cdot E_{calibrator},$$

where ΔA — reduction of absorption during 10 min of incubation at 37 °C; $E_{calibrator} = 82.1$ (protocol B HLMANN ACE colometric kit, Switzerland). ACE activity was expressed in U/l, which corresponds to ACE enzyme quantity, which separates 1 μM hippuric acid at 37 °C per minute per liter for blood serum and per mg of protein for areas of the brain (fronto-coronal cortex and hippocampus).

The obtained results were statistically processed, average values and standard deviations were calculated. Statistical analysis of differences was made using *t*-test. Values at $P < 0.05$ were considered significant.

Results and Discussion

Fig. 1 presents data about increase in ACE activity in hippocampus (direct spot of Aβ42_Human injection) and blood serum and absence of reliable changes in this parameter in cerebral cortex of the rats with AD experimental model. It is first of all due to ACE synthesis induction by one of the substrates local excess, namely Aβ [36]. Nasal therapy with CUA liposome form significantly reduced ACE activity compared to the effect of empty liposomes (Fig. 1) in both investigated brain sections of the rats and in blood serum.

On physiological level, the intrahippocampal injection of Aβ42_Human brought suppression of conditioned avoidance response in the rats of group 1 (Fig. 2). Study of mnestic features and memory showed reduction in the share of positive responses and increase of latent period in these animals compared to the reference group. The share of positive responses in the rats with AD experimental model was not different from that of in the sham operated animals, which is a consequence of intracranial intervention. Curcumin in liposomes was responsible for recovery of mnestic features and memory parameters in the rats with AD experimental model, which was not the case when empty liposomes were used (Fig. 2).

The most substantial cytokine activation was registered in hippocampus of the animals with AD experimental model (Table 1): Concentration of TNFα increased by 26%, IL-6 — by 27% and IL-10 — by 95%, respectively. These data show that Aβ42_

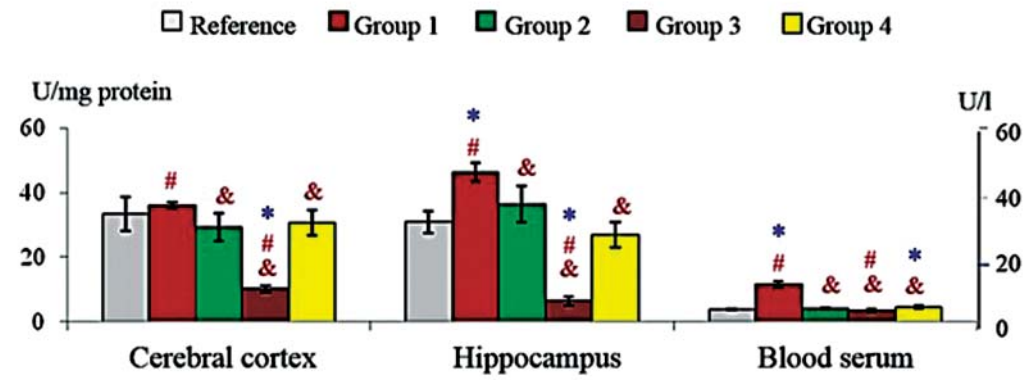

Fig. 1. **Effect of 42_Human β-amyloid peptide and curcumin liposome form on angiotensin-converting activity in brain sections (cerebral cortex and hippocampus) and blood serum of the rats**

Hereinafter: * — $P \le 0.05$ compared to control (intact animals, $n = 6$); # — $P \le 0.05$ when comparing the groups 1 (model of Alzheimer's disease, $n = 6$); 2 (sham operated animals, $n = 6$); 3 (nasal therapy of the AD model animals with liposome curcumin, $n = 6$); 4 (nasal therapy of AD model animals with empty liposomes, $n = 6$), respectively; & — $P \le 0.05$ compared to the group 1 (Alzheimer's disease model, $n = 6$).

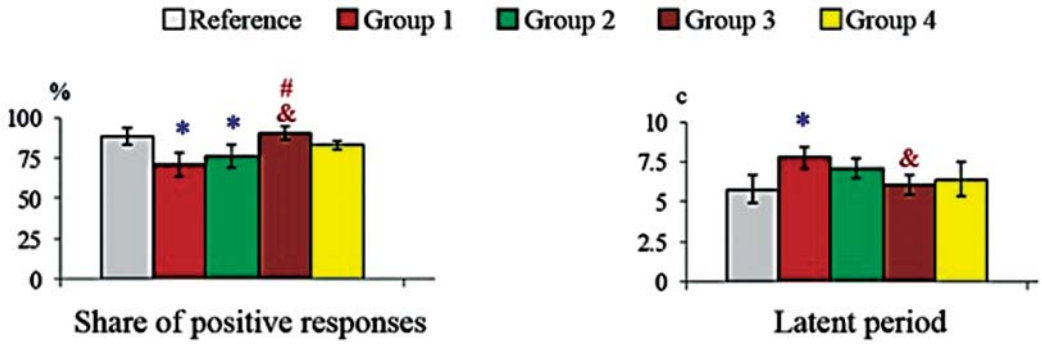

Fig. 2. **Dynamics of mnestic ability and memory parameters (share of positive responses and latent period) in effect of 42_Human β-amyloid peptide and curcumin liposome form therapy in the rats**

Human in hippocampus of the experimental rats causes neuroinflammation specifically and mainly in the spot of injection. But in the brain cerebral cortex the activation of neuroinflammation was also shown, although to lower extent (Table 2). Namely, only the IL-6 level reliably increased by nearly 54%. Specificity of Aβ42_Human inflammatory effect in the brain of the rats was also proved by difference in the levels of the studied cytokines between groups 1 and 2 (Tables 1 and 2).

Effect of liposome curcumin on cytokine levels in hippocampus of the animals was marked by essential suppression of inflammation (Table 1): TNFα level decreased by 56%, IL-6 — by 39% and IL-10 — by 52%, respectively. But not a single cytokine normalized its concentration, unlike in the case with the effect of empty liposomes (Table 1). Effect of CUA as component of liposomes in the cerebral cortex of the rats with AD gave similar suppression of cytokine response (Table 2): TNFα level decreased by 71%, IL-6 — by 67% and IL-10 — by 41%, respectively. The obtained results are in agreement with our previous data for curcumin water solution only for the brain cerebral cortex of the animals with intrahippocampal injection of Aβ42_Human [37]. In hippocampus of the rats with AD model the CUA liposome form showed more intensive suppression of cytokine chain of neuroinflammation compared to its water solution.

The level of peripheral cytokines (TNFα, IL-6 and IL-10 in blood serum) did not reflect neither specific neuroinflammatory effect of 42_Human β-amyloid peptide in the brain of the rats, nor suppression effect of liposome CUA (Table 3). 20–50% rise in TNFα concentration, 54–67% decrease in IL-10 concentration and absence of changes in IL-6 content in blood serum of the rats of all the

Table 1. **Effect of curcumin liposome form on TNFα, IL-6 and IL-10 in hippocampus of the rats with the model of Alzheimer's disease**

Cytokine	Reference $n = 6$	Group 1 $n = 6$	Group 2 $n = 6$	Group 3 $n = 6$	Group 4 $n = 6$
TNFα	50.7±2.1	63.8±3.5*#	46.8±1.9&	28.3±1.7*#&	46.3±2.3&
IL-6	57.3±8.3	72.8±6.8#	98.3±6.8*&	44.7±5.9*&	58.5±8.2
IL-10	130.4±11.0	254.3±16.7*#	152.8±12.9&	122.4±13.4*#&	151.0±12.4&

Note. Hereinafter: the results are represented as $M \pm m$, ng/g of protein.

Table 2. **Effect of curcumin liposome form on TNFα, IL-6 and IL-10 in cerebral cerebral cortex of the rats with the model of Alzheimer's disease**

Cytokine	Reference $n = 6$	Group 1 $n = 6$	Group 2 $n = 6$	Group 3 $n = 6$	Group 4 $n = 6$
TNFα	50.8±2.5	46.2±2.4#	40.6±2.9*&	13.2±0.9*#&	47.1±2.8
IL-6	52.5±4.2	80.8±7.4*	68.5±5.8	26.8±2.0*#&	49.3±3.9&
IL-10	179.5±13.0	150.8±10.6#	206.4±24.2&	89.4±7.6*#&	177.0±12.8&

Table 3. **Effect of curcumin liposome form on TNFα, IL-6 and IL-10 in blood serum of the rats with the model of Alzheimer's disease**

Cytokine	Reference $n = 6$	Group 1 $n = 6$	Group 2 $n = 6$	Group 3 $n = 6$	Group 4 $n = 6$
TNFα	7.9±0.8	9.5±0.6 *	10.7±1.0 *	10.4±0.4 *#	11.9±0.9 *&
IL-6	48.3±10.4	37.5±6.9	53.2±11.3	44.8±7.7	47.0±14.1
IL-10	19.5±2.4	9.8±1.2 *#	6.5±0.9 *	7.0±1.8 *#&	9.3±2.5 *

experimental groups compared to the reference were marked.

The obtained results showed activation of cytokine system in the brain of the rats with AD experimental model (Tables 1, 2). These data are in agreement with other studies on activation of neuroinflammation by Aβ aggregates [38–41]. Aβ deposits are responsible for activation of microglia [38]. Aβ conduces to higher inflammatory response to NFκB stimulation, the nuclear factor which is involved in regulation of ERK (extracellular signal-regulated kinases) and MAPK (mitogen-activated protein kinases) routes which lead to cytokines and chemokines production [39]. Modification of the inflammatory condition of microglia/macrophages plays prominent role in the course of amyloidosis [40].

Nasal therapy of AD model rats with curcumin liposome form was responsible for suppression of ACE activity and cytokine chain of neuroinflammation. Revealed anti-inflammatory activity of CUA resulted in recovery of memory parameters and mnestic functions in the animals. Therefore, the previous assumption that its liposome form may be an efficient anti-inflammatory factor in the effect of exogenous β-amyloid peptide was confirmed by experimental data. This natural polyphenol prevents activation of NFκB transcription nuclear factor suppressing phosphorylation and degradation of IκBα (NFκB inhibitor). Since curcumin effect lies in inhibition of IB kinase (IKK) activation, needed for NFκB activation [42–44], it is just this fact that explains the revealed anti-cytokine effect of curcumin in the experimental animals. The mechanism of curcumin effect on ACE activity is substantiated by the proved suppressor effect of this polyphenol on expression of enzyme gene [45]. Above-mentioned data show high anti-cytokine potential of especially the liposome form of curcumin.

REFERENCES

1. *Minati L., Edginton T., Bruzzone M. G., Giaccone G.* Current concepts in Alzheimer's disease: a multidisciplinary review. *Am. J. Alzheim. Dis. & Other Dement*. 2009, V. 24, P. 95–121.
2. *Birks J.* Cholinesterase inhibitors for Alzheimer's disease. *Cochrane Database Syst. Rev.* 2006, CD005593.
3. *Gotti C., Riganti L., Vailati S., Clementi F.* Brain neuronal nicotinic receptors as new targets for drug discovery. *Curr. Pharm. Des.* 2006, V. 12, P. 407–428.
4. *Palmer G. C.* Neuroprotection by NMDA receptor antagonists in a variety of neuropathologies. *Curr. Drug. Targets.* 2001, V. 2, P. 241–271.
5. *Ostrowski S. M., Wilkinson B. L., Golde T. E., Landreth G.* Statins reduce amyloid-beta production through inhibitionof protein isoprenylation. *J. Biol. Chem*. 2007, V. 282, P. 26832–26844.
6. *Tamburri A., Dudilot A., Licea S., Bourgeois C., Boehm J.* NMDA-receptor activation but not ion flux is required for amyloid-beta induced synaptic depression. *PLoS One*. 2013, V. 8, P. e65350.
7. *Takamura A., SatoY., Watabe D., Okamoto Y., Nakata T., Kawarabayashi T., Oddo S., Laferla F.M., Shoji M., Matsubara E.* Sortilin is required for toxic action of Aβ oligomers (AβOs): extracellular AβOs trigger apoptosis, and intraneuronal AβOs impair degradation path ways. *Life Sci.* 2012, V. 91, P. 1177–1186.
8. *Slack B. E., Wurtman R. J.* Regulation of synthesis and metbolism of the amyloid precursor protein by extracellular signals. *Res. Progr. Alzheimer's Dis. Dement*. 2007, V. 2, P. 1–25.
9. *Mattson M. P.* Pathways towards and away from Alzheimer's disease. *Nature*. 2004, V. 430, P. 631–639.
10. *Mehan S., Arora R., Sehgal V., Sharma D., Sharma G.* Inflammatory diseases — immunopathology, clinical and pharmacological bases; in Khatami M (ed): *Dementia: A Complete Literature Review on Various Mechanisms Involved in Pathogenesis and an Intracerebroventricular Streptozotocin-Induced Alzheimer's Disease. Rijeka, InTech*. 2012, P. 3–19.
11. *Swardfager W., Lanct t K., Rothenburg L., Wong A., Cappell J., Herrmann N.* A meta-analysis of cytokines in Alzheimer's disease. *Biol. Psychiatry*. 2010, V. 68, P. 930–941.
12. *Hunter C.A., Timans J., Pisacane P., Menon S., Cai G., Walker W., Aste-Amezaga M., Chizzonite R., Bazan J. F., Kastelein R. A.* Comparison of the effects of interleukin-1α, interleukin-1β and interferon-γ inducing factor on the production of interferon-γ by natural killer. *Eur. J. Immunol*. 1997, V. 27, P. 2787–2792.
13. *Dinarello C. A.* Proinflammatory cytokines. Chest. 2000, V. 118, P. 503–508.
14. *Soscia S. J., Kirby J. E., Washicosky K. J., Tucker S. M., Ingelsson M., Hyman B., Burton M. A., Goldstein L. E., Duong S., Tanzi R. E., Moir R. D. Bush, Ashley I.* The Alzheimer's disease-associated amyloid β-protein is an antimicrobial peptide. *PLoS One*. 2010, V. 5, P. e9505.
15. *Huber T. S., Gaines G. S., Welborn M. B., Roseberg J. J., Seeger J. M., Moldawer L. L.* Anticytokine therapies for acute inflammation and the systemic inflammatory response syndrome: IL-10 and ischemia/reperfusion injury as a new paradigm. *Shock*. 2000, V. 13, P. 425–434.
16. *Akiyama H., Barger S., Barnum S., Bradt B., Bauer J., Cole G. M., Cooper N. E., Eikelenboom P., Emmerling M., Fiebich B. L., Finch C. E., Frautschy S., Griffin W. S., Hampel H., Hull M., Landreth G., Lue L., Mrak R., Mackenzie I. R., Mcgeer P. L., O'Banion M. K., Pachter J., Pasinetti G., Plata-Salaman C., Rogers J., Rydel R., Shen Y., Streit W., Strohmeyer R., Tooyoma I., Van Muiswinkel F. L., Veerhuis R., Walker D., Webster S., Wegrzyniak B., Wenk G., Wyss-Coray T.* Inflammation and Alzheimer's disease. *Neurobiol Aging*. 2000, V. 21, P. 383–421.
17. *Stewart W. F., Kawas C., Corrada M., Metter E. J.* Risk of Alzheimer's disease and duration of NSAID use. *Neurology*. 1997, V. 48, P. 626 –631.
18. *Shezad A., Lee Y. S.* Molecular mechanisms of curcumin action: signal transduction. *Biofactors*. 2013, V. 39, P. 27–36.
19. *Bharti A. C., Takada Y., Aggarwal B. B.* Curcumin (diferuloylmethane) inhibits receptor activator of NF-κB ligand-induced NF-κB activation in osteoclast precursors and suppresses osteoclastogenesis. *J. Immunol.* 2004, V. 172, P. 5940–5947.
20. *Teiten M. N., Dicato M., Diederich V.* Curcumin as a regulator of epigenetic events. Mol. Nutr. *Food Res.* 2013, V. 57, P. 1619–1629.
21. *Lee W. H., Loo C. Y., Bedawy M., Luk F., Mason R. S., Rohanizadeh R.* Curcumin and its derivatives: their application in neuropharmacology and neuroscience in the 21st century. *Curr. Neuropharmacol*. 2013, V. 11, P. 338–378.
22. *Jackson J. K., Higo T., Hunter W. L., Burt H. M.* The antioxidants curcumin and quercetin inhibit inflammatory processes associated with arthritis. *Inflamm. Res.* 2006, 55 (4), 168–175.
23. *Banerjee M., Tripathi L. M., Srivastava V. M., Puri A., Shukla R.* Modulation of inflammatory mediators by ibuprofen

and curcumin treatment during chronic inflammation in rat. *Immunopharmac. Immunotoxic*. 2003, 25 (2), 213–224.
24. *Kunnumakkara A. B., Anand P., Aggarwal B. B.* Curcumin inhibits proliferation, invasion, angiogenesis and metastasis of different cancers through interaction with multiple cell signaling proteins. *Cancer Lett*. 2008, 269 (2), 199–225.
25. *Ono K., Hasegawa K., Naiki H., Yamada M.* Curcumin has potent anti-amyloidogenic effects for Alzheimer's beta-amyloid fibrils in vitro. *J. Neurosci. Res*. 2004, 75 (6), 742–750.
26. *Yang F., Lim G. P., Begum A. N., Ubeda O. J., Simmons M. R., Ambeqaokar S. S., Chen P. P., Kayed R., Glabe C. G., Frautschy S. A., Cole G. M.* Curcumin inhibits formation of amyloid beta oligomers and fibrils, binds plaques, and reduces amyloid in vivo. *J. Biol. Chem*. 2005, 280 (7), 5892–5901.
27. *Zhang L., Fiala M., Cashman J., Sayre J., Espinosa A., Mahanian M., Zaghi J., Badmaev V., Graves M.C., Bernard G., Rosenthal M.* Curcuminoids enhance amyloid-beta uptake by macrophages of Alzheimer's disease patients. *J. Alzheimers Dis*. 2006, 10 (1), 1–7.
28. *Shulga S. M*. Obtaining and characteristic of curcumin liposomal form. *Biotechnologia Acta*. 2014, 7 (5), 55–61.
29. *Miners J. S., Baig S., Palmer J., Palmer L. E., Kehoe P. G., Love S.* A β-degrading enzymes in Alzheimer's disease. *Brain Pathol*. 2008, V. 18, P. 240–252.
30. *Hu J., Igarashi A., Kamata M., Nakagawa H.* Angiotensin-converting enzyme degrades Alzheimer amyloid beta-peptide (Abeta); retards Abeta aggregation, deposition, fibril formation; and inhibits cytotoxicity. *J. Biol. Chem*. 2001, 276 (5), 47863–47868.
31. *Hemming M. L., Selkoe D. J.* Amyloid β-protein is degraded by cellular angiotensin-converting enzyme (ACE) and elevated by an ACE inhibitor. *J. Biol. Chem*. 2005, 280 (45), 37644–37650.
32. *Vorobjova T. M*. Role of limbic and reticular systems in selfstimulation. *The federation of American societies for experimental biology*. 1969, V. 70, P. 95–101.
33. *Bures J., Petran M., Zachar J.* Electrophysiological methods in biological research. *Ed. 2 Publishing House*. 1960, 516 p.
34. *Lowry O. H., Rosebrough N. J., Farr A. L., Randall R. J.* Protein measurement with Folin phenol reagent. *J. Biol. Chem*. 1951, V. 193, P. 265–275.
35. *Ronca-Testoni S.* Direct spectrophotometric assay for angiotensin-converting enzyme. *Clin. Chem*. 1983, V. 29, P. 1093–1096.
36. *Arregui A., Perry E. K., Rossor M., Tomlinson B. E.* Angiotensin converting enzyme in Alzheimer's disease increased activity in caudate nucleus and cortical areas. *J. Neurochem*. 1982, V. 38, P. 1490–1492.
37. *Sokolik V. V., Shulga S. M.* Curcumin influence on the background of intrahippocampus administration of β-amyloid peptide in rats. *Biotechnol. acta*. 2015, 8 (3), 78–88.
38. *Sadigh-Eteghad S., Sabermarouf B., Majdi A., Talebi M., Farhoudi M., Mahmoudi J.* Amyloid-Beta: A Crucial Factor in Alzheimer's Disease. *Med. Princ. Pract*. 2015, V. 24, P. 1–10.
39. *Ridolfi E., Barone C., Scarpini E., Galimberti D.* The role of the innate immune system in Alzheimer's disease and frontotemporal lobar degeneration: an eye on microglia. *Clin. Dev. Immunol*. 2013, P. 939786.
40. *Boutajangout A., Wisniewski T.* The innate immune system in Alzheimer's disease. *Int. J. Cell. Biol*. 2013, P. 576383.
41. *Smith J.A., Das A., Ray S.K., Banik N.L.* Role of pro-inflammatory cytokines released from microglia in neurodegenerative diseases. *Brain Res. Bull*. 2012, V. 87, P. 10–20.
42. *Aggarwal B. B., Gupta S. C., Sung B.* Curcumin: an orally bioavailable blocker of TNF and other pro-inflammatory biomarkers. *Br. J. Pharmacol*. 2013, V. 169, P. 1672–1692.
43. *Jobin C. C., Bradham A., Russo M. P., Juma B., Narula A. S., Brenner D. A., Sartor R. B.* Curcumin blocks cytokine-mediated NF-κB activation andproinflammatory gene expression by inhibiting inhibitory factor IB kinase activity. *J. Immunol*. 1999, V. 163, P. 3474.
44. *Pan M. H., Lin-Shiau S. Y., Lin J. K.* Comparative studies on thesuppression of nitric oxide synthase by curcumin and its hydrogenated metabolites through down-regulation of IB kinase and NF-κB activation in macrophages. *Biochem. Pharmacol*. 2000, V. 60, P. 1665.
45. *Fazal Y., Fatima S. N., Shahid S. M., Mahboob T.* Effects of curcumin on angiotensin-converting enzyme gene expression, oxidative stress and anti-oxidant status in thioacetamide-induced hepatotoxicity. *J. Renin Angiotensin Aldosterone Syst*. 2014, Epub 2014, pii: 1470320314545777.

ВПЛИВ ЛІПОСОМНОЇ ФОРМИ КУРКУМІНУ НА АНГІОТЕНЗИН-ПЕРЕТВОРЮВАЛЬНУ АКТИВНІСТЬ, ЦИТОКІНИ І КОГНІТИВНІ ВЛАСТИВОСТІ ЩУРІВ З МОДЕЛЛЮ ХВОРОБИ АЛЬЦГЕЙМЕРА

В. В. Соколік[1]
С. М. Шульга[2]

[1]ДУ «Інститут неврології, психіатрії і наркології НАМН України», Харків
[2]ДУ «Інститут харчової біотехнології і геноміки НАН України», Київ

E-mail: Shulga5@i.ua

Метою дослідження було вивчення впливу ліпосомної форми куркуміну на активність ангіотензинперетворювального ензиму, цитокіни і мнестичні властивості щурів з експериментальною моделлю хвороби Альцгеймера. У тварин з інтрагіпокампальним уведенням Aβ42_Human застосовували назальну терапію ліпосомною формою куркуміну. Реєстрували концентрацію цитокінів і активність ангіотензинперетворювального ензиму у відділах головного мозку (лобно-фронтальна кора і гіпокамп) та сироватці крові, а також показники умовно-рефлекторної реакції уникнення. У результаті терапії куркуміном встановлено пригнічення активності цитокінів, ангіотензинперетворювального ензиму та відновлення мнестичних показників у щурів із хворобою Альцгеймера. Назальна терапія ліпосомної форми куркуміну мала наслідком зменшення активності ангіотензинперетворювального ензиму та антицитокінового ефекту в цільових відділах головного мозку (лобно-фронтальна кора і гіпокамп), що сприяло відновленню мнестичних властивостей і пам'яті щурів.

Ключові слова: куркумін, ліпосоми, β-амілоїдний пептид, цитокіни, ангіотензинперетворювальний ензим.

ВЛИЯНИЕ ЛИПОСОМНОЙ ФОРМЫ КУРКУМИНА НА АНГИОТЕНЗИН-ПРЕВРАЩАЮЩУЮ АКТИВНОСТЬ, ЦИТОКИНЫ И КОГНТИТИВНЫЕ СВОЙСТВА КРЫС С МОДЕЛЬЮ БОЛЕЗНИ АЛЬЦГЕЙМЕРА

В. В. Соколик[1]
С.М. Шульга[2]

[1]ГУ «Институт неврологии, психиатрии и наркологии НАМН Украины», Харьков
[2]ГУ «Институт пищевой биотехнологии и геномики НАН Украины», Киев

E-mail: Shulga5@i.ua

Целью исследования было изучение влияния липосомной формы куркумина на активность ангиотензин-превращающего энзима, цитокины и мнестические свойства крыс с экспериментальной моделью болезни Альцгеймера. У животных с интрагипокампальным введением Aβ42_Human применяли назальную терапию липосомной формой куркумина. Регистрировали концентрацию цитокинов и активность ангиотензинпревращающего энзима в отделах головного мозга (лобно-фронтальная кора и гиппокамп) и сыворотке крови, а также показатели условно-рефлекторной реакции избегания. В результате терапии куркумином установлено угнетение активности цитокинов, ангиотензинпревращающего энзима и восстановление мнестических показателей у крыс с болезнью Альцгеймера. Назальная терапия липосомной формой куркумина обусловила уменьшение активности ангиотензинпревращающего энзима и антицитокинового эффекта в целевых отделах головного мозга (лобно-фронтальная кора и гиппокамп), что способствовало восстановлению мнестических свойств и памяти крыс.

Ключевые слова: куркумин, липосомы, β-амилоидный пептид, цитокины, ангиотензинпревращающий энзим.

УДК 579:662.7 doi: 10.15407/biotech8.06.056

PROPERTIES OF CHEMOLITHOTROPHIC BACTERIA NEW STRAINS ISOLATED FROM INDUSTRIAL SUBSTRATES

I. A. Blayda[1]
T. V. Vasyleva[1]
V. I. Baranov[2]
K. I. Semenov[1]
L. I. Slysarenko[1]
I. M. Barba[1]

[1]Mechnykov Odesa National University, Ukraine

[2]Franko Lviv National University, Ukraine

E-mail: iblayda@ukr.net

Received 23.07.2015

The purpose of the research was determination of strains *Acidithiobacillus ferrooxidans* MFLv37 and *Acidithiobacillus ferrooxidans* MFLad27, isolated from aboriginal consortium of coal beneficiation dumps and fly ash from coal combustion, resistance to heavy metals, forming part of these waste, as well as adaption ability of the strains to new substrates. New strains increased resistance to heavy metal ions as compared to *A. ferrooxidans* standard and collection strains is found; minimal inhibitory concentrations of heavy and toxic metals are determined; a number of metals that have negative impact on growth of isolated cultures are identified. It is shown that the minimal metals concentrations, at which strains growth still happens, are several times higher than their concentrations in technogenic waste. It has been found that isolated strains differed in their ability to adapt, as well as in growth rate and substrates oxidation. This is due to the specific conditions of microbiocenoses formation in making and further storage of rock dumps and fly ash, whereof the appropriate strains are isolated. The investigations indicate the necessity in directional selection of strains that are resistant to the toxic compounds and are able to oxidize various mineral substrates, as well as in their adaptation to new substrates for the extraction of heavy metals.

Key words: fly ash, rock dumps, aboriginal bacterial community, acidophilic chemolithotrophic bacteria, strains, leaching activity, ions of heavy metals.

The members of the genera *Acidithiobacillus* and *Sulfobacillus* have the greatest activity regarding leaching of metals from raw natural ores and technogenic substrates [1–3]. In previous investigations it was found that the most active group of microorganisms in the aboriginal consortium of coal beneficiation dumps and fly ash from coal combustion substrates is the group of acidophilic chemolithotrophic microorganisms as small mesophilic and most numerous moderately thermophilic ones — the members of the genera *Acidithiobacillus* and *Sulfobacillus* [4, 5]. The study of the properties of the most active pure cultures of the microorganisms isolated from the substrates aboriginal association has allowed to classify them as the representatives of *Acidithiobacillus ferrooxidans* and assign them the strain numbers MFLv37 and MFLad27 in a view of their habitats — Lviv-Volyn Coal Basin coal beneficiation dumps and fly ash from the coal combustion at Ladyzhynskaya thermal power station, respectively.

Acidithiobacillus ferrooxidans group is the most studied among acidophilic chemolithotrophic bacteria receiving energy from the oxidation of ferrous iron, elemental sulfur and its reduced compounds and sulfide minerals; it has a high level of resistance to heavy metals. Resistance is an important property of microorganisms of different taxonomic groups, thanks to which resistant forms of microorganisms in the environment with a high content of heavy metals appear. So, in [6] it is shown that the differences between the strains in substrate oxidation activity are caused by environment and conditions of microbiocenosis formation whereof the strains were isolated. *A. ferrooxidans* strain, isolated from a complex mineralogical composition substrate, is characterized by a higher growth

rate and oxidation degree of various pyrite types than the strain *A. ferrooxidans* from poorer composition ore dump. In addition, in environmental objects with a high content of heavy metals, steadier to heavy metals (resistant) forms of microorganisms of different taxonomic groups appear and formed. There are data about the study of *A. ferrooxidans* strains, isolated from the natural environment, adaptation to various sulfide ores [7–9]. However, the issue of technogenic mineral raw materials usage for energy obtaining by representatives of *A. ferrooxidans* has been insufficiently studied. Therefore, the study of properties of new resistant highly active strains capable of adaptation and growth on the environmental objects with a high content of heavy metals is an urgent task of biotechnology.

The objective was to study the properties of the new isolated from technogenic waste strains of chemolithotrophic bacteria *Acidithiobacillus ferrooxidans* MFLv37 and MFLad27 — as resistance to heavy metals, and the ability to adapt to new substrates compared with highly active collection (*A. ferrooxidans* VKM468) and standard (*A. ferrooxidans* ATCC23270) strains.

Materials and Methods

Isolated strains *Acidithiobacillus ferrooxidans* MFLv37 and MFLad27, collection *Acidithiobacillus ferrooxidans* VKM468 and standard *Acidithiobacillus ferrooxidans* ATCC23270 strains are stored in the Museum of Microbiology, Virology and Biotechnology Department of Mechnykov Odesa National University, which is a branch of the National Collection of Microorganisms. Strains *A. ferrooxidans* ATCC23270 and *A. ferrooxidans* VKM468 are used in biohydrometallurgical processes for the bacterial leaching of metals from sulphide ores [10]. In addition, *A. ferrooxidans* ATCC23270 is capable of solubilizing the sulfur from the coal surface [11].

New strains *A. ferrooxidans* MFLv37 and MFLad27 are characterized by the following features. There are Gram-negative rods, 0.2–0.4 microns in size, mobile. They are obligate anaerobes, chemolithoautotrophs, strictly acidophilic, mesophilic (optimum temperature for growth is 35.0 ± 2.0 °C). They are cultivated in media with iron, sulfur, thiosulfate, use thiourea as the single energy source, capable of growth in mixotrophic conditions. They are stored on an agar culture medium in the fridge with passages on fresh medium every 1–2 months. To cultivate the strains for biomass accumulation and metal ions leaching from substrates the medium 9K is used (g/dm^3): $(NH_4)_2SO_4$ — 3,0; KCl — 0,1; $MgSO_4$ — 0,5; K_2HPO_4 — 0,5; $Ca(NO_3)_2$ — 0,01. The only source of energy is $FeSO_4 \cdot 7H_2O$ in concentrations: 44.5 g/dm^3 for maximum strains biomass accumulation and 12.0 g/dm^3 for the most effective leaching of metals from the studied substrates. The original titer of all tested strains is the same and is equal to $(4.1 \pm 0.3)\times10^3$ cells/ml.

The objects of the research were the substrates of: rock dumps resulting from the coal beneficiation of mines of Lviv-Volyn Coal Basin by gravity and flotation methods at the Central Concentrating Factory (CCF) “Chervonogradska” of the joint stock company (JSC) “Lviv Coal Company”, and fly ash from high temperature combustion of mixture of domestic fossil coals at Ladyzhynskaya thermal power station.

Rock dumps substrate has the following characteristics. This is clay earth material, crystallized with the overwhelming majority of fairly large (5–7 mm) particles, represented by argillites, kaolinite, quartz sandstone-type mineral, pyrite, containing coal up to 17.0%, sulfur — up to 1.5% and organic mass — up to 2.0%. Chemical composition (%): Fe — 4.46; Al — 1.39; Si — 15.90; Ti — 0.42; Ca — 1.72; Cu — $6.22\cdot10^{-3}$; Zn — $1.13\cdot10^{-2}$; Mn — $3.18\cdot10^{-2}$; Pb — $0.42\cdot10^{-2}$; Ni — $1.34\cdot10^{-2}$; Cd — $2.82\cdot10^{-4}$; Sn — $3.52\cdot10^{-2}$; Cr — $0.99\cdot10^{-2}$; V — $1.50\cdot10^{-2}$; Co — $1.16\cdot10^{-2}$; Sr — $2.11\cdot10^{-2}$; Ba — $5.19\cdot10^{-2}$; Zr — $1.73\cdot10^{-2}$; Rb — $1.41\cdot10^{-2}$; Nb — $1.40\cdot10^{-3}$; La — $4.80\cdot10^{-3}$; Ce — $6.90\cdot10^{-3}$; Ga –$1.21\cdot10^{-3}$; Ge — $2.60\cdot10^{-3}$. Storage life in dumps is 1 year. The number of aboriginal acidophilus chemolithotrophic bacteria is: of mesophilic ones $(6.4 \pm 0,6)\times10^4$ and of moderately thermophilic ones $(7.4 \pm 0,3)\times10^8$ cells/ml [12].

Fly ash substrate is an amorphous poorly crystallized pulverized product with an overwhelming majority of quartz, carbonate and silicate phases, oxides of iron and aluminum. Chemical composition (%): Fe — 5.93; Al — 3.89; Si — 12.10; Ti — 4.16; Ca — 0.20; Cu — $6.82\cdot10^{-3}$; Zn — $3.27\cdot10^{-2}$; Mn — $5.73\cdot10^{-2}$; Pb — $1.09\cdot10^{-2}$; Ni — $1.77\cdot10^{-2}$; Cd — $5.31\cdot10^{-4}$; Sn — $2.07\cdot10^{-2}$; Cr — $2.18\cdot10^{-2}$; V — $2.15\cdot10^{-2}$; Co — $3.05\cdot10^{-2}$; Sr — $6.56\cdot10^{-2}$; Ba — $6.34\cdot10^{-2}$; Zr — $2.37\cdot10^{-2}$; Rb — $1.16\cdot10^{-2}$; Nb — $1.90\cdot10^{-3}$; La — $4.20\cdot10^{-3}$; Ce — $7.40\cdot10^{-3}$; Ga –$1.02\cdot10^{-3}$; Ge — $2.80\cdot10^{-3}$; S — 1.24; C (incomplete combustion) — 9.98.

Storage life in dumps is 1 year. The number of native acidophilus chemolithotrophic bacteria is: of mesophilic ones $(5.9 \pm 0.6) \cdot 10^4$ and of moderately thermophilic ones $(6.4 \pm 0.5) \cdot 10^7$ cells/ml.

The increase in biomass was determined by the number of cells counted in Goryaev chamber with the light microscope Primo Star PC (Germany). Analysis of solutions for metal content was performed using atomic absorption spectroscopy with devices AAS-1 (Germany) and C-115PK Selmi (Ukraine). The reliability of the results was evaluated by Student's t test with a probability of $P < 0.05$. The ratio (%) of the amount of metal that passed into the solution as a result of contact a nutrient medium with a substrate in microorganisms presence to the initial amount of metal in the original solid substrate is referred to as "degree of metal extraction". Indicator 100% corresponds to complete metal transition from the substrate into the solution.

Results and Discussion

In the initial phase the resistance of new strains *A. ferrooxidans* MFLv37 and *A. ferrooxidans* MFLad27 to heavy metals, which are the part of technogenic waste, has been studied.

Determination of copper, iron, zinc, lead, cadmium, manganese and germanium ions minimal concentration, at which *A. ferrooxidans* MFLv37 and *A. ferrooxidans* MFLad27 cells growth still happens, carried out in the course of their cultivation on an agar medium 9K with iron, adding sulfates of these metals in ever increasing concentrations. The minimal inhibitory concentration (MIC), at which the growth of the test strains may be still recorded, was determined. The term of cultivation was 7 days at 30.0 ± 2.0 °C. The results are shown in the table.

The findings indicate a high resistance level to heavy metals of strains isolated from technogenic waste of coal and energy industry. It is found that the minimal metal concentrations, at which strains growth still happens, are several times greater than their content in waste itself. The both new strains equally reacted to impact of manganese, zinc, copper and germanium. *A. ferrooxidans* MFLv37 and *A. ferrooxidans* MFLad27 strains are the most sensitive to cadmium; the most stable — to iron. By the negative influence on the growth of new isolated strains the following row is made:

$$Fe < Zn < Mn < Cu < Pb < Ge < Cd.$$

When comparing the stability of new strains with standard and collection ones it has been found that the latest were more sensitive to metals, forming part of technogenic waste. This could be explained by the fact that new strains are isolated from the aboriginal community, formed during the production and storage of technogenic objects with complex mineralogical composition and high concentrations of heavy metals. The high level of thiobacteria stability to metals is associated with the fact that the genetic basis of the resistance is extrachromosomal stability factors presence in bacteria — plasmids and transposons [13], and also with poor permeability of the cell wall for the heavy metal ions, formation of a large amount of slime, which binds and inactivates metals, et al. [14].

The next step is studying the adaptation of isolated strains *A. ferrooxidans* MFLv37 and

Minimal inhibitory metal concentrations (mg/dm^3) for *A. ferrooxidans* strains

Element	MIC, mg/dm^3				Determined concentration in substrates, mg/kg	
	A. ferrooxidans MFLv37	*A. ferrooxidans* MFLad27	*A. ferrooxidans* VKM 468	*A. ferrooxidans* ATCC23270	Rock dump	Fly ash
Cu	1200.0	1500.0	7.0	5.0	62.18	68.18
Zn	4500.0	4500.0	5.0	5.0	112.52	327.33
Mn	1500.0	1650.0	7.0	5.0	317.72	572.60
Pb	600.0	850.0	2.0	1.0	42.20	108.74
Cd	25.0	25.0	2.0	2.0	2.82	5.31
Fe	$150.0 \cdot 10^3$	$150.0 \cdot 10^3$	$10.0 \cdot 10^3$	$10.0 \cdot 10^3$	$44.57 \cdot 10^3$	$59.31 \cdot 10^3$
Ge	150.0	150.0	12.0	15.0	26.00	28.00

A. ferrooxidans MFLad27 to new technogenic waste as a new source of energy. Experiments were performed using the standard 9K medium and technogenic substrates samples as a sole energy source. Ratio of solid and liquid phases (S:L) in the experiments was the following: 1:2, 1:3 and 1:10; temperature of 30.0 ± 2.0 °C, pH ≤ 3. Successive reinoculations with growing volumes of new substrates were performed when the strains reached maximum quantity of biomass in each passage. Control was an indicator of strains biomass growth in the medium 9K with 12.0 g/dm^3 of $FeSO_4 \cdot 7H_2O$ (as the sole source of energy).

Fig. 1 and 2 show the results of strains *A. ferrooxidans* MFLv37 and *A. ferrooxidans* MFLad27 biomass growth with various amounts of substrates usage as power sources. Obviously, the both strains, which were grown for a long time using Fe^{2+}, require lengthy adaptation as to substrate from which they were isolated, and to a new substrate.

As follows from Fig. 1, when switching from ferrous iron oxidation to old substrate (dumps) and new one (ash) oxidation there is a decrease in *A. ferrooxidans* MFLv37 bacteria cell number in the first 6 hours of cultivation. Subsequently, the active biomass growth occurs on both substrates with pronounced inversely proportional dependence on its quantity: less substrate with respect to the medium, more active biomass increasing on it. In the case of the test strain cultivation at S:L = 1: 2 the time to reach the stationary phase of growth for *A. ferrooxidans* MFLv37 was 36 and 42 hours, respectively, for the new (ash) and old (dumps) substrates. Upon that, the quantity of biomass was respectively 4.0–6.0 times less than in the control experiment. With a decrease in the amount of the solid substrate to the S:L = 1: 3 the time to reach the stationary phase of growth for *A. ferrooxidans* MFLv37 was 48 hours for the new (ash) and 66 hours for the old (dumps) substrates. In addition, the quantity of biomass was respectively 1.7–2.0 times less than in the control. During the further test strain cultivation the cell number did not increase, but they remain viable. With a decrease in technogenic waste number to S:L = 1:10 *A. ferrooxidans* MFLv37 growth was observed over the entire period of cultivation, the number of bacteria was even higher than data in the control group. The sharp decrease in the number of bacteria in the early adaptation period and a minor amount of bacteria with an excess of the substrate (S:L = 1: 2, and S:L = 1: 3) may be explained by attaching a significant number of formed cells to the surface of substrate particles [15].

Similar results were obtained while studying the biomass growth of *A. ferrooxidans* MFLad27 strain on the old and the new substrates (Fig. 2) with expressed adaptation period in the first 6–12 hours, and with an excess of a substrate — up to 36 hours of cultivation. In the process of *A. ferrooxidans* MFLad27 adaptation to the growing volume of rock dumps the same pattern as that for *A. ferrooxidans* MFLv37 to fly ash are marked, with the only difference being that the strain *A. ferrooxidans* MFLad27 is much worse adapted to other technogenic substrate as an energy source.

In the next stage of the work the oxidative capacity of adapted to new substrates strains has been studied compared with maladapted strains, standard *A. ferrooxidans* ATCC23270 and collection *A. ferrooxidans* VKM468. The leaching process was performed at a ratio of

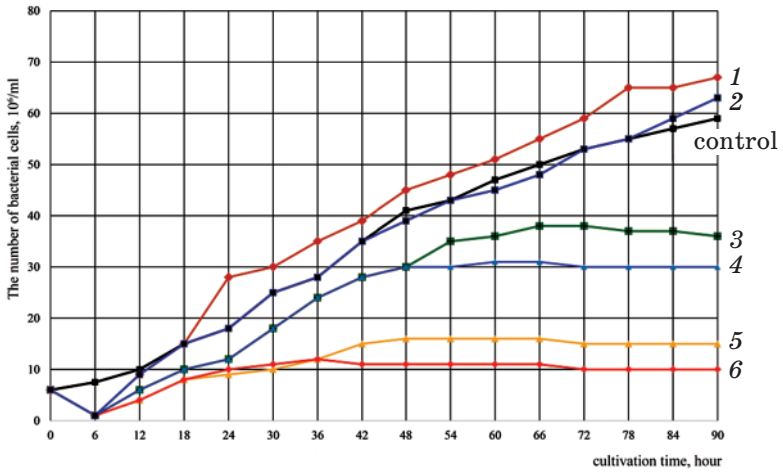

Fig. 1. **The amount of *A. ferrooxidans* MFLv37 biomass with growth on:**
1 — dumps S:L = 1:10; *2* — ash S:L = 1:10; *3* — dumps S:L = 1: 3; *4* — ash S:L = 1: 3; *5* — dumps S: L = 1: 2; *6* — ash S:L = 1: 2

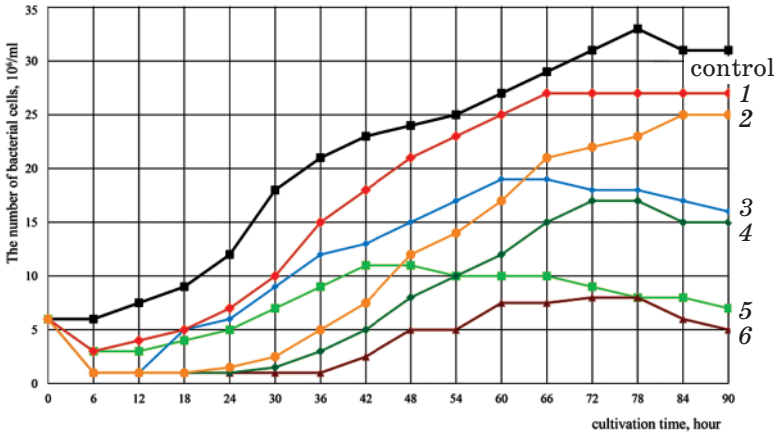

Fig. 2. **The amount of *A.ferrooxidans* MFLad27 biomass with growth on:**
1 — ash S:L = 1:10; *2* — dumps S:L = 1:10; *3* — ash S:L = 1: 3; *4* — dumps S:L = 1: 3;
5 — ash S:L = 1: 2; *6* — dumps S:L = 1: 2

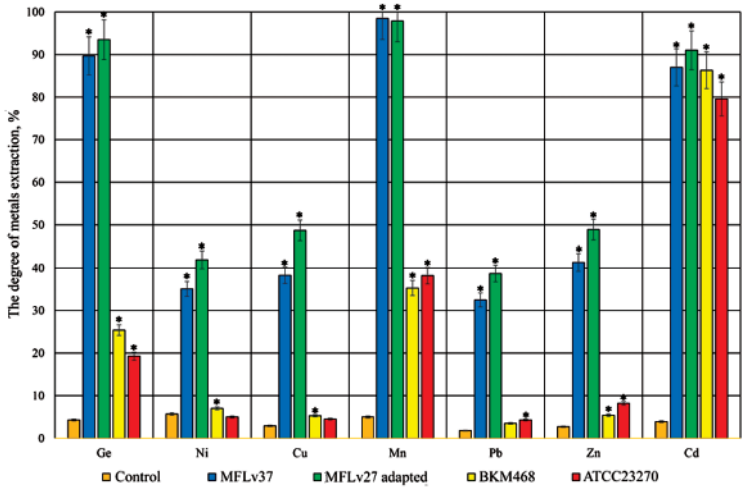

Fig. 3. **Metals recovery (%) from fly ash by *A. ferrooxidans* strains**
Hereinafter: * — $P < 0.05$ compared with the control

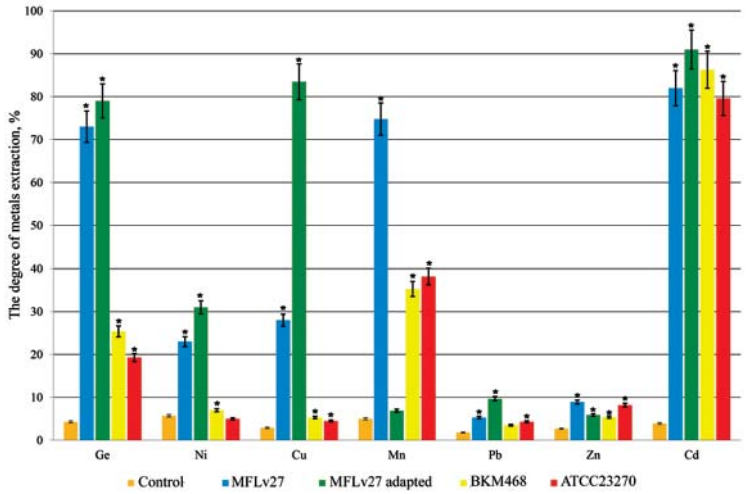

Fig. 4. **Metals recovery (%) from rock dumps by *A. ferrooxidans* strains**

S:L = 1:10, at temperature of 30.0 ± 2.0 °C, pH ≤ 2, for 7 days. The control was the results of metals leaching from substrates by nutrient medium under sterile conditions in the absence of microorganism strains. Fig. 3 and 4 show the results of these experiments.

Analysis of the results indicates that the both new isolated strains had a much higher oxidizing ability compared to the standard and the collection strains. Furthermore, adapted strains in most cases leached metals into solution more active compared to maladapted strains.

Comparison of the two strains showed that *A. ferrooxidans* MFLad27, isolated from fly ash obtained from coal combustion, exhibits less adaptability relative to growth rate (Fig. 2) and oxidation degree (Fig. 4). This indicates that *A. ferrooxidans* MFLv37 has more pronounced regulatory mechanisms, when reinoculating from one medium ($FeSO_4 \cdot 7H_2O$) to another (dump or ash substrate) an enzyme systems activation occurs that associated with the oxidation of sulfur compounds, and consequently the growth and oxidation degree increase [6, 9]. This is due to the specific conditions of rock dumps and fly ash microbiocenoses formation, whereof appropriate strains are obtained.

The results indicate that the main factors affecting the diversity of *A. ferrooxidans* strains are their formation and habitation in different ecological niches, in the substrates of different origin, as well as physico-chemical properties specificity. Search and directed selection of strains with high resistance and oxidative capacity, adaptation to the new natural and technogenic substrates are urgent tasks.

REFERENCES

1. *Ivanov M. V., Karavayko G. I.* Geological microbiology. *Mikrobiologiya.* 2004, 5 (73), 581–597. (In Russian).
2. *Norris P. R., Burton N. P., Foulis N. A. M.* Acidophiles in bioreactor mineral processing. *Extremophiles.* 2000, V. 4, P. 71–76.
3. *Blayda I. A.* Extraction of valuable metals from industrial waste biotechnological methods (Review). *Energotekhnologii i resursosberezhenie.* 2010, V. 6, P. 39–45. (In Russian).
4. *Blayda I. A., Vasileva T. V., Slyusarenko L. I., Barba I. N., Ivanitca V. A.* Composition and leaching activity of energy industrial waste microbiocenosis. *Problemy ekolohichnoi biotekhnolohii.* 2013, V. 1. Available at: http://jrnl.nau.edu.ua /index.php/ecobiotech/article/view/4592. (In Russian).
5. *Blayda I. A.* Composition and activity of bacterial community of coal tailing. *Biotechnol. acta.* 2014, 7 (5), 94–100. doi: 10.15407/biotech7.05.094.
6. *Tupikina O. V., Kondrateva T. F., Samorukova V. D., Rassulov V. A., Karavayko G. I.* Dependence of the strains *Acidithiobacillus ferrooxidans* phenotypic characteristics from the physical, chemical and electrical properties of pyrites. *Mikrobiologiya.* 2005, 74 (5), 596–603. (In Russian).
7. *Karavayko G. I., Kuznetsov S. I., Golomzik Ye. I.* The Role of Microorganisms in the leaching of metals from ores. *Moskva: Nauka.* 1972, 248 p. (In Russian).
8. *Silver M.* Metabolic mechanisms of iron-oxidizing thiobacilli. *Metallurgical applications of bacterial laeching and related microbiological phenomena.* Murr L. E., Torma A. E., Brierley J. A. (Eds). *New York: Academic Press.* 1978, P. 3–17.
9. *Grudev S. N.* The differences between the strains of *Thiobacillus ferrooxidans* on the ability to oxidize sulfide minerals. *Biogeotehnologija metallov.* Karavayko G. I., Grudev S. N. (Red.). *Moskva: Centr mezhdunarodnykh proektov GKNT.* 1985, P. 85–99. (In Russian).
10. *Tuovinen O. H., Fry I. J.* Bioleaching and mineral biotechnology. *Curr. Opin. Biotechnol.* 1993, V. 4, P. 344–355.
11. *Juszczak A., Domka F., Kozlowski M., Wachowska H.* Microbial desulfurization of coal with *Thiobacillus ferrooxidans* bacteria. *Fuel.* 1994, 74 (5), 725–728.
12. *Vasileva T. V.* Diversity of the microorganisms community in the technogenic ecosystems of Ukraine fuel-and-energy complex. *Problemy ekolohichnoi biotekhnolohii.* 2014, V. 1. Available at: http://ecobio.nau.edu.ua / index.php/ecobiotech/article/view /6660. (In Ukrainian).
13. *Khmelev I. A.* Plasmids and evolution of microorganisms. *Uspekhi sovremennoy biologii.* 1985, 99 (3), 323–337. (In Russian).
14. *Kenji Iwahorl, Fumiaki Takeuchi, Kazuo Kamimura, Tsuyoshi Sugio.* Ferrorous Iron-Dependent Volatilization of Mercuri by the Plasma Membrane of *Thiobacillus ferrooxidans. Apll. Envir. Microbiol.* 2000, P. 3823–3827.
15. *Kondrateva T. F., Ageeva S. N., Pivovarova T. A., Karavayko G. I.* Characteristics of chromosomal DNA restriction profiles strains *Acidithiobacillus ferrooxidans,* adapted to different substrates oxidation. *Mikrobiologiya.* 2002, 71 (4), 514–520. (In Russian).

ВЛАСТИВОСТІ НОВИХ ШТАМІВ ХЕМОЛІТОТРОФНИХ БАКТЕРІЙ, ЩО ЇХ ВИДІЛЕНО З ТЕХНОГЕННИХ СУБСТРАТІВ

І. А. Блайда[1]
Т. В. Васильєва[1]
В. І. Баранов[2]
К. І. Семенов[1]
Л. І. Слюсаренко[1]
І. М. Барба[1]

[1]Одеський національний університет імені І. І. Мечникова, Україна
[2]Львівський національний університет імені Івана Франка, Україна

E-mail: iblayda@ukr.net

Метою роботи було встановлення резистентності виділених з аборигенного консорціуму породних відвалів вуглезбагачення і золи-виносу від спалювання вугілля штамів *A. ferrooxidans* МФLv37 і *A. ferrooxidans* МФLad27 до важких металів, що входять до складу цих відходів, а також здатності штамів до адаптації до нових субстратів. Встановлено підвищену стійкість нових штамів до іонів важких металів порівняно з типовим і колекційним штамами *A. ferrooxidans*, визначено мінімальні інгібуючі концентрації важких металів, виявлено низку металів, що негативно впливають на ріст ізольованих культур. Показано, що мінімальні концентрації металів, за яких ще відбувається ріст штамів, у декілька разів перевищують їх вміст у техногенних відходах. Встановлено, що виділені штами відрізнялися за здатністю до адаптації, а також за швидкістю росту і окиснення субстратів. Це зумовлено специфічними умовами формування мікробіоценозів у процесі утворення і подальшого зберігання породних відвалів та золи-виносу, з яких виділено відповідні штами. Проведені дослідження свідчать про необхідність спрямованої селекції культур, стійких до токсичних сполук і здатних окиснювати різні мінеральні субстрати, а також їх адаптації до нових субстратів для вилучення важких металів.

Ключові слова: зола-винос, породні відвали, аборигенне бактеріальне угруповання, ацидофільні хемолітотрофні бактерії, штами, активність вилуговування, іони важких металів.

СВОЙСТВА НОВЫХ ШТАММОВ ХЕМОЛИТОТРОФНЫХ БАКТЕРИЙ, ВЫДЕЛЕННЫХ ИЗ ТЕХНОГЕННЫХ СУБСТРАТОВ

И. А. Блайда[1]
Т. В. Васильева[1]
В. И. Баранов[2]
К. И. Семенов[1]
Л. И. Слюсаренко[1]
И. Н. Барба[1]

[1]Одесский национальный университет имени И. И. Мечникова, Украина
[2]Львовский национальный университет имени Ивана Франко, Украина

E-mail: iblayda@ukr.net

Целью работы было установление резистентности выделенных из аборигенного консорциума породных отвалов углеобогащения и золы-уноса от сжигания угля штаммов *A. ferrooxidans* МФLv37 и *A. ferrooxidans* МФLad27 к тяжелым металлам, входящим в состав этих отходов, а также способности штаммов к адаптации к новым субстратам. Установлена повышенная устойчивость новых штаммов к ионам тяжелых металлов по сравнению с типовым и коллекционным штаммами *A. ferrooxidans*, определены минимальные ингибирующие концентрации тяжелых металлов, выявлен ряд металлов, оказывающих негативное влияние на рост изолированных культур. Показано, что минимальные концентрации металлов, при которых еще происходит рост штаммов, в несколько раз превышают их содержание в техногенных отходах. Установлено, что выделенные штаммы отличались по способности к адаптации, а также скорости роста и окисления субстратов. Это обусловлено специфическими условиями формирования микробиоценозов в процессе образования и дальнейшего хранения породных отвалов и золы-уноса, из которых выделены соответствующие штаммы. Проведенные исследования свидетельствуют о необходимости направленной селекции культур, устойчивых к токсичным соединениям и способных окислять различные минеральные субстраты, а также их адаптации к новым субстратам для извлечения тяжелых металлов.

Ключевые слова: зола-унос, породные отвалы, аборигенное бактериальное сообщество, ацидофильные хемолитотрофные бактерии, штаммы, активность выщелачивания, ионы тяжелых металлов.

UDC 611.018.5.013.8.088.3:577.121.7:57.43 **doi: 10.15407/biotech8.06.063**

ENERGY METABOLISM OF PACKED WHITE CELLS AFTER CRYOPRESERVATION AND REHABILITATION IN A MEDIUM CONTAINING A CORD BLOOD LOW-MOLECULAR FRACTION

A. K. Gulevsky[1]
Yu. S. Akhatova[1]
A. A. Sysoev[2]
I. V. Sysoeva[2]

[1]Institute for Problems of Cryobiology and Cryomedicine of the National Academy of Sciences of Ukraine, Kharkiv
[2]Kovalevsky Institute of Biology of the Southern Seas of the National Academy of Sciences of Ukraine, Sevastopol

E-mail: Julija_Veselovskaja@meta.ua

Recieved 09.09.2015

To study the bioenergy indicators of leykokontsentrate cells after cryopreservation and possibility of their recovery after incubation in a medium with a low-molecular fraction from cow cord blood were the aim of work. Leykokontsentrate was obtained from donor blood by sedimentation; cryopreservation was carried out in the slow freezing regimen with 5% dimethylacetamide; amount of ATP, ADP and AMP was determined by chemiluminescence; glycogen — by cytochemical method. Evidence of energy disbalance of leukoconcentrate cells after cryopreservation was obtained. It was shown that the cord blood low-molecular fraction (0.15 mg/ml) activated glycogenolysis and increased contents of ATP, ADP and AMP in leukoconcentrate cells after cryopreservation. It was also shown that the cord blood low-molecular fraction contained energy substrates and metabolites, hormones and macro- and micronutrients. Use of the low-molecular fraction (below 5 kDa) from cord blood as a component of rehabilitating medium for frozen-thawed leukoconcentrate cells contributed to improvement of their energy status, which was manifested as augmentation in the total adenylic pool and glycogenolysis activation.

Key words: leykokontsentrat, cryopreservation, energy metabolism, cord blood.

Current methods of low-temperature storage of packed white cells cannot guarantee their high safety, which is due to heterogeneity of cell population in terms of composition and functional characteristics and, therefore, difficulty of unification of optimal cryopreservation conditions. The experimental research conducted to date both in Ukraine and abroad aimed at finding of better methods of leukocytes cryopreservation [1–5], which requires separation of packed white cells into individual populations and are not always clinically justified. Despite some progress, frozen-thawed leukocytes need to recovery of their functional status before clinical application. It is known that in leukocytes intensity bioenergetic processes changes after cryopreservation, it leads to abnormalities in energy-dependent reactions [6, 7] and hence to impairment of their functional activity.

Recovery from cryoinjuries, first of all, requires energy costs, which can be replenished via glycolysis and oxidative phosphorylation. To solve this problem, use of special rehabilitating media capable of stimulating energy generation processes is promising.

We present the results of studying energy metabolism of donor blood packed white cells cryopreserved with dimethylacetamide. Evidence of a stimulating effect of a low-molecular fraction from cow cord blood (CBF) on ATP, ADP and AMP contents and glycolysis in the test cells is adduced.

Materials and Methods

Obtaining leukocyte mass

Leukoconcentrate was obtained from human donor blood by sedimentation of erythrocytes in 6% dextran solution (m.m. 50,000–70,000, “Biokhim”, Russia) [8].

Cryopreservation of leukocyte mass

Cryopreservation of cell suspension samples (0.5 mL, 2×10^7 cells/ml) was carried out according to the following regimen of slow freezing with 5% dimethylacetamide (DMAc):

at the rate of 3 °C/min from 22 °C to the crystallization point (−16 °C) with a shutdown of process for 6.5 min; then at the rate of 5 °C/min to −100 °C followed by immersion of samples in liquid nitrogen (−196 °C) [9]. Suspension was thawed in a water bath at 38 °C with intensive shaking containers [10]. After thawing the cryoprotectant was removed by slow dilution of cell suspension samples with autoplasma containing 2% dextran (1:2) followed by centrifugation (7 min at 200 g) [11].

Integrity of Leukocytes

The leukocyte integrity was assessed by trypan blue exclusion test [12].

Determination of ATP, ADP and AMP Contents

Cell suspension samples (0.5 ml) were incubated at 37 °C for 20 min with or without CBF (0.15 mg/ml). The incubation time was based on the experimental studies of granulocyte energy metabolism, viz., ATP and lactate production rates [13, 14]. After incubation adenylates were extracted.

Adenylates were extracted from cells by boiling leukocyte suspension samples (10^7 cells/ml) in Tris-buffer. 3 ml of boiling 0.1 M Tris-0.01M EDTA-acetate buffer (pH = 7.75) were added to an aliquot of cell suspension (0.5 ml); the aliquot was exposed in a boiling water bath for 5 min. Extracts were cooled down to the ambient temperature and stored at −18 °C for further analytic procedures.

ATP content in the resulting extract was determined by a chemiluminescence method [14] using a firefly enzyme, luciferase, and luciferin (Sigma, USA) (ATP Luminometer — 1250, LKB, Sweden). The maximum values of light reaction were registered.

To calibrate dependence of light reaction on ATP concentration, values of light emission of standard ATP solutions obtained at the beginning and end of an experimental series were used. To match light reaction values with ATP concentrations readings of light emission of ATP standard solutions were obtained at the beginning and end of each series of runs. ATP concentrations were calculated on the basis of relations of light impulse values to ATP standard solution concentrations adjusted for dilution, extract volumes and sample weights equivalent to protein. Background adenylate content in cell-free medium was also accounted in the calculations.

ADP and AMP contents were determined via preliminary restitution of these nucleotides to ATP using phosphoenolpyruvate (Sigma, USA), pyruvate kinase (Sigma, USA), and myokinase (Sigma, USA). The amount of synthesized ATP was again estimated by chemiluminescence assay. Adenylic nucleotide concentrations were conversed to molar unit.

Calculation of Adenylic Pool: adenylic pool is the sum of ATP, ADP and AMP concentrations.

*Calculation of A*denylic Energy Charge*:* adenylic energy charge (AEC) was calculated by the following formula [15]:

$$AEC = \frac{C_{ATP} + \frac{1}{2} C_{ADP}}{C_{ATP} + C_{ADP} + C_{AMP}} .$$

AEC characterizes the state of adenylic system charge; for example, if the whole pool of adenylic nucleotides is purely represented by ATP (maximum of high-energy bonds) AEC equals one; if there is only AMP in the cell (no high-energy bonds) AEC equals zero [15].

Determination of Glycogen Content

Glycogen in leukoconcentrate neutrophil cytoplasm was analyzed by cytochemically method [16] using Schiff reagent (PAS reaction) (Merck, Germany). Before the test leukoconcentrated was washed out by centrifuging (7 min at 200 g) in glucose-free medium of the following composition: 5% bovine serum albumin (Serva, Germany) in physiologic saline, 10% dextran in physiologic saline ("Reopoliglyukin-Novofarm"®, Novofarm-Biosynthesis, Ukraine). The ration leukocyte suspension/dextran/albumin was 1:1:1. Supernatant was removed; precipitate was resuspended in fresh solution. Glycogen content was semiquantitatively estimated with calculation of the average cytochemical coefficient (ACC) according to Kaplow [16]: ACC=(3A+2B+C)/100, where A — number of cells with strong positive staining, B — number of cells with staining of medium intensity, C — number of cells with weak positive staining and/or negative staining. To inhibit glycolysis, sodium iodoacetate was used at the final concentration of 1 mM [17]. To activate cells, packed white cells were incubated for 1 hour at 37 °C after inoculation of one-day culture of *Staphylococcus aureus* strain 209 in physiologic saline (inactivated by 1-hour exposure in a water bath at 80 °C) at the concentration of ~2 bln cells/ml by the turbidity standard.

CBF (below 5 kDa) Extracting

The extraction of the fraction containing components with molecular weights below 5 kDa from the cryodestructed whole cattle blood was performed by ultrafiltration [18] using a membrane module Sartorius (Germany). Ultrafiltrate was lyophilized in a freeze-drying chamber under the pressure of 5×10^{-2} mmHg; the total duration of drying was 28–30 h. Lyophilized samples

were stored at −80 °C. CBF was added to the incubation medium at the final concentration of 0.15 mg/ml.

Determination of CBF Composition

CBF was assessed for estradiol, free triiodothyronine, cortisol, and progesterone contents using a closed test system for quantitative analysis of hormones *in vitro* by electrochemiluminescent immunoassay (ECLIA) on an automatic Elecsys 1070/2010 analyzer and a Modular Analytics E170 analyzer (Hoffmann-La Roche, Switzerland). To estimate micro/macroelements and metabolite concentrations (calcium, magnesium, phosphorus, zinc, glucose, creatinine, etc.) a closed test system for quantitative analysis of substances in biological liquids by electrochemiluminescent assay and automatic Elecsys 1070/2010 and Cobas C311 chemistry analyzers were used (Hoffmann-La Roche, Switzerland).

Inhibitory Assay

To explain the mechanism of action of CBF on energy processes native leukoconcentrate suspension was pre-incubated with a glycolysis inhibitor, sodium iodoacetate (IA) (Serva, Germany), which blocks one of the key glycolytic enzymes — glyceraldehyde-3-phosphate dehydrogenase at 37 °C for 20 min. IA was added to leukocyte suspension (10^7 cells/ml) before CBF at the final concentration of 1 mM [17].

The non-parametric Mann–Whitney test was used for statistical analysis.

Results and Discussion

The analysis of safety of native packed white cells obtained from human blood by sedimentation showed that suspension had 97.81±0.42% of viable nucleated cells. After cryopreservation with DMAc at the final concentration of 5% the number of provisionally viable cells in samples was 79.96±1.75%.

To understand changes occurring in the adenylic energy system after cryopreservation of cells, we assessed ATP, ADP and AMP contents, the total adenylic pool, adenylic energy charge and ratios between individual adenylic nucleotides.

The investigation of the baseline energy status of packed white cells revealed that they had the full set of adenylic nucleotides represented by ATP, ADP and AMP. AEC of freshly-isolated cells was 0.79±0.003 rel. u., which suggests predominance of ATP in the total adenylic pool and, therefore, abundance of energy in the adenylic system of cells (Table 1). The data in Table 1 show that after cryopreservation balance of the cell energy system is impaired.

Thus, it was demonstrated that the total adenylic pool significantly reduced mainly due to the decrease in ATP content by 2.6 times (23.42±2.9 vs. 8.9±0,93 nmol/mg protein). It is noteworthy that the drastic drop in ATP content in frozen-thawed cells was not accompanied by expected rise in relative concentrations of ADP and AMP via their interconversion, that is why the ration ATP:ADP:AMP considerably shifted to di- and monophosphates. We assume that this can be attributed to loss of adenylic nucleotides through transmembrane pores that form during cryopreservation and capable for self-healing [19]. It is important to note that the selected method of cryopreservation, despite the distortion in ratios between individual adenylic nucleotides, provides preserving AEC on the level of 0.64±0.070 rel. u.

Table 1. **Characterization of General Status of the Adenylic System of Packed Human White Cells**

Index	Before cryopreservation	After cryopreservation	After cryopreservation + CBF
ATP, nmol/mg of protein	23.42 ± 2.9	8.9 ± 0.93 *	11.9 ± 0.68 *#
ADP, nmol/mg of protein	9.68 ± 1.21	8.37 ± 2.6	16.87 ± 4.4 #
AMP, nmol/mg of protein	3.02 ± 0.39	4.6 ± 1.7	9.56 ± 2 #
Adenylic Pool, nmol/mg of protein	37.49 ± 4.09	21.47 ± 5.6 *	37.9 ± 5.9 #
AEC, rel. u.	0.79 ± 0.003	0.64 ± 0.070	0.56 ± 0.080
Ratio ATP: ADP: AMP	7.75: 3.2: 1	1.2: 1.8: 1	1: 1.8:1

Footnotes: * — significant difference in comparison with the before-cryopreservation control ($P < 0.05$); # — significant difference in comparison with the after-cryopreservation control ($P < 0.05$).

It is known that in energy metabolism in cells of leukocytic series glycogen metabolism plays a key role, being used as energy substrate by cells. In particular, this referrers to phagocyting types of leukocytes, which function under acute hypoxia in tissues, at the same time keeping a high level of metabolism [20]. Need of leukocytes in large stock of glycogen is predominantly related to a drastic increase of energy expenditure by stimulated cells. Given the above, at the next stage of our experimental work we performed cytochemical analysis of glycogen content in neutrophils from packed white cells after cryopreservation with DMAc.

The data showed that freshly-isolated cells contain large amounts of PAS-positive matter, glycogen, which uniformly or as conglomerates and granules fills the whole cytoplasm. ACC was 2.139±0.01 rel. u., which corresponded to the normal range (Fig. 1).

Further incubation of cells in glucose-free medium for 1 hour did not lead to visible changes in glycogen content in cytoplasm, consequently, no ACC changes were recorded (1.98±0.02 rel. u.). Activation of freshly-isolated cells by inoculating *Staphylococcus aureus* suspension under these conditions did not promote glycogenolysis (ACC = 1.9±0.02 rel. u.). Analyzing these results, we can conclude that native neutrophils do not need mobilization of cytoplasmic stock of glycogen under these conditions, at least within 1-hour incubation. DMAc exerted no impact on this parameter.

At the same time a completely different pattern was observed for glycogen content in neutrophils from packed white cells cryopreserved with 5% DMAc. The glycogen amount in neutrophils from frozen-thawed packed white cells remained unchanged in comparison with that in freshly-isolated cells: ACC was 1.93±0.018 and 2.139±0.01, respectively (Fig. 2). However, after 1-hour incubation of quiescent cells a statistically significant decline in glycogen content was observed (ACC 1.73±0.01 rel. u.), which was seen in stained slides as weakening of staining intensity in cytoplasm.

Unlike freshly-isolated cells, phagocyting neutrophils from frozen-thawed leukoconcentrate actively used glycogen stock, which was seen as changes in intensity and nature of cytoplasmic staining and a significant reduction in ACC to 1.66±0.007 rel. u. (Fig. 2). Microscopic analysis of slides demonstrated decreased intensity of cytoplasmic staining, absence of glycogen conglomerates, and in slides PAS-negative neutrophils regularly occurred.

Thus, DMAC-containing cryoprotective solution provides preserving sufficiently large numbers of viable cells, nevertheless, taking into account the above-mentioned data, we can conclude that leukoconcentrate quality after cryopreservation still worsens, and there is an unmet need in recovery of functional status of cells before transfusion to guarantee the best therapeutic benefit.

Previously we demonstrated that application of rehabilitating medium containing a low-molecular fraction (below 5 kDa) from cord blood contributed to recovery of functional status of frozen-thawed leukocytes, namely augmentation in parameters of their phagocytic activity [9, 21, 22]. All phagocytic stages are known to depend largely on energy supply of cells via glycolysis and oxidative phosphorilation, and in phagocyting cells the contribution of glycolysis

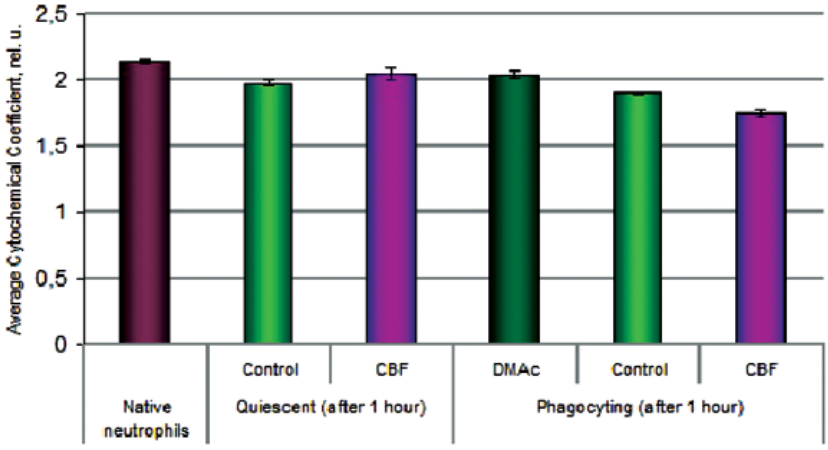

Fig. 1. **Glycogen Content in Neutrophils from Packed Human White Cells prior to Cryopreservation Depending on Incubation Medium Components**

in the total energy pool is significantly higher [13, 14]. Therefore, we assumed that mechanisms of the CBF stimulating effect were mediated through influence of its components on energy metabolism.

As one can see in Table 1, CBF contributed to increase in ATP, ADP and AMP concentrations in frozen-thawed cells by 1.34, 2 and 2 times, respectively, resulting in the gain in the total adenylic pool by 76.5%, which reached the level of freshly-isolated cells. However, CBF had no impact on AEC. It could be explained both by intensified ATP consumption due to activation of recovery processes aimed at elimination of injuries and by ADP and AMP *de novo* synthesis, since these both processes lead to a shift in ratios between individual adenylic nucleotides in favor of ADP and AMP.

To elucidate mechanisms of CBF action on the test parameters, we used glycolysis inhibitor, sodium iodoacetate, for freshly-isolated cells (Fig. 3). It was found that addition of sodium iodoacetate to incubation medium was associated with the decline in intracellular ATP by 1.7 times, however, as early as after 20-minute incubation of inhibitor-treated cells with CBF we noticed the increase in this parameter by 1.4 times.

At the same time there was no return of ATP concentration to the level observed in CBF-treated cells without inhibitor: in Fig. 3 one can see that iodoacetate suppresses the stimulating effect of the fraction on ATP production by 1.9 times (35.42±3.91 vs. 18.78±2.05 nmol/mg protein). This indicates that in addition to glycolysis, other pathways of ATP synthesis can be influenced by low-molecular components of CBF.

The most conspicuous reduction in ACC was observed, when CBF was added to frozen-thawed quiescent (down to 1.61±0.017 rel/ u.) and phagocyting (down to 1.31±0.005 rel. u.) cells (Fig. 2). This attests to the fact that CBF upon activation of phagocytes with cryopreservation-impaired metabolism assists mobilization of cytoplasmic glycogenic stock, thereby satisfying the need of cells in glucose, which is likely to be used for energy production in glycolytic reactions.

To confirm this assumption, we used inhibitor analysis with sodium iodoacetate again. Fig. 2 shows that treatment of cells with glycolysis inhibitor resulted in conservation of glycogen stock in cytoplasm — staining intensity was the same as in control, and ACC was 2.09±0.02 rel. u. In CBF presence the blocking effect of inhibitor persisted;

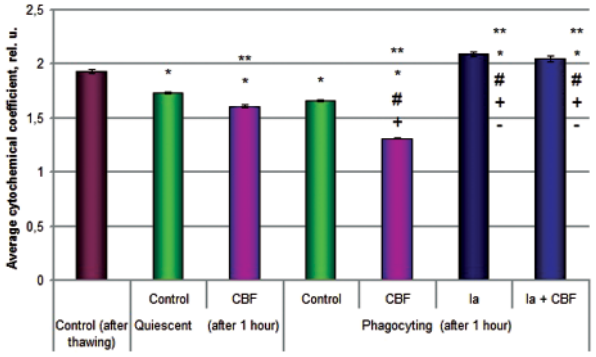

Fig. 2. **Glycogen Content in Neutrophils from Packed Human White Cells afterCryopreservation Depending on Incubation Medium Components:**
* — significant difference in comparison with control after cryopreservation ($P < 0.05$);
** — significant difference in comparison with quiescent control ($P < 0.05$);
# — significant difference in comparison with phagocyting control ($P < 0.05$);
+ — significant difference in comparison with quiescent cells incubated with CBF ($P < 0.05$);
– significant difference in comparison with phagocyting cells incubated with CBF ($P < 0.05$).

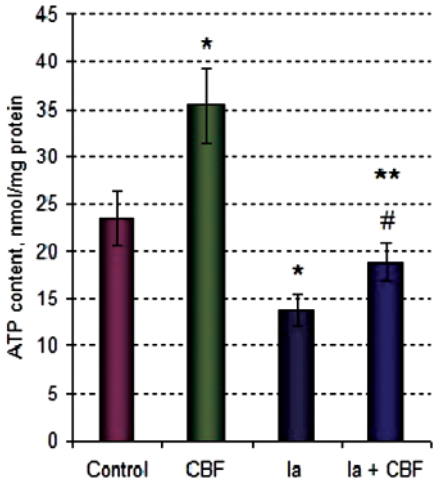

Fig. 3. **Effect of CBF on ATP Content in Freshly-Isolated Packed White Cells Treated with Iodoacetate:**
* — significant difference in comparison with the before-cryopreservation control ($P < 0.05$);
** — significant difference in comparison with incubation of leukoconcentrate cells with Ia ($P < 0.05$);
# — significant difference in comparison with incubation of leukoconcentrate cells with CBF ($P < 0.05$)

Table 2. **Composition of the Cattle Cord Blood Low-Molecular (below 5 kDa) Fraction**

Component	Content of CBF solution (1 mg/ml)
Estradiol	20.78 pg/ml
Free Triiodothyronine	0.76 pmol/L
Cortisol	0.415 nmol/L
Progesterone	0.03 ng/ml
Polypeptides	0.15 mg/ml
Calcium ionized	0.2 mmol/L
Magnesium	0.3 mmol/L
Phosphorus	0.195 mmol/L
Zinc	2.52 μmol/L
Glucose	0.39 mmol/L
Lactate	0.15 mmol/L
Creatinine	154 μmol/L
Chondroitin sulfates general	0.9 mg/L
Uronic acid	2.98 mg/L
Glycoproteins	25.3 mg/L
Total GAG	0.007 U
ATP	1,18 nmol/ml
ADP	0,818 nmol/ml
AMP	0,25 nmol/ml

staining intensity in cytoplasm and ACC (2.05±0.029 rel. u.) did not change in comparison with the baseline values. These results confirm the fact that addition of CBF to incubation medium promotes glycogenolysis in frozen-thawed neutrophils, and glucose produced in this process is used in glycolytic reactions for further ATP synthesis.

Since CBF is isolated from cord blood rich in bioactive substances, one cannot exclude that its beneficial effect on cell energy status is attributed to energy substrates such as glucose, adenylic precursors or regulatory biomolecules contained in it. In view of this we analyzed CBF composition (Table 2).

The data summarized show that there are energy substances and metabolites represented by glucose, creatinine, lactate, ATP, ADP, and AMP as well as metabolism regulators represented by hormones, calcium ions and macro/microelements in the fraction. Currently, it turns to be impossible to ascribe the biological activity of CBF to a certain component; its mechanism of action is most likely to be due to a complex action of low-molecular substances.

Thus, the study results showed that DMAc as a component of protective solution for cryopreservation of packed white cells provides preserving sufficiently large numbers of viable cells. However, taking into consideration the data on impairment in bioenergy balance of cells, we can conclude that leukoconcentrate quality still worsens after cryopreservation.

Use of the low-molecular fraction (below 5 kDa) from cord blood as a component of rehabilitating medium for frozen-thawed leukoconcentrate cells contributed to improvement of their energy status, which was manifested as augmentation in the total adenylic pool and glycogenolysis activation.

Using glycolysis inhibition, we revealed that CBF effect on energy system of cells could be mediated at least by two mechanisms. First, it is possible that CBF low-molecular components are directly involved in glycolytic reactions, since glycolysis pathway of energy generation is the major one for cells of leukocytic series. Second, we cannot rule out CBF influence on other pathways of ATP synthesis, in particular on oxidative phosphorilation.

REFERENCES

1. *Vian A. M. Higgins A. Z.* Membrane permeability of the human granulocyte to water, dimethyl sulfoxide, glycerol, propylene glycol and ethylene glycol. *Cryobiology*. 2014, 68 (1), 35–42. doi: 10.1016/j.cryobiol.2013.11.004.
2. *Aziz N., Margolick J. B., Detels R., Rinaldo C. R., Phair J., Jamieson B. D., Butch A. W.* Value of a quality assessment program in optimizing cryopreservation of peripheral blood mononuclear cells in a multicenter study. *Clin. Vaccine Immunol.* 2013, 20 (4), 590–595. doi: 10.1128/CVI.00693-12.
3. *Koryakina A., Frey E., Bruegger P.* Cryopreservation of human monocytes for pharmacopeial monocyte activation test. *J. Immunol. Meth.* 2014, 40 (5), 181–191. doi: 10.1016/j.jim.2014.01.005.
4. *Nazarpour R., Zabihi E., Alijanpour E., Abedian Z., Mehdizadeh H., Rahimi F.* Optimization of human peripheral blood mononuclear cells (PBMCs) cryopreservation. *Int. J. Mol. Cell. Med.* 2012, 1 (2), 88–93.
5. *Nair S. R., Geetha C. S., Mohanan P. V.* Analysis of IL-1 β release from cryopreserved pooled lymphocytes in response to lipopolysaccharide and lipoteichoic acid. *Biomed. Res. Int.* 2013, Article ID 689642, 10 p.: doi.org/10.1155/2013/689642.
6. *Svedentsov E. P., Chtcheglova O. O., Tumanova T. V., Solomina O. N.* Conservation leukocytes in the conditions of cryoanabiosis (-40 ^{O}C). *J. Stress Physiol. Biochem*. 2006, 2 (1), 29–34. (In Russian).
7. *Lane T. A., Lamkin G. E.* Defective energy metabolism in stored granulocytes. *Transfusion*. 1982, V. 5, P. 368–373.
8. *Grishina V. V., Timokhina Ye. V. Andreeva L. Yu.* Collection and fractionation cord blood stem cells. *Voprosy ginekologii, akusherstva i perinatologii.* 2004, 6 (3), 50–54. (In Russian).
9. *Gulevsky A. K., Akhatova Yu. S., Moiseeva N. N., Gorina O. L., Chizhevsky V. V., Stepanyuk L. V.* Assessment of phagocytic activity of leukoconcentrate neutrophils cryopreserved with dimethyl acetamide after post-thaw rehabilitation in medium containing cord blood low-molecular fraction (below 5 kDa). *Problems of Cryobiology*. 2012, 22 (1), 71–79. (In Ukrainian).
10. *Svedentsov Ye. P., Tumanova T. V., Hudyakov A. N., Zaitseva O. O., Solomina O. N., Utemov S. V., Sherstnev F. S.* Preservation of biological membranes of nuclear blood cells at –80 °C. *Biol. membrany*. 2008, 1 (25), 18–24. (In Russian).
11. *Rumjancev A. G., Maschan A. A.* Transplantation of haemopoetic cells in children. *Moskva: MIA*. 2003, 911 p. (In Russian).
12. *Avelar-Freitas B. A., Almeida V. G., Pinto M. C., Mour o F. A., Massensini A. R., Martins-Filho O. A., Rocha-Vieira E., Brito-Melo G. E.* Trypan blue exclusion assay by flow cytometry. *Braz. J. Med. Biol Res.* 2014, 47 (4), 307–315. doi: 10.1590/1414-431X20143437.
13. *Majanskij A. N.* Mitochondria of neutrophils: physiology especially and important in apoptosis. *Immunology.* 2004, V. 5, P. 307–311. (In Russian).
14. *Borregaard N., Herlin T.* Energy metabolism of human neutrophils during phagocytosis. *J. Clin. Invest*. 1982, 9 (70), 550–557.
15. *Nikolaev A. Ya.* Biological Chemistry. *Moskva: MIA*. 2004, 565 p. (In Russian).
16. Clinical laboratory analytics. V. 2. Several analytical techniques in the clinical laboratory. *Moskva: RAMLD*. 1999, P. 115–117. (In Russian).
17. *Yang J. H., Yang L., Qu Z., Weiss J. N.* Glycolytic oscillations in isolated rabbit ventricular myocytes. *J. Biol. Chem.* 2008, 283 (52), 36321–36327. doi: 10.1074/jbc.M804794200.
18. *Brock T. D.* Membrane Filtration: A User's Guide and Reference Manual. *Science Tech Publishers, Madison, WI*. 1983, 381 p.
19. *Gulevsky A. K., Bondarenko V. A., Belous A. M.* The barrier properties of the biological membrane at low temperatures. *Kyiv: Naukova dumka*. 1988, 205 p. (In Ukrainian).
20. *Afonso A., Macedo P. M., Ellis A. E. Silva M. T.* Glycogen granules in resting and inflammatory rainbow trout phagocytes — an ultrastructural study. *Dis. Aquat. Organ*. 2000, 42 (2), 101–110.
21. *Gulevsky A. K., Moiseyeva N. N., Gorina O. L.* Influence of low-molecular (below 5 kDa) fraction from cord blood and actovegin on phagocytic activity of frozen-thawed neutrophils. *CryoLetters*. 2011, 2 (32), 131–140.
22. *Gulevsky A. K., Akhatova Yu. S., Moiseeva N. N., Gorina O. L.* Immunomodulatory effect of a low-molecular fraction from cord blood on human blood monocytes. *Ukr. J. Hematol. Transfusiol.* 2013, V. 5, P. 24–28. (In Ukrainian).

ЕНЕРГЕТИЧНИЙ ОБМІН ДЕКОНСЕРВОВАНИХ КЛІТИН ЛЕЙКОКОНЦЕНТРАТУ ПІСЛЯ РЕАБІЛІТАЦІЇ В СЕРЕДОВИЩІ, ЩО МІСТИТЬ НИЗЬКОМОЛЕКУЛЯРНУ ФРАКЦІЮ КОРДОВОЇ КРОВІ

О. К. Гулевський[1]
Ю. С. Ахатова[1]
О. О. Сисоєв[2]
І. В. Сисоєва[2]

[1]Інститут проблем кріобіології та кріомедицини НАН України, Харків
[2]Інститут біології південних морів ім. О. О. Ковалевського НАН України, Севастополь

E-mail: Julija_Veselovskaja@meta.ua

Метою роботи було визначити біоенергетичні показники клітин лейкоконцентрату після кріоконсервування та можливість їх відновлення після інкубації в середовищі з низькомолекулярною фракцією кордової крові. Лейкоконцентрат одержували з донорської крові методом седиментації; кріоконсервування проводили в режимі повільного заморожування під захистом 5%-го диметилацетаміду; кількість АТФ, АДФ і АМФ визначали хемолюмінесцентним, а глікоген — цитохімічним методами. Встановлено, що після кріоконсервування відбувається порушення енергетичного балансу клітин лейкоконцентрату. Показано, що низькомолекулярна фракція кордової крові (0,15 мг/мл) сприяє глікогенолізу і підвищенню вмісту АТФ, АДФ і АМФ в деконсервованих клітинах. До складу фракції кордової крові входять енергетичні субстрати й метаболіти, гормони, макро- та мікроелементи.

Використання фракції кордової крові у складі реабілітувального середовища для деконсервованих клітин лейкоконцентрату сприяє поліпшенню їхнього енергетичного статусу, що виявляється у збільшенні загального аденілатного пулу і активації процесів глікогенолізу.

Ключові слова: лейкоконцентрат, кріоконсервування, енергетичний обмін, кордова кров.

ЭНЕРГЕТИЧЕСКИЙ ОБМЕН ДЕКОНСЕРВИРОВАННЫХ КЛЕТОК ЛЕЙКОКОНЦЕНТРАТА ПОСЛЕ РЕАБИЛИТАЦИИ В СРЕДЕ, СОДЕРЖАЩЕЙ НИЗКОМОЛЕКУЛЯРНУЮ ФРАКЦИЮ КОРДОВОЙ КРОВИ

А. К. Гулевский[1]
Ю. С. Ахатова[1]
А. А. Сысоев[2]
И. В. Сысоева[2]

[1]Институт проблем крибиологии и криомедицины НАН Украины, Харьков
[2]Институт биологии южных морей им. А. О. Ковалевского НАН Украины, Севастополь

E-mail: Julija_Veselovskaja@meta.ua

Целью работы было определение биоэнергетических показателей клеток лейкоконцентрата после криоконсервирования и возможности их восстановления после инкубации в среде с низкомолекулярной фракцией кордовой крови. Лейкоконцентрат получали из донорской крови методом седиментации; криоконсервирование проводили в режиме медленного замораживания под защитой 5%-го диметилацетамида; количество АТФ, АДФ и АМФ определяли хемолюминесцентным, а гликоген — цитохимическим методами. Установлено, что после криоконсервирования происходит нарушение энергетического баланса клеток лейкоконцентрата. Показано, что низкомолекулярная фракция кордовой крови (0,15 мг/мл) способствует гликогенолизу и повышению содержания АТФ, АДФ и АМФ в деконсервированных клетках. В состав фракции кордовой крови входят энергетические субстраты и метаболиты, гормоны, макро- и микроэлементы.

Использование фракции кордовой крови в составе реабилитирующей среды для деконсервированных клеток лейкоконцентрата способствует улучшению их энергетического статуса, что выражается в увеличении общего аденилатного пула и активации процессов гликогенолиза.

Ключевые слова: лейкоконцентрат, криоконсервирование, энергетический обмен, кордовая кровь.

UDK 669.187.526.001.5 **doi: 10.15407/biotech8.06.071**

THE LIME PURIFICATION OF SUGAR-CONTAINING SOLUTION USING HIGH VISCOSITY COLLOIDAL SOLUTIONS

Liapina K. V.[1]
Dulnev P. G.[2]
Marynin A. I.[3]
Pushanko N. N.[3]
Olishevskiy V. V.[3]

[1]Paton Electric Welding Institute of the National Academy of Sciences of Ukraine, Kyiv
[2]Institute of Bioorganic Chemistry and Petrochemistry of the National Academy of Sciences of Ukraine, Kyiv
[3]National Institute of Food Technologies, Kyiv, Ukraine

E-mail: kirulya@mail.ru

Received 16.07.2015

Aim of the work was to determine the efficiency of combined application of lime and high-viscous suspensions, containing the aluminium nanoparticles as a precursor in treatment of sugar-containing solutions.

At the first stage the aluminium nanopowder, encapsulated into a salt matrix, was produced by the combined precipitation from a gas phase of metal and halogenide of alkali metal (NaCl). For the long-term stabilization of aluminum nanoparticles the method, developed by the authors, for dispersing these powders in the composition of polyethylene glycols was used, providing the colloidal solution of high viscosity (gel).

At the second stage, as an object of investigation a juice of sugar beet, produced in the laboratory conditions by water extracting from the beet chips, was applied. In the produced juice the main characteristics of its quality were determined: the content of solids, sucrose, its purity was calculated (ratio of sucrose to solids content, in%). The content of protein and pectin components was also determined (as the main components of the colloidal fraction of the diffusion juice). Conventionally, as a basic reagent for the process of a lime pretreatment a lime milk of 1.18 g/cm^3 density, prepared by liming the burned lime using hot water, was used.

During the experiments the effectiveness of reagents, containing aluminum in nanoform, their influence on the degree of removal of the colloidal dispersion substances in the process of juice purification in sugar beet production and improvement of its quality, is shown. However, the obtained results show that, depending on the method of producing, the additional reagents with aluminium nanoparticles have different effect on change of diffusion juice purity in the process of its treatment by the lime milk.

Key words: nanopowders, defecosaturation treatment, sugar-containing solutions.

Today, to attain the required quality of sugar, it is necessary to have the high quality of semi-products, it concerns, in particular, juices after the defecosaturation treatment by using a lime milk and saturation gas. Due to the fact that the beet of a low technological quality is supplied often into processing, the diffusion juice has a high content of different compounds (so-called non-sugars), which reduce greatly its purity [1]. To purify this juice it is necessary either to increase the consumption of the lime milk and saturation gas or to apply additionally in the technology such reagents which could improve sufficiently the effectiveness of the carried out processes of the juice purification, and also reduce the consumption of conventional reagents. The use of the additional reagents in the technology of treatment of the sugar-containing solutions is the rather urgent problem for the sugar complex of Ukraine, as this is the most simple and economic way for the improvement of characteristics of the ready products. This problem was studied in many works, in particular in [2–8]. However, the variety of processes, proceeding under conditions of a diffusion juice treatment, does not give an opportunity to evaluate precisely the mechanism of interaction of added additional chemical reagents with non-sugars of the diffusion juice. First of all, it concerns the process of coagulation of colloids. On the other hand, the adding of additional reagents to the processes of the juice treatment should be in

compliance with a number of conditions, in particular these are a minimum dose of reagent at high efficiency, the absence of interaction with the sucrose, removal in the process of production together with other wastes [9–13].

On the basis of investigations of properties of colloidal high-viscosity solutions, produced by encapsulation of metallic aluminium particles into a salt coat, the present work deals with their effect on the quality of semi-products at applying the nanoreagents for an additional treatment of the sugar-containing solutions in the beet sugar production. The work considered the possibility of applying the additional reagents on the base of aluminium nanoparticles in the process of lime pretreatment of the diffusion juice.

Materials and Methods

The nanopowders of biogenic metals were produced by the combined precipitation of metals and halogenide of alkali metals from the gas phase [14, 15]. Encapsulation of metallic particles into a chemically inert matrix limits them by sizes on the one hand and on the other hand it provides formation of a protective coat on their surface (Fig. 1). This does not only prevent the processes of consolidation of particles during storage, but also protects them from their interaction with environment.

Statistic processing of results of measurement using the computer program Image Pro Plus is given in Table 1, that allowed plotting a diagram of distribution of nanoparticles by sizes, given in Fig. 2. It is seen from the diagram that the sizes of these particles are 6–7 nm.

Such composite structure allows the encapsulated nanoparticles to be stored for a long time in ordinary atmosphere and then to be used by dissolution of the salt coat for producing the colloidal solution [16–18].

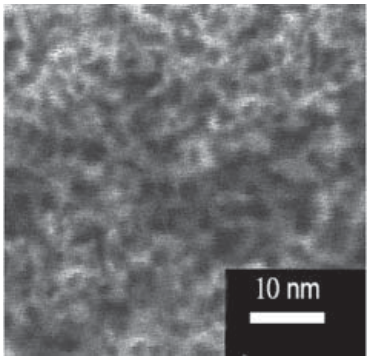

Fig. 1. **Electron-microscopic image of condensate: light background**

To provide a long-time stabilization of the nanopowders in the form of a colloidal solution, a method of dispersion of these powders into compositions of PEG (PEG 1500–8000 in the volume of 4–7 parts and PEG 400–600 in the volume of 3–6 parts) was developed. The initial powder, placed into fluid, was subjected to dispersion for 60 min, accompanied by heating up to 60–80 °C. However, the same as any colloid, this system will tend to agglomeration under the action of external factors. Therefore, to prevent this phenomenon, the rapid cooling of the colloidal solution is used at the last stage of producing. Such an approach makes it possible to store the produced gel for a long time in a compact form. The appearance of high-viscosity colloidal solution (gel) is shown in Fig. 3.

To reduce the viscosity of this gel is possible by introducing into the water suspension. The properties of this produced suspension were

Table 1. **Statistic processing of the nanoparticles observation using the computer program Image Pro Plus**

Diameter of particles, nm	Frequency, %	Number of investigated particles
4	15	298
5	16	325
6	21	421
7	12	236
8	15	292
9	9	185
10	6	124
11	6	128

Hereinafter: * — $P < 0.05$.

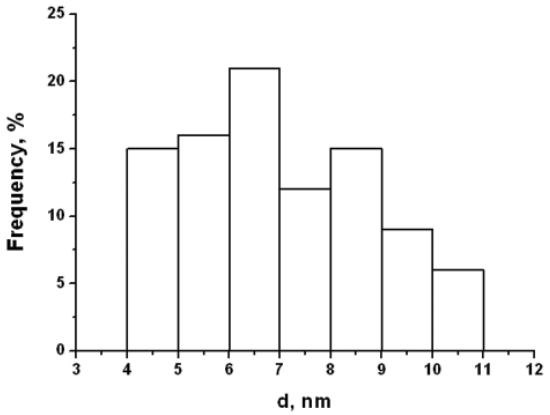

Fig. 2. **Distribution of particles by sizes**

investigated by using the device Malvern Zetasizer Ver. 7.11. From Fig. 4, at which the distribution of particles by sizes is presented, it is seen that such reducing of viscosity does not cause an aggregation process. The size of particles remains within the nanorange [19].

By comparing Fig. 2 and 4, it is possible to conclude that the average size of particles in the solution is smaller than in a precursor. It can be assumed that the particles in the precursor are more agglomerated, and in the process of solution producing the division of agglomerated particles is occurred, in particular, under the ultrasound effect.

Effectiveness of reagents for additional treatment of sugar-containing solutions

During investigations a diffusion juice was used, produced in the laboratory conditions by water extraction from beet chips. In the produced juice the main its quality characteristics were determined, namely: content of solids, sucrose, its purity was calculated (ratio of sucrose content to solids content, in %). Content of protein and pectin components (as main components of colloidal fraction of diffusion juice) was also determined, which makes the proceeding of treatment processes difficult to the greatest extent. As a main reagent for carrying out the process of lime treatment, a lime milk of 1.18 g/cm^3 density was used, prepared by liming of burned lime by hot water [20].

Fig. 3. **Appearance of high-viscosity colloidal solution (gel)**

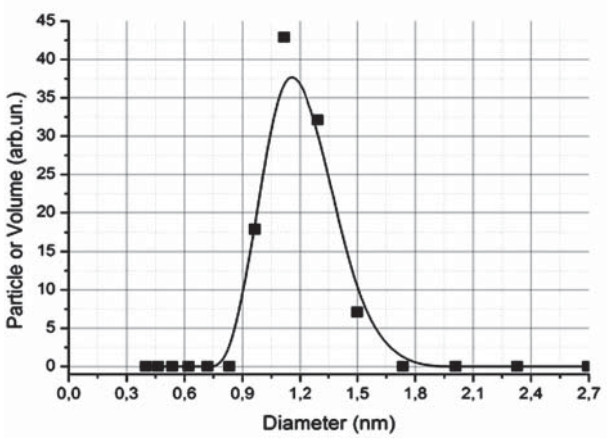

Fig. 4. **Distribution of aluminium particles by sizes**

As the main aim of the lime pretreatment of the diffusion juice consists in maximum precipitation of components of colloidal dispersity (protein and pectin components) by the lime milk and producing a well-structured precipitate [20], then at the first stage of the investigations the task was put for determination of effect of additional reagents, containing aluminium in a nanoform, on colloidal component of the diffusion juice proper. Two modifications of reagents were used: DAl4 (No.807) and DAl5(No.805). Characteristic of these reagents is given in Table 2.

Experiment was made according to the following procedure. Six test samples of diffusion juice of 100 cm^3 volume were heated up to 60 °C temperature (typical temperature of carrying out the process of lime pretreatment of juice). The preliminary calculated value of reagent in the range of 0.25...1.5 g (with content of Al nanoparticles in the limits of 0.0013...0.0078 g) was added to the preheated samples at continuous stirring. The obtained samples were stirred for 10 min at constant temperature and then at stirring during 15 min the lime milk was added up to producing of value pH of mixture of 11.2...11.3 (final point of lime pretreatment). Then, precipitate was separated in the obtained samples by a filtering and in the filtrates the purity, content of protein and pectin components were determined. The obtained results are given in Tables 1 and 2. For comparison, the treatment of the diffusion juice was also made by the lime milk without adding of Al nanoparticles (reference sample). In this case the quality of initial diffusion juice was the following: purity — 83.3%, content of protein components — 0.887 g/100 g of juice; pectin components — 0.29 g/100 g of juice.

The obtained results show that the additional reagents have a different effect on value of changing in purity of the diffusion juice in the process of its treatment. Thus, when adding the reagent DAl4(No.807) in the amount of 0.0052...0.0078 g/100 g of juice the improvement of its quality characteristics is observed (purity, content of protein and pectin

Table 2. **Characteristic of colloidal solutions of high viscosity (gels)**

No. of reagent	Characteristic of reagent		
	Volume fraction of nanoparticles in precursor	Concentration of nanoparticles of Al in colloid high-viscosity solution	Dav, nm
DAl4 (No.807)	25%	52 mg/10 g	1.2–1.5
DAl5 (No.805)	30%	51 mg/10 g	1.2–1.5

Table 3. **Results of interaction of reagent DAl4(No.807) in the process of diffusion juice treatment with a lime milk**

No. of test sample	Quantity of DAl4(No.807), g/100 g of juice	Purity,%	Content in test sample	
			Protein components, g/100 g of juice	Pectin components, g/100 g of juice
0 Control	0	84.3	0.414	0.212
1	0.0013	84.55	0.406	0.210
2	0.0026*	84.84	0.368	0.206
3	0.0039	85.20	0.350	0.200*
4	0.0052	85.36	0.344	0.198*
5	0.0065	85.40	0.346*	0.192*
6	0.0078	85.39	0.350	0.201

Hereinafter: * — $P < 0{,}05$ compared with control

Table 4. **Results of interaction of reagent DAl5(No.805) in the process of diffusion juice treatment with a lime milk**

No. of test sample	Quantity of DAl5(No.805), g/100 g of juice	Purity, %	Content in test sample	
			Protein components, g/100 g of juice	Pectin components, g/100 g of juice
0 Control	0	84.3	0.414	0.212
1	0.0013	84.25	0.226*	0.110*
2	0.0026	84.10	0.210*	0.100*
3	0.0039	82.12	0.115*	0.094*
4	0.0052	80.29*	0.112*	0.086*
5	0.0065	77.34*	0.100*	0.080*
6	0.0078	77.39*	0.098*	0.079*

components) as compared with a control sample without the reagent addition. The visual inspection for the formation and quality of the precipitate showed that at such consumptions the active formation and quick precipitation of the precipitate particles is observed. This gives an opportunity to separate this precipitate and avoid its effect on proceeding of further processes of the diffusion juice treatment (for example, main lime pretreatment, carried out under the conditions of high alkalinity and temperature, which destroy the earlier formed precipitate).

For the reagent DAl5(No.805) the results of experiments showed its negative effect on the result of treatment of the juice samples. Though the effect of removal of protein and pectin components is rather higher than that in reagent DAl4(No.807), but the purity of this juice is occurred to be very low, that proves about the additional removal of sucrose from the juice. The decrease in content of sucrose for treatment of the diffusion juice can be, probably, explained by the formation by an aluminium saccharate, which is precipitated into the precipitate together with other colloidal particles in system [$Al(OH)_3$ +

$C_{12}H_{24}O_{12} \rightarrow C_{12}H_{21}O_{12}Al + 3H_2O$]. For the technology of sugar production from the beet this effect is not admissible. The visual inspection for the formation of the precipitate showed the similar results. Therefore, this reagent has, possibly, the higher purifying effect on other semi-products of the beet sugar production, which do not contain sucrose, for example, feed water for proceeding the process of sugar extraction from the beet.

Thus, during experiments the effect of the reagents, containing aluminium in the nanoform, on degree of removal of components of the colloidal dispersity in the process of the diffusion juice purification in the beet sugar production, is shown. In future these investigations will be continued for determination of an optimum time of interaction and effect of applying the additional reagents on the efficiency of the processes.

REFERENCES

1. *Shtangeev V. O., Kober V. T., Belostotskiy L. G., Lagoda V. A., Shestakovskij V. A.* Sovremennie technologii I oborudovanie sveklosaharnogo proizvodstva. *Tcukor Ukrainy*. 2003, V. 1, 352 p. (In Russian).
2. *Reva L. P., Pushanko N. N., Zamura S. A.* Ispolzovanie aktivnoj kremnievoj kisloti dlya dopolnitelnoj ochistki diffuzionnogo soka. *Tcukor Ukrainy*. 2008, N 3, P. 11–16. (In Ukrainian).
3. *Verchenko L. M., Tkachenko S. V., Marinin A. I., Lopatko K. G.* Pervij opit ispolzovaniya reagenta v nanorazmernom sostoyanii dlya dopolnitelnoj ochistki diffuzionnogo soka v sveklosaharnom proizvodstve. *Tcukor Ukrainy*. 2012, N 12, P. 11–16. (In Ukrainian).
4. *Duran N., Marcato P. D.* Nanobiotechnology perspectives. Role of nanotechnology in the food industry: a review. *Int. J. Food Sci. Technol*. 2013, N 48, P. 1127–1134.
5. *Zimon A. D.* Kolloidnaya chimiya nanochastic. Chast 1. Osobennosti i svojstva nanochastic. Uchebnoe posobie dlya studentov technologicheskih specialnostej vseh form obucheniya. *MGutu*. 2010, 370 p. (In Russian).
6. *Amin M. T., Alazba A. A., Manzoor U.* A review of removal of pollutants from water/wastewater using different types of nanomaterials. *Alamoundi Water Res.* 2014, N 3, P. 10–38.
7. *Dongsheng W., Shuifeng W., Chihpin H., Chow C.* Hydrolyzed Al(III) clusters. Speciation stability of nano-Al13. *J. Environm. Sci.* 2011, P. 706–710.
8. *Wang Y., Gao B., Xu X., Xu W.* The effect of total hardness and ionic strength on the coagulation performance and kinetics of aluminum salts to remove humic acid. *Chem. Engin. Jl*. 2010, N 1, P. 150–156.
9. *Xu W., Gao B., Du B.* Influence of shear force on floc properties and residual aluminum in humic acid treatment by nano-Al13. *J. Hazardous Mat*. 2014, N 271, P. 1–9.
10. *Xu H., Wang D., Ye* C. Survey of treatment process in water treatment plant and the characteristics of flocs formed by two new coagulants. *Coll. Surfaces*. 2014, N 456, P. 211–221.
11. *Lopatko K. G., Tkachenko S. V., Olishevskij V. V., Verchenko L. M., Marinin A. I., Arodinskij O. V.* Nanotechnologii v chukrovij promislovosti. *Naukovyj vicnyk NUBiPU. Seria «Technika ta energetyka APK»*. 2012, 170 (1), 361–366. (In Ukrainian).
12. *Reva L. P., Pushanko N. N., Zamura S. A.* Sposib ochijennya difuzijnogo soku. *UA Patent №93206*. January 25, 2011. (In Ukrainian).
13. *Reva L. P., Pushanko N. N., Alekseeva L. V.* Pidvijennya efektivnosti ochijennya difuzijnogo sokuobroblennyam iogo filtroperlitom. *Tcukor Ukrainy*. 2008, N 2, P. 24–27. (In Ukrainian).
14. *Ustinov A. L., Melnichenko T. V., Liapina K. V., Chaplyuk V. I.* Method of producing encapsulated nanopowders and installation for its implement. *U. S. Patent 8491972B2*. July 23, 2013.
15. *Ustinov A. L., Melnichenko T. V., Liapina K. V., Chaplyuk V. I.* Sposob polucheniya inkapsulirovannih nanoporoshkov i ustanovka dlya ego realizacii. *UA Patent №82448*. April 10, 2008. (In Russian).
16. *Dulnev P. G., Liapina K. V., Davidova O. E., Ustinov A. I.* Sposob dispergirovaniya i stabilizacii nanochastic medi v vodnich sredah. *UA Patent №91374*. July 10, 2014. (In Russian).
17. *Liapina K. V., Dulnev P. G., Marinin A. I., Melnichenko T. V., Ustinov A. I.* Method to produce suspensions using encapsulated nanopowders of 3-d metals as precursors. *Title for the book: Nanomaterials Imaging Techniques, Surface Studies, and Applications Publisher: Springer Springer Physics series.* 2013.
18. *Marinin A. I., Olishevskij V. V., Pushanko N. N., Dulnev P. G.* The influence of colloidal solutions on the basis of aluminium on clearing of sugar manufacture products. *III International research and practice conference «Nanotechnology and nanomaterials»*. Lviv, Ukraine, August 26–29, 2015.
19. *Dulnev P. G., Marinin A. I. , Melnichenko T. V., Ustinov A. I.* Preparation and properties of the collodial solution based on biogenic metal nanoparticles. *Biotechnol. acta.* 2014, V. 7, N 6.
20. Pravila vedennya technichnogo procesu virobnictva cukru z buryakiv (Pravila ustalenoi praktiki 15.83-37-106:2007). *Kyiv: Naukova dumka*. 2007, 419 p. (In Ukrainian).

ВАПНЯКОВЕ ОЧИЩЕННЯ ЦУКРОВМІСНОГО РОЗЧИНУ КОЛОЇДНИМИ РОЗЧИНАМИ ВИСОКОЇ В'ЯЗКОСТІ

К. В. Ляпіна[1], *П. Г. Дульнєв*[2], *А. І. Маринін*[3], *Н. М. Пушанко*[3], *В. В. Олішевський*[3]

[1]Інститут електрозварювання ім. Є. О. Патона НАН України, Київ
[2]Інститут біоорганічної хімії та нафтохімії НАН України, Київ
[3]Національний інститут харчових технологій, Київ, Україна

E-mail: kirulya@mail.ru

Метою роботи було визначити ефективність сумісного використання вапняку та суспензій високої в'язкості, що містять як прекурсор наночастинки алюмінію, під час очищення цукровмісних розчинів.

На першому етапі отримували інкапсульований у сольову матрицю нанопорошок алюмінію спільним осадженням із парової фази металу та галогеніду лужного металу NaCl. Для тривалої стабілізації наночастинок алюмінію застосовували розроблений авторами спосіб диспергування цих порошків у композиції поліетиленгліколей, одержуючи колоїдний розчин високої в'язкості — гель. На другому етапі як об'єкт дослідження використовували дифузійний сік, отриманий в лабораторних умовах екстрагуванням водою бурякової стружки. Визначали основні показники якості соку: вміст сухих речовин, сахарози, протеїнових і пектинових речовин (як основних складових колоїдної фракції дифузійного соку), а також його чистоту — співвідношення вмісту сахарози і сухих речовин (у %). Як основний реагент для проведення процесу попереднього вапнування використовували вапняне молоко зі щільністю 1,18 г/см^3, приготоване шляхом гасіння обпаленого вапна гарячою водою.

У ході експериментів показано ефективність препаратів, що містять алюміній у наноформі, їх вплив на ступінь видалення речовин колоїдної дисперсності у процесі очищення дифузійного соку в цукробуряковому виробництві та підвищення його якості. Одержані результати свідчать про те, що залежно від способу отримання досліджувані додаткові реагенти з наночастинками алюмінію справляють різний ефект на зміну чистоти дифузійного соку в процесі його оброблення вапняним молоком.

Ключові слова: нанопорошок алюмінію, вапнякове очищення цукровмісного розчину.

ИЗВЕСТКОВАЯ ОЧИСТКА САХАРОСОДЕРЖАЩЕГО РАСТВОРА КОЛЛОИДНЫМИ РАСТВОРАМИ ВЫСОКОЙ ВЯЗКОСТИ

К. В. Ляпина[1], *П. Г. Дульнев*[2], *А. И. Маринин*[3], *Н. Н. Пушанко*[3], *В. В. Олишевский*[3]

[1]Институт электросварки им. Е. О. Патона НАН Украины, Киев
[2]Институт биоорганической химии и нефтехимии НАН Украины, Киев
[3]Национальный институт пищевых технологий, Киев, Украина

E-mail: kirulya@mail.ru

Целью работы было определение эффективности совместного использования извести и высоковязких суспензий с содержанием в качестве прекурсора наночастиц алюминия при очистке сахаросодержащих растворов.

На первом этапе получали инкапсулированный в соляную матрицу нанопорошок алюминия совместным осаждением из паровой фазы металла и галогенида щелочного металла NaCl. Для длительной стабилизации наночастиц алюминия применяли разработанный авторами способ диспергирования этих порошков в композиции полиэтиленгликолей, получая коллоидный раствор высокой вязкости — гель. На втором этапе в качестве объекта исследования использовали сок сахарной свеклы, полученный в лабораторных условиях экстрагированием водой свекловичной стружки. Определяли основные показатели качества сока: содержание сухих веществ, сахарозы, протеиновых и пектиновых веществ (как основных составляющих коллоидной фракции диффузионного сока), а также его чистоту — соотношение содержания сахарозы и сухих веществ (в %). В качестве основного реагента для проведения процесса предварительного известкования использовали известковое молоко с плотностью 1,18 г/см^3, приготовленное путем гашения обожженной извести горячей водой.

В ходе экспериментов показана эффективность препаратов, содержащих алюминий в наноформе, их влияние на степень удаления веществ коллоидной дисперсности в процессе очистки диффузионного сока в свеклосахарном производстве и повышение его качества. Полученные результаты свидетельствуют, что в зависимости от способа получения исследуемые дополнительные реагенты с наночастицами алюминия оказывают различный эффект на изменение чистоты диффузионного сока в процессе его обработки известковым молоком.

Ключевые слова: нанопорошок алюминия, известковая очистка сахаросодержащего раствора.

UDK 582. 923.1.+ 58.084 **doi: 10.15407/biotech8.06.077**

ADAPTATION OF *Gentiana lutea* L. PLANTS OBTAINED *in vitro* TO *ex vitro* AND *in situ* CONDITION

O. Yu. Mayorova
L. R. Hrytsak
N. M. Drobyk

Hnatiuk Ternopil
National Pedagogical University, Ukraine

E-mail: majorova@i.ua

Received 21.10.2015

The aim of the research was to develop the technology of introduction of the *Gentiana lutea* L. plants obtained by microclonal propagation into conditions *in situ*. Methods of cultivation of plant objects *in vitro* were used. There were chosen optimal conditions for rooting *G. lutea* shoots obtained through microclonal propagation *in vitro:* MS/2 medium with twice decreased concentration of NH_4NO_3without vitamins and sucrose supplemented with 3 g/l of mannite and 0.05 mg/l kinetin, and agar (4 g/l) in combination with perlite (16 g/l) used as a maintaining substrate; or the nutrient medium (MS/2 without vitamins and smaller concentration of NH_4NO_3) with gradual decrease of carbohydrates from 10 g/l to 2 g/l, and further rooting experimental shoots in tap water. Rooted plants were adapted to conditions *ex vitro* through planting them into flowerpots with soil and gradual changing hothouse regime for exposed one. The share of adapted to *in situ* conditions plants (21% after a year of planting) proves the used method to be resultative and promising. Thus, there was suggested the most efficient technology for revival of disturbed *G. lutea* populations that includes repatriation of rooted and adapted to *ex vitro* conditions plants obtained through microclonal propagation *in vitro*.

Key words: *Gentiana lutea* L., rooting *in vitro*, adaptation ex *vitro*, repatriation *in situ*.

Within a concept of preserving biodiversity of plant and animal world, the investigations aimed at finding ways to stabilize the number of disturbed populations and revival of destroyed natural populations of rare plant species are of current relevance. While protecting such plant species, it is necessary to apply not only passive preservation methods (inventory, including into local lists of rare plants and Red Books of various ranks, conserving on reserved territories), but use active methods (growing in botanical gardens, increasing number of rare species in natural conditions by seeding and planting of obtained *in vitro* cultures) too [1].

Rare plant species, requiring protection and revival, include medicinal *Gentiana lutea* L. The complexity of *G. lutea* seed restoration, excessive pastoral load and recreation have led to reducing areas and violated structures of this species population. *G. lutea* value for conventional and nontraditional medicine, determined by the pharmacological properties and potential need in raw material, has caused the necessity to estimate the species resources in Ukraine for creating fundamental principles of preservation and developing new approaches to its population revival.

The recent years being marked by the developed methods of *G. lutea* microclonal propagation in *vitro* [2, 3], the repatriation of propagated in *vitro* plants into natural conditions has become of great importance. The essential condition for successful repatriation is the use of individuals grown in most approximated to natural conditions, and therefore minimally changed genetically [4].

The objective of the investigation was to develop a scheme of reintroducing *G. lutea* plants developed by microclonal propagation into *in situ* conditions.

Materials and Methods

The object of the investigation was *G. lutea* — a perennial with indefinitely long life cycle (over 50 years) and lasting pre-generative period (5–10 years) [5]. The initial seed

material was gathered during expeditions in the Ukrainian Carpathians in mountainous populations on Petros Marmarosky, Pozhyzhevska, Sheshul-Pavlyk, Menchul Kvasy mountains and Lemska and Rogneska mountainous valleys.

For choice of rooting *G. lutea* shoots *in vitro* we took into consideration biological and ecological peculiarities of the species and the results of *G. lutea* introduction *in vitro* culture, obtained in the laboratory of ecology and biotechnology of Volodymyr Hnatiuk Ternopil National Pedagogical University. For rooting, we used *G. lutea* shoots obtained by microclonal propagation and then grown for 1.5–3 months until they became 15–20 mm high with 3–5 pairs of leaves. Each testing variant included three samplings with 8–10 shoots.

Fourteen variants of media were tested (tables 1, 2). In eight tested variants, the cultivated *in vitro* shoots were planted in Murashige and Skoog medium (1962) with half concentration of macro- and microsalts (MS/2) without sucrose and vitamins (table 1). There were experimented two MS modifications media: MS/2 (variants I, II, III, IV); and MS/2 with twice decreased concentration of NH_4NO_3 (variants V, VI, VII, VIII), as the decrease of macro- and micro-elements and nitrogen concentration are known to promote rooting wild strawberry, apple-tree and other plant cuttings [6–9]. In addition, the research of the component soil composition from natural *G. lutea* areas showed that the amount of both available and general nitrogen in them was comparatively low. Growth regulators are known to negatively influence adaptation of plants to *ex vitro* conditions [9], so kinetin (Kin) concentration in all media was reduced to 0.05 mg/l.

For each modification of nutrient medium, we used various maintaining substrates such as agar (8 g/l) (I, V); agar (4 g/l) and perlite (16 g/l) (IV, VIII); agar (4 g/l) and ground perlite (16 g/l) (III, VII); foam (II, VI); vermiculite (IX). We also attempted to enroot shoots in a sterilized soil from natural *G. lutea* habitats combined with peat and perlite in correlation 1:1:1 (X).

There was tested nutrient medium MS/2 without vitamins with twice decreased concentration of NH_4NO_3 which was added with 2 g/l sucrose (as the main CO_2 source) (XI); two variants with different concentrations of sucrose and mannite in correlation 1:1 (XII, XIII); a variant with mannite only (XIV) with its concentration 3 g/l (table 2). Agar (4 g/l) combined with perlite (16 g/l) was used as a maintaining substrate. Adding mannite was caused by its being osmotically active substance providing antioxidant protection and promoting plant survival in stress [10, 11]. Plants were cultivated for 120 days on the media mentioned above.

G. lutea was cultivated in jars with ventilatory covers. The plants, infected during relocation or not forming roots on nutrient media, were placed into settled tap water. Rooted specimens were planted into flowerpots with soil, having their roots previously washed with distilled water to relieve them from the medium remains.

To avoid dehydration of the plants and create the greenhouse effect the flowerpots were covered with glass. Every day the plants were sprayed and once a week they were watered with settled tap water. Air expositions were used to make them adapt to *ex vitro* conditions. In 1–1.5 months the flowerpots were definitely opened, watering was done in dependence on soil drying (1–2 times a week), and spraying was daily.

In early June (after 8–10 months of the experiment beginning) the adapted to *ex vitro* conditions and then grown for 3–4 months *G. lutea* were planted *in situ* conditions in the places of bare soil near adult gentian individuals.

General state of plants in *ex vitro* and *in situ* conditions was estimated by morphological values (plant height, number of shoots, pairs of leaves and number of internodes per plant). The obtained data were processed statistically [12].

Results and Discussion

The adaptation efficiency of the obtained *in vitro* plants to *ex vitro* conditions depends in the first place on their successful rooting, as the existence of well-developed root system provides better adaptation of plants to growth in soil and unstable conditions of unsterile environment (fluctuations of humidity, temperature, etc.). Thus, the research included three stages: rooting obtained by microclonal propagation plants *in vitro*, adaptation of rooted plants to *ex vitro* conditions, transfer of adapted to *ex vitro* plants to conditions *in situ*.

Rooting G. lutea sprouts obtained by microclonal propagation. The results of the research show that both the composition of nutrient medium and the type of maintaining substrate (table 1) influenced *G. lutea* rooting. *G. lutea* shoots planted in agarized media (8 g/l) (I, V) and in vermiculite (IX) necrotized on the

20–30th day of cultivation, and those placed in media with agar (4 g/l) in combination with ground perlite (16 g/l) (III, VII) — on 20–40th day. Evidently, the consistency of nutrient medium decelerates absorbing of nutrient substances by plant roots that leads to their death. This result is confirmed by scientific literature data, pointing to the fact that growth and development of roots *in vitro* are dependent on aeration of nutrient medium that, in its turn, is dependent on agar concentration. Rooting plant cuttings is decelerated; the development of secondary roots does not take place [7].

The shoots planted into the nutrient media with foam substrate and decreased concentration of agar (up to 4 g/l) in combination with perlite (16 g/l) survived and rooted in dependence on medium composition. The individuals cultivated in MS/2 without vitamins and sucrose (II, VI), died on the 20th (II) and 30th (VI) day. Twice decreased concentration of NH_4NO_3 in MS/2 medium (VI, VIII) was more efficient. As a result, the share of viable specimens on the 50th day of cultivation constituted 45% (VI) and 66% (VIII), and on the 120th day, it was 10 % and 15% respectively. Obviously, the composition of nutrient medium serves as a limiting factor in such a combination of nutrient medium and maintaining substrate.

Thus, one can assume that using MS/2 medium with twice decreased NH_4NO_3 concentration and maintaining substrates such as foam and agar (4 g/l) combined with perlite (16 g/l) positively influences rooting shoots. As the results of shoots survival on conditions of using foam and agar with perlite did not sufficiently differ, one can use both variants for further cultivation. However, referring to the objective of the research, we find the use of the second variant more efficient as semi-solid maintainig substrate will enable better adaptation of plant root system to growth conditions in soil. Other researchers prove positive effect of using agar combined with perlite as a maintaining substrate: plants of wild strawberries, apples, pears, ashes, lilac formed a well-developed root system on such a substrate [7].

On conditions of rooting *G. lutea* shoots in sterilized soil with adding peat and perlite in correlation 1:1:1 all the tested shoots died on 20–30th day. Evidently, soil sterilization

Table 1. **Rooting of *G. lutea* shoots *in vitro***

Days	Percentage of viable shoots, %								
	MS/2 medium without vitamins and sucrose supplemented with 0.05 mg/l Kin				MS/2 medium without vitamins and sucrose; with twice decreased concentration of NH_4NO_3, supplemented with 0.05 mg/l Kin				Vermiculite
	Maintaining substrate								
	Ag	F	Ag+gPr	Ag+Pr	Ag	F	Ag+gPr	Ag+Pr	
	I	II	III	IV	V	VI	VII	VIII	IX
10	51±3.8	84±3.5	42±2.4	100	49±3.2	100*	100*	100*	100
20	0	0	0	27±1.8	0	100*	18±1.4*	93±5.4*	43±3.2
30	0	0	0	0	0	100*	44±2.8*	93±5.4*	0
40	0	0	0	0	0	85±5.4*	0	71±4.7*	0
50	0	0	0	0	0	45±3.6*	0	66±4.2*	0
60	0	0	0	0	0	30±3.1*	0	48±3.9*	0
90	0	0	0	0	0	10±1.5*	0	43±3.3*	0
120	0	0	0	0	0	10±1.5*	0	15±1.8*	0

Notes: Ag, F, Ag + gPr, Ag + Pr — maintaining substrates;

Ag — agar (8 g/l), F — foam, Ag + gPr — agar (4 g/l) combined with ground perlite (16 g/l), Ag + Pr — agar (4 g/l) combined with perlite (16 g/l);

* — marked variants of the experiment in which the parameters of share of viable shoots during use of modified variants MS/2 media with twice decreased concentration of NH_4NO_3 reliable ($P \leq 0.05$) differ from the results on nutrient media MS/2 with full NH_4NO_3 concentration.

leads to death of mycorrhizal organisms that negatively affects growth and development of *G. lutea*, which is a mycorrhizal species [13].

An attempt to enroot *G. lutea* shoots on the medium suggested by Petrova and colleagues [14] and which was efficient for rooting and further adaptation of obtained *in vitro G. lutea* plants to *ex vitro* conditions, and then to *in situ* in Natural Park of Vitosha (Bulgaria) failed to have any positive results in our case. None of the cultivated *in vitro* shoots formed roots that is probably caused by genotype peculiarities and heterogeneity of natural habitats of plants.

The shoots cultivated on the medium without sucrose and additional supply of CO_2 died probably because of the complexity of adaptation to autotrophic type of nutrition, little photosynthetic activity and scarcity of oxygen. Therefore, for further cultivation, we used nutrient medium MS/2 without vitamins with twice decreased concentration of NH_4NO_3 and added carbohydrates (XI, XII, XIII, XIV) (Table 2).

The shoots cultivated on XI, XII and XIII variants of the medium were viable on the 30th day, but they did not form roots. That is why all the specimens for rooting were planted in tap water, covered with caps, which were gradually opened to adapt the plants to *ex vitro* conditions. On the 20th day after planting into water 38% of specimens demonstrated rhizogenesis, and on the 90th day 94% of the specimens formed roots. The *G. lutea* shoots grown on XIV variant of the medium also formed roots (Fig.1), the percentage of adaptation on the 120th day of cultivation was 97 (Table 2).

The analyzed results show that efficiency of rooting *G. lutea* shoots can be provided only by combination of optimal composition of nutrient medium and favourable for rooting maintaining substrate. The optimal medium among those tested proved to be MS/2 medium with twice decreased concentration of NH_4NO_3 without vitamins and sucrose supplemented with 3 g/l mannite and 0.05 mg/l Kin and agar (4 g/l) combined with perlite (16 g/l) used as a maintaining substrate. Gradual diminishing carbohydrates from 10 g/l to 2g/l in the nutrient medium (MS/2 without vitamins and twice decreased concentration of NH_4NO_3) with further rooting of the shoots in tap water proved equally efficient (Fig. 1).

Adaptation of the rooted plants to ex vitro conditions. Repatriation in disturbed populations of plants obtained through microclonal propagation *in vitro* first requires solving the problem of their adaptation

Table 2. **Rooting of *G. lutea* shoots**

<table>
<tr><td rowspan="3">Days</td><td colspan="4">Percentage of viable shoots, % / Percentage of rooted plants, %</td></tr>
<tr><td colspan="4">MS/2 medium with twice decreased concentration of NH_4NO_3 without vitamins, supplemented with 0.05 mg/l Kin, and agar (4 g/l) in combination with perlite (16 g/l) used as a maintaining substrate</td></tr>
<tr><td>2 g/l sucrose</td><td>2 g/l sucrose,
2 g/l mannite</td><td>1 g/l sucrose,
1 g/l mannite</td><td>3 g/l mannite</td></tr>
<tr><td></td><td>XI</td><td>XII</td><td>XIII</td><td>XIV</td></tr>
<tr><td>10</td><td>100/0</td><td>100/0</td><td>100/0</td><td>100/0</td></tr>
<tr><td>20</td><td>100/0</td><td>100/0</td><td>100/0</td><td>100/0</td></tr>
<tr><td rowspan="2">30</td><td>100/0</td><td>100/0</td><td>100/0</td><td rowspan="2">100/54±3.2</td></tr>
<tr><td colspan="3">Shoots planted into tap water</td></tr>
<tr><td>40</td><td colspan="3">100*/0</td><td>97±4.7*/97±4.7</td></tr>
<tr><td>50</td><td colspan="3">100*/38±2.8</td><td>97±4.7*/97±4.7</td></tr>
<tr><td>60</td><td colspan="3">94±5.3*/72±6.1</td><td>97±4.7*/97±4.7</td></tr>
<tr><td>90</td><td colspan="3">94±5.3*/94±5.3</td><td>97±4.7*/97±4.7</td></tr>
<tr><td>120</td><td colspan="3">94±5.3*/94±5.3</td><td>97±4.7*/97±4.7</td></tr>
</table>

Note: * — marked variants of the experiment in which the parameters of the share of viable shoots, on conditions of using modified variants of MS/2 media with twice decreased concentration of NH_4NO_3 supplemented with carbohydrates reliable ($P \leq 0.05$) differ from the results on the nutrient MS/2 medium with twice decreased concentration of NH_4NO_3 without carbohydrates (Table 1, VIII variant of nutrient medium).

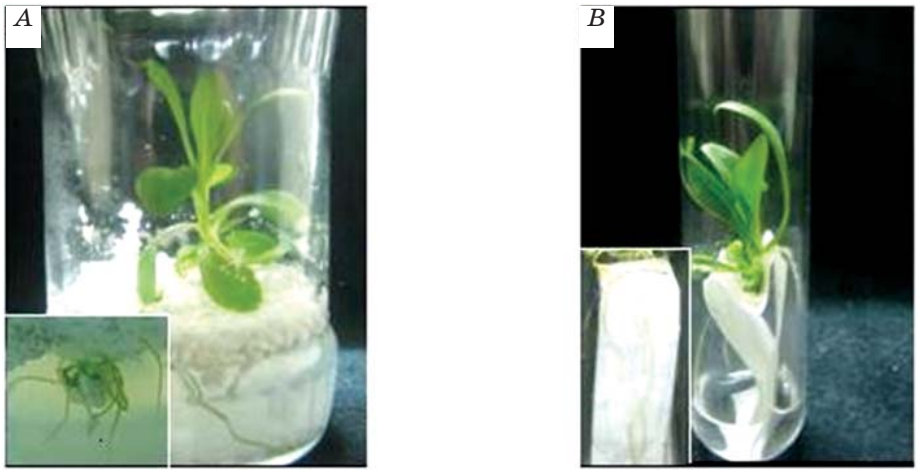

Fig. 1. **Rooting *G. lutea* shoots *in vitro*:**
A — rooting in the medium MS/2 with twice decreased concentration of NH_4NO_3 without vitamins and sucrose, supplemented with 3 g/l mannite and 0.05 mg/l Kin, the maintaining substrate is agar (4 g/l) combined with perlite (16 g/l); *B* — rooting in tap water

to *ex vitro* conditions. According to the research literature data [15–17], this process is labour intensive, as specific conditions of *in vitro* culture in many cases cause the formation of microshoots with defective physiological processes, morphological and anatomical structure. After transplantation from cultivation-vessels to *ex vitro* conditions such plants may be damaged because of altered cultivation conditions and therefore they require adaptation.

For adaptation *G. lutea* to *ex vitro* conditions the plants which formed roots in tap water and in the medium with twice decreased concentration of NH_4NO_3 and mannite were planted in soil (Fig. 2) To avoid drying of plants and their better adaptation to *ex vitro* conditions the flowerpots with planted specimens were covered by glass. Air expositions were done for 4–6 weeks, the duration and frequency of openings were gradually increased.

Percentage of adaptation for plants from various experimental variants somewhat differed (Fig. 3). Thus, on the 30th day the share of adaptation for plants which previously formed roots in water was higher compared to the plants cultivated in nutrient medium (XIV). However, the percentage of viable plants from both variants did not significantly differ hereafter and on the 150th day constituted 72.4% (rooted in tap water) and 70.8% (rooted in nutrient medium).

To estimate the condition of *G. lutea* individuals, we determined some morphometric parameters: height of plants (to clarify their adaptive capacity), number of pairs of leaves (leaves are the main organs of photosynthetic activity), and the number of internodes (to show adaptive changes of plants to *ex vitro* conditions, as internodes formation is the peculiarity of *G. lutea* plants cultivated *in vitro*).

It was shown that within the period from the 1st to 30th day the accretion of plants rooted

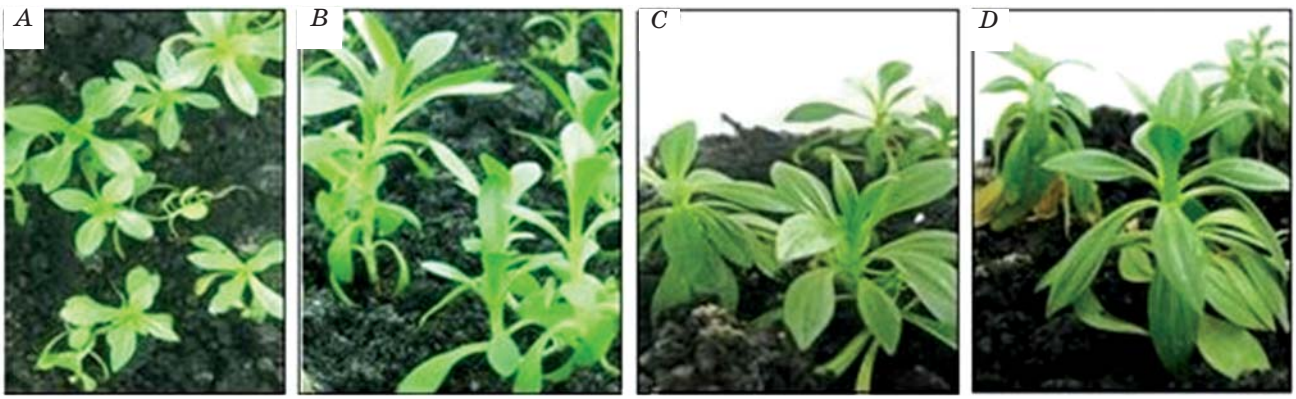

Fig. 2. ***G. lutea* planted in soil:**
vegetation duration 30 (*A*), 60 (*B*), 90 (*C*), 120 (*D*) days

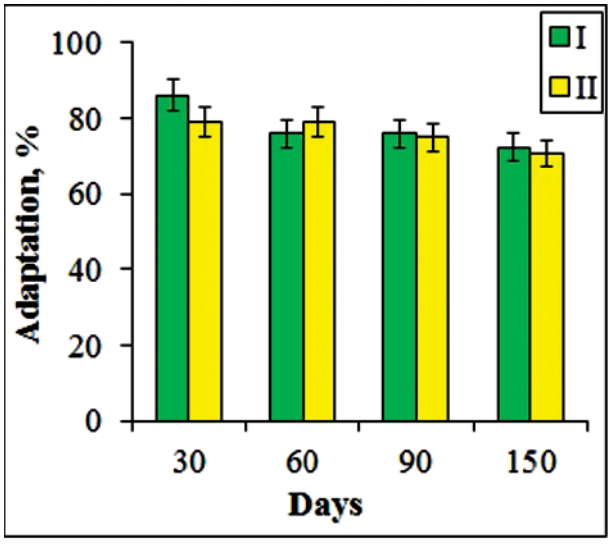

Fig. 3. **Adaptation in soil for plants rooted *in vitro*:**
I — percentage of adaptation for plants which formed roots in tap water;
II — percentage of adaptation for plants rooted in the nutrient medium MS/2 with twice decreased concentration of NH_4NO_3 without vitamins and sucrose, supplemented with 3 g/l mannite and 0.05 mg/l Kin, the maintaining substrate is agar (4 g/l) combined with perlite (16 g/l)

in the nutrient medium was 1.6 times higher compared with the plants which formed roots in water (Table 3). This phenomenon can be explained by the available reserve of nutrient substances stored in the organs of plants from the nutrient medium. From 30th to 90th day, the results were the opposite: accretion of the rooted in water plants was twice bigger that may testify to faster adaptation to *ex vitro* conditions. From 90th to 120th day the accretion of plant height was 1.3 times bigger for specimens rooted in the nutrient medium.

During growing in soil, the rooted in tap water plants formed on average 4–5 pairs of leaves and those rooted in the nutrient medium — 2–3 ones. That proves more intense photosynthetic activity, better viability and adaptation to *ex vitro* conditions. The number of internodes was the same in both variants. Besides, merome formation decreased in the process of cultivation and on 150th day it stopped (Table 3). Evidently, in *ex vitro* conditions *G. lutea* acquire morphological structure of intact plants, as the formation of radical rosette is representative for this species in nature [18].

Thus, the percentage of adaptation and accretion of plants rooted in tap water and in the nutrient medium did not practically differ. For rooting and further adaptation to *ex vitro* conditions, *G. lutea* can be planted in both water and medium MS/2 with twice decreased concentration of NH_4NO_3 without vitamins and sucrose, supplemented with 3 g/l mannite and 0.05 mg/l Kin. It is reasonable to use agar (4 g/l) combined with perlite (16 g/l) as a maintaining substrate.

Transplantation of adapted ex vitro plants into conditions in situ. At the beginning of June all viable and adapted to *ex vitro* conditions individuals were planted in natural conditions on Pozhyzhevska mountain (territory of the Carpathian National Natural Park) (Fig. 4). The area is located on the slope of northern-western exposition with steepness 20–40° 1450 m high above sea level.

According to literature data [19, 20], which were confirmed by our research, germination and taking to root of undergrowth for *Gentiana* species, including *G. lutea*, take place best in conditions of disturbed gramineous sodding. That is why the individuals were planted in places of bare soil to reduce the level of interspecies competition and provide optimal conditions for *G. lutea* adaptation and growth.

On the 3rd day of growth in natural conditions, we observed the loss of turgor in 15 ± 1.2% plants; on the 30th day the share of adapted plants constituted 97 ± 2.5%. The plants were viable, 2.5–7.5 cm high, with 6–16 pairs of leaves (Table 4). Evidently, their adaptation *in situ* was favoured by weather conditions of highland, as it rained almost every day in June–July, 2013. On the 60th day of growing the share of viable plants was 51 ± 1.8%. However, almost 40% of individuals died, having been eaten by small animals (rodents, lizards). Next year the share of viable plants equaled 21%.

General accretion of *G. lutea* height after 60 days of growing in natural conditions was insignificant (5.8 mm) that is probably caused not only by the complexity of adaptation, but biological peculiarities of the species too. Particularly, in the first years of ontogenesis *G. lutea* are known to grow slowly (2–5 cm/per year), forming 5–8 pairs of leaves [5]. The accretion of plants height from 30th to 60th day compared with the same value from 1st to 30th day was almost 3 times bigger that proves the successful adaptation. From 1st to 30th day the number of leaves was observed to increase, and from the 30th to 60th day — to decrease (Table 4). Probably the lack of rains in the first half of August resulted in drying out lower pairs of leaves.

Table 3. **Morphometric parameters of *G. lutea* planted in soil**

Morphometric parameters of plants rooted in tap water							
Parameters		at the time of planting	30th day	60th day	90th day	150th day	Total accretion
PH, mm	X± Sx	29±3.2	34±2.5	42±3.4	44±4.0	53±6.2	–
	Accretion	–	5±0.4*	8±0.6*	2±0.2*	9±0.6*	24±0.7
NPL, pieces	X± Sx	7.8±0.77	9.3±0.82	10.1±0.75	10.3±0.76	12.0±0.89	–
	Accretion	–	1.5±0.2*	0.8±0.1	0.2±0.1	1.7±0.2*	4.2±0.3
NI, pieces	X± Sx	3.1±0.35	4.2±0.33	4.3±0.33	4.5±0.43	4.5±0.37	–
	Accretion	–	1.1±0.1	0.1±0.04	0.2±0.05	0	1.4±0.2
Morphometric parameters of plants rooted in the nutrient medium[1]							
PH, mm	X± Sx	43±4.3	51±6.4	56±7.9	57±8.1	69±6.8	–
	Accretion	–	8±0.5	4±0.4	1±0.2	12±0.7	25±0.8
NPL, pieces	X± Sx	8.8±0.73	9.5±0.80	10.2±0.84	10.5±1.10	10.8±1.16	
	Accretion	–	0.7±0.1	0.7±0.1	0.3±0.05	0.3±0.05	2.0±0.2
NI, pieces	X± Sx	3.9±0.83	4.7±0.99	5.1±0.96	5.3±0.30	5.3±0.30	–
	Accretion	–	0.8±0.1	0.4±0.09	0.2±0.06	0	1.4±0.2

Notes: PH — plant height, NPL — number of pairs of leaves, NI — number of internodes; [1] — the medium MS/2 with twice decreased concentration of NH_4NO_3 without vitamins and sucrose, supplemented with 3 g/l mannite and 0.05 mg/l Kin, the maintaining substrate is agar (4 g/l) combined with perlite (16 g/l);
* — marked variants of the experiment in which the morphometric parameters of plants rooted in the nutrient medium MS/2 with twice decreased concentration of NH_4NO_3 without vitamins and sucrose, supplemented with 3 g/l mannite and 0.05 mg/l Kin reliable ($P \leq 0.05$) differ from the parameters of plants rooted in tap water.

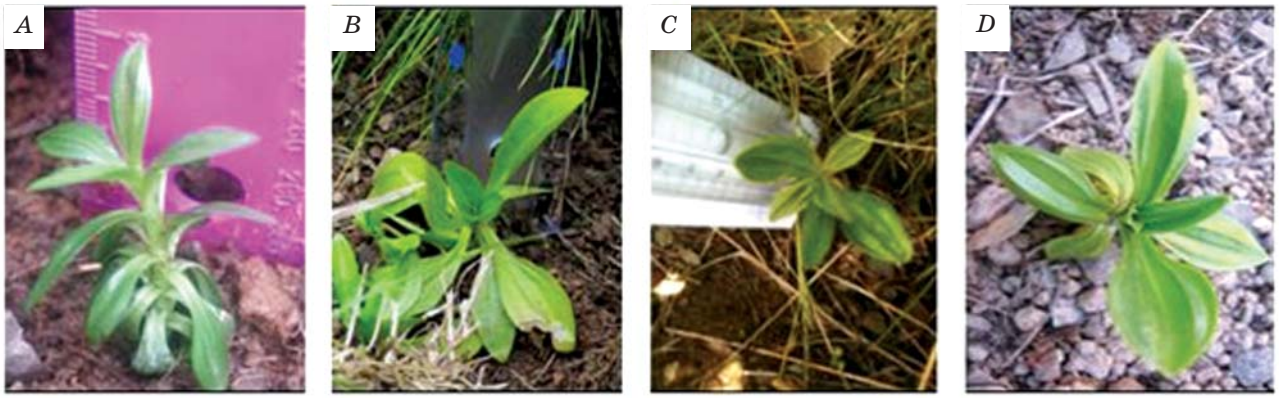

Fig. 4. ***G. lutea*** **planted in natural conditions:**
on 3rd (*A*), 30th (*B*), 60th (*C*) days of vegetation and a year after planting (*D*)

Within 60 days' period of *G. lutea* growing in natural conditions the length and width of lamina increased 7.8 and 2.9 times respectively. The formation of internodes stopped, and on the 60th day sporadic individuals had 1–2 internodes left, that proves that the plants acquired characteristic for the species habitus [18].

Thus, the conditions for rooting *G. lutea* shoots obtained by microclonal propagation have been chosen. It has been established that the biggest share of rooting shoots was provided by optimal combination of nutrient medium composition and supporting substrate. The medium MS/2 with twice decreased concentration of NH_4NO_3 without vitamins and sucrose, supplemented with 3 g/l mannite

Table 4. **Morphometric parameters of *G. lutea* planted *in situ* (Mt. Pozhyzhevska, 1450 m a.s.l.)**

Parameters		Time of measurement			Increase of morphometric parameters		
		1st day	30th day	60th day	1–30th day	30–60th day	60–90th day
Plant height, mm	X	41.4	42.9	47.2	1.5	4.3	5.8
	Sx	1.3	1.3	0.35			
	Sx′	1.84	1.63	1.70			
	Min	20.0	25.0	30.0			
	Max	70.0	75.0	75.0			
Number of internodes per plant, pieces	X	4.19	2.23	0.6	−2.67	−1.63	−4.30
	Sx	1.12	0.41	0.02			
	Sx′	1.47	0.58	0.13			
	Min	1.0	0	0			
	Max	10.0	4.0	1.0			
Number of pairs of leaves per plant, pieces	X	8.54	9.16	8.75	0.62	−0.41	0.21
	Sx	2.49	2.38	0.71			
	Sx′	2.69	2.64	2.97			
	Min	4.0	6.0	4.0			
	Max	13.0	16.0	14.0			
Length of lamina, mm	X	7.8	8.2	10.9	0.4	2.7	3.1
	Sx	0.08	0.1	0.13			
	Sx′	0.26	0.35	0.39			
	Min	5.0	5.0	7.0			
	Max	12.0	15.0	20.0			
Width of lamina, mm	X	3.6	4.7	6.8	1.1	2.1	3.2
	Sx	0.02	0.04	0.05			
	Sx′	0.09	0.1	0.17			
	Min	1.5	3.0	5.0			
	Max	4.5	7.0	10.0			

and 0.05 mg/l Kin and agar (4 g/l) combined with perlite (16 g/l) as a maintaining substrate proved to be the most efficient among all tested variants. Quite effective was also gradual diminishing of carbohydrates from 10 g/l to 2 g/l in the nutrient medium (MS/2 without vitamins and decreased concentration of NH_4NO_3) and further rooting of shoots in tap water.

There are chosen conditions for adaptation of rooted *in vitro* plants to conditions *ex vitro*. It has been found that plants rooted on both mentioned above variants can be used for this purpose. The obtained initial results of repatriation of *G. lutea* plants (21%) in natural habitats testify to efficiency of the suggested technology and rationality of its use for revival of disturbed gentian populations.

REFERENCES

1. *Rodinka O.* Methods of rare species protection in Sumy region. *Visnyk Lvivskoho universytetu. Seriia biolohichna*. 2004, N 36, P. 91–95. (In Ukrainian).
2. *Strashniuk N. M., Grycak L. R., Leskova O. M., Melnyk V. M.* Introduction in culture *in vitro* of some *Gentiana* L. genus species. *Fiziolohiia i biokhimiia kulturnykh roslyn*. 2004, 36 (4), 327–334. (In Ukrainian).
3. *Strashniuk N. M., Melnyk V. M., Grycak L. R., Leskova O. M., Kunah V. A.* Method of microclonal propogation of *Gentiana lutea* L. and *Gentiana acaulis* L. species. *Ukraine. Patent* 21499 UA, МПК C12N 5/00; A01H 4/00; C12N 5/04, March 15, 2007.
4. *Sobko V. G. Introduction* of rare and endangered species of the Ukrainian flora. *Kyiv: Naukova dumka*. 1996, 284 p. (In Ukrainian).
5. *Moskaliuk B. I.* The modern state of the populations of the high-mountain of *Gentiana* L. genus and the scientific base of their protection within the Ukrainian Carpathians. Ph.D. dissertation. *Natsionalnyi botanichnyi sad imeni M. M. Hryshka NANU*. Kyiv, Ukraine. 2010.
6. *Murashige T., Skoog F.* A revised medium for rapid growth and bioassays with tobacco tissue cultures. *Physiol. Plant*. 1962, 15 (13), 473–497.
7. *Demenko V. Y., Shestibratov K. A., Lebedev V. G.* The rooting is the key stage of the plant's propagation *in vitro*. *Izvestiya TSKhA*. 2010, N 1, P. 73–85. (In Russian).
8. *Krasinskaya T. A., Kuharchik N. V.* Effect of ion exchange substrate Biona-112 *Cerasus* Mill. plants morfological development during *ex vitro* adaptation. *Vesti Natsionalnoy akademii nauk Belarusii. Seriya agrarnykh nauk*. 2006, N 3, P. 54–59. (In Russian).
9. *Korosteleva N. I., Gromova T. V., Zhukova I. G.* Biotechnology. *Barnaul: izd-vo AGAU*. 2006, 127 p. (In Russian).
10. *Dolgova L. G., Samoylova M. V.* Proline contain — indicator of alien *Amelancheir* family plant persistance. Available at http://sites.znu.edu.ua/bio-eco-chem-sci/issues/index.php?lang=rus (accessed, N 3, 2009). (In Russian).
11. *Lobachevska O. V.* Content of free proline and activity of antioxidant protection in mosses under stress conditions. *Chornomorskyi botanichnyi zh*. 2008, 4 (2), 230–236. (In Ukrainian).
12. *Zaycev G. N.* Mathematical statistics in experimental botany. *Moskva: Nauka*. 1984, 424 p. (In Russian).
13. *Sykorova Z., Rydlova J.,* Vosatk*a M.* Establishment of mycorrhizal symbiosis in *Gentiana verna*. *Folia Geobotanica*. 2003, V. 38, P. 177–190.
14. *Petrova M., Zayova E., Vitkova A.* Effect of silver nitrate on *in vitro* root formation of *Gentiana lutea*. *Rom. Biotechnol. Lett*. 2011, 16 (6), 53–58.
15. *Nitish Kumar, Arpan R. Modi, Amritpal S. Singh.* Assessment of genetic fidelity of micropropagated date palm (*Phoenix dactylifera* L.) plants by RAPD and ISSP markers assay. *Physiol. Mol. Biol. Plants*. 2010, 16 (2), 207–213.
16. *Doi N., Takahachi R., Hikage T., Takahata Y.* Embryogenesis and doubled haploid production fromanther culture in gentian (*Gentiana triflora*). *Plant Cell Tiss. Organ Cult*. 2010, V. 102, P. 27–33.
17. *Medvedieva T. M.* The problems of acclimatization of micropropagated plants. *Fiziolohiia i biokhimiia kulturnykh roslyn*. 2008, 40 (1), 299–309. (In Ukrainian).
18. Red data Book of Ukraine. Vegetable kingdom. Vidp. za red. Ja. P. Diduh. *Kyiv: Globalkonsaltyng*. 2009, 900 p. (In Ukrainian).
19. Viability of plant populations of high-mountain zone of the Ukrainian Carpathians. *Z*a red. Y. Tsaryka. *Lviv: Merkator*. 2009, 172 p. (In Ukrainian).
20. *Geddes C., Miller G. R.* Long-term changes in the size of an Alpine Gentian, *Gentiana nivalis* L., population in Scotland. *Watsonia*. 2010, V. 28. P. 65–73.

АДАПТАЦІЯ ОДЕРЖАНИХ *in vitro* РОСЛИН *Gentiana lutea* L. ДО УМОВ *ex vitro* ТА *in situ*

О. Ю. Майорова
Л. Р. Грицак
Н. М. Дробик

Тернопільський національний педагогічний університет імені Володимира Гнатюка, Україна

E-mail: majorova@i.ua

Метою роботи було розробити технологію перенесення одержаних шляхом мікроклонального розмноження рослин *Gentiana lutea* L. в умови *in situ*. Використовували методи культивування рослинних об'єктів *in vitro*. Підібрано оптимальні умови для вкорінення отриманих мікроклональним розмноженням пагонів *G. lutea in vitro:* живильне середовище МС/2 з половинним вмістом NH_4NO_3 без вітамінів та сахарози, доповнене 3 г/л маніту та 0,05 мг/л кінетину, з використанням як підтримувального субстрату агару (4 г/л) у поєднанні з перлітом (16 г/л) або поетапне зменшення в середовищі МС/2 без вітамінів та зі зменшеною концентрацією NH_4NO_3 концентрації вуглеводів з 10 г/л до 2 г/л із подальшим укоріненням цих пагонів у водопровідній воді. Укорінені рослини адаптовано до умов *ex vitro* шляхом висаджування їх у горщики з ґрунтом та поступовим переведенням тепличного режиму до відкритого. Частка адаптованих до умов *in situ* рослин — 21% через рік після висаджування — свідчить про перспективність розробленого способу культивування. Таким чином, запропоновано один з ефективних способів відновлення ушкоджених популяцій *G. lutea*, що включає репатріацію в них укорінених та адаптованих до умов *ex vitro* рослин, отриманих мікроклональним розмноженням *in vitro*.

Ключові слова: *Gentiana lutea* L., вкорінення *in vitro*, адаптація *ex vitro*, репатріація *in situ*.

АДАПТАЦИЯ ПОЛУЧЕННЫХ *in vitro* РАСТЕНИЙ *Gentiana lutea* L. К УСЛОВИЯМ *ex vitro* И *in situ*

О. Ю. Майорова
Л. Р. Грицак
Н. М. Дробык

Тернопольский национальный педагогический университет имени Владимира Гнатюка, Украина

E-mail: majorova@i.ua

Цель работы — разработка технологии перенесения полученных путем микроклонального размножения растений *Gentiana lutea* L. в условия *in situ*. Использовали методы культивирования растительных объектов *in vitro*. Подобраны оптимальные условия укоренения полученных микроклональным размножением побегов *G. lutea in vitro*: питательная среда МС/2 с половинным содержанием NH_4NO_3 без витаминов и сахарозы, дополненная 3 г/л маннита и 0,05 мг/л кинетина, с использованием в качестве поддерживающего субстрата агара (4 г/л) в сочетании с перлитом (16 г/л) либо поэтапное уменьшение в среде МС/2 без витаминов и с уменьшенной концентрацией NH_4NO_3 концентрации углеводов с 10 г/л до 2 г/л с последующим укоренением этих побегов в водопроводной воде. Укоренившиеся растения адаптировали к условиям *ex vitro*, высаживая их в горшки с почвой, и постепенным переводом тепличного режима в открытый. Количество адаптированных к условиям *in situ* растений — 21% через год после высаживания свидетельствует о перспективности разработанного способа культивирования. Таким образом, предложен один из эффективных способов восстановления поврежденных популяций *G. lutea*, состоящий в репатриации в природные места произрастания укорененных и адаптированных к условиям *ex vitro* растений, полученных микроклональным размножением *in vitro*.

Ключевые слова: *Gentiana lutea* L., укоренение *in vitro*, адаптация *ex vitro*, репатриация *in situ*.

UDK 544.723:612.82:616.831-005.1-06-07 **doi: 10.15407/biotech8.06.087**

THE STATE OF THE WATER IN BRAIN TISSUE IN PRESENCE OF TS-100 SILICA NANOPARTICLES

T. V. Krupska[1]
S. V. Pakrishen[2]
O. V. Serov[2]
O. T. Volik[3]
V. V. Turov[1]

[1]Chuiko Institute of Surface Chemistry of the National Academy of Sciences of Ukraine, Kyiv
[2]The Post-mortem Department of Alexander Hospital, Kyiv, Ukraine
[3]The Medical and Pharmaceutical Faculty of Kyiv International University, Ukraine

E-mail: krupska@ukr.net

Received 24.09.2015

By the method of low-temperature ^{1}H NMR spectroscopy the structure of the hydrate layers of water associated with brain cells, the changes of these parameters during necrotic lesions (stroke) and in the presence of trifluoroacetic acid, which suggest to differentiate intracellular water clusters according to their ability to dissolve the acid, were studied. Also the impact of silica TS-100 nanoparticles on the state of water in brain tissue, namely on the water binding parameters in the air and in the presence of a weakly polar solvent was considered.

The distributions by the radii and change of Gibbs free energy for clusters of strongly bound interfacial water were obtained. It was shown that the hydration properties of the native brain tissue differ from the hydration properties of necrotic damaged tissue by the structure of weakly bound water clusters. In intact tissue all the water is associated and is a part of clusters and domains, most of which have a radii R = 2 and 20 nm. The media with chloroform stabilizes water polyassociates with the radius up to R = 100 nm and trifluoroacetic acid stabilizes water polyassociates with radii R = 7–20 nm. It was found that the partial dehydration of the investigated tissue samples is accompanied by decreasing of weakly bound water amount and some increasing of strongly bound water that indicates a change of molecular interactions between the components of cells-nanoparticles composite system. The ischemic necrosis area presence leads to decrease of water binding due to the average size water polyassociates increasing. This effect is observed both in air and in a weakly polar organic solvent medium (deuterochloroform).

Key words: ischemic stroke, the strongly and weakly bound water, ^{1}H NMR spectroscopy.

There are great achievements in the study of electrophysical characteristics of the different parts of brain at biotechnology development [1, 2], which can be compared with details of its morphological structure determined by magnetic resonance tomography (MRT) [3, 4]. It is known, there is 84% of intracellular water in brain (in neurons and glia). The presence of so much water amount in brain suggests the possibility of its active participation in the brain function not only as a medium providing delivery of nutrients to the cells and removing decomposition products (it is carried out by neuroglia cells) but also in specific functions performing.

The water in brain tissue cells is studied by NMR spectroscopy for more than 50 years [6–9] which served largely as the basis for creation and wide spreading of MRT methods. As a basic research method the low-temperature ^{1}H NMR spectroscopy was chosen [10–13], whereby we can determine the amount of strongly and weakly bound water by changes in the intensity of the NMR signal during the thawing process of samples, and using Gibbs-Thomson equations — the nonfreezing water clusters radii distribution [14, 15]. The magnitude of water chemical shift made it possible to calculate the average association degree of water molecules in polyassociates. This takes into account the fact that protons of not associated (weakly associated) water have a chemical shift δ_H = 1–1.5 ppm, ice-like structures characteristic for hexagonal ice have δ_H = 7 ppm [16], and liquid water has δ_H = 4.5–5 ppm.

Decreasing of the brain tissue cells interaction may be realized by silica nanoparticles administration into intercellular space. This allows determining the contribution of intercellular interactions in the thermodynamic properties of water associated with brain cells.

The aim of the work was to determine water parameters associated with brain cells, their parameters change in the case of necrotic lesions (stroke) and in the presence of an acidic agent (trifluoroacetic acid — TFA) allowing differentiation of intracellular water clusters by their capability to solve the acid [17, 18].

Materials and Methods

Materials. Samples of brain tissue were obtained by dissection of 50 years man's cadaver with the postmortem diagnosis: cerebrovascular disease, ischemic cerebral stroke (death occurred within 10 days after the onset of the disease). An autopsy of the body of the deceased was carried out in 6 hours followed by the detection of biological death. Sampling was carried out directly from the section of ischemic necrosis and distant part of the brain (macroscopically — the zone of intact tissue). Macroscopic description of the brain, photography in macro mode on Digital Cameras Canon Pover Shot A510 (Canon, China), selection of brain tissue samples for histological and NMR spectroscopic studies were carried out.

For the manufacture of histological preparations the fragments of the tissue after fixation with 10% neutral formalin solution according to a standardized method were dehydrated in increasing concentrations of ethanol and then embedded in paraffin blocks. Block sections with thickness of 3–5 microns were prepared using a sledge microtome, stained with hematoxylin-eosin by standard procedure.

Histological preparations (slices) were photographed by the camera Canon Power Shot A510 (Canon, China) using the separation capacity of 5 megapixels on the microscope Leica DM LS2, a lens 10×, 20×, ocular 10× and sim out adapter Leica DM LS2 (Leica Microsystems Wetzlar GmbH, Germany) using the program Remote Capture (Canon, China).

For NMR studies the tissue slice of about 2 cm thick was used. Tissues were frozen and stored at a temperature of 258 K. For the initial sample (Norm) obtaining the substance from the inside of frozen brain slice was taken by the puncture with 4 mm glass tube and placed in a 5 mm NMR ampoule and then in a pre-cooled to 210 K NMR spectrometer sensor. The intensity of the water signal was measured during the thawing of the sample up to a final temperature of T = 300 K.

To study the effect of the hydrophobic liquid media (deuterochloroform — $CDCl_3$) 0.5 g of frozen tissue was ground up to pieces of 1–3 mm^3 size, pieces were thawed and placed in $CDCl_3$ medium and maintained for 1 h. Then the tissue was placed in a 5-mm measuring ampoule and cooled up to 210 K, and then the measurements of ^1H NMR spectra during defrosting were carried out.

Effect of the solid medium was studied by administering the brain tissue in a matrix of silica TS-100 (manufactured by Cabot Corporation, USA). For this purpose 0.5 g of tissue was mixed with 100 mg of silica. Five minutes after the mixing of tissue with silica a homogeneous powder mass was formed in which the pieces of tissue up to 100 microns, and possibly a small group of individual cells, were coated with silica particles. Then a composite powder was placed in a 5-mm NMR ampoule in which in one and the same sample the state of the water in the initial sample and chloroform and (or) other organic substances additive containing sample could be studied. Partial dehydration of tissues containing particles of TS-100 silica was carried out at 313 K with an electronic scales provided with a heating device (a halogen lamp). In this way, the water content in the samples was adjusted to 50% of the original.

Low-temperature ^1H NMR spectroscopy. NMR spectra were recorded on the NMR spectrometer of high resolution (Varian "Mercury") with an operating frequency of 400 MHz. Eight 60°- sounding pulses of duration 1 μs at a bandwidth of 20 kHz were used. The temperature in the sensor was regulated by the Bruker VT-1000 temperature controller with an accuracy of ± 1 degree. The signal intensity was determined by measuring the peak areas using the procedure of signal decomposition into its components, assuming a Gaussian waveform and optimizing the zero line and phase with an accuracy that for well-resolved signals did not fall below 5% and for overlapping signals of ±10% . In order to prevent water super-cooling in the studied objects, the concentration of non-freezing water was measured at heating the samples, pre-cooled to a temperature of 210 K. The temperature dependences of NMR signals intensity were obtained in an automated cycle, when incubation of samples at a

constant temperature was 9 minutes, and the measurement time was 1 minute.

As the main parameter that determines the structure of water hydrogen bond network, the chemical shift of the protons (δ_H) was used. It was assumed that the water in which each molecule is involved in four hydrogen bonds forming (two due to protons and two due to unshared electron pairs of oxygen atoms) has a chemical shift $\delta_H = 7$ ppm (for hexagonal ice), and weakly associated water (not involved in the formation of hydrogen bonds as proton-donor) has the chemical shift $\delta_H = 1–1.5$ ppm [10–13]. For the geometric dimensions of the adsorbed water clusters determination, the Gibbs-Thomson equation, relating the radius of the spherical or cylindrical water cluster or domain (R) with the depression value of the freezing temperature [14,15], was used:

$$\Delta T_m = T_m(R) - T_{m,\infty} = \frac{2\sigma_{sl} T_{m,\infty}}{\Delta H_f \rho R}, \qquad (1)$$

where $T_m(R)$ is the melting temperature of the ice localized in the pores of radius R, $T_{m,\infty}$ is the bulk ice melting temperature, r is the solid phase density, s_{sl} is the solid-liquid interface energy and ΔH_f is the bulk enthalpy of melting. For practical use, equation (1) can be used in the form $\Delta T_m = (k/R)$, where the constant k for many heterogeneous water containing systems is close to 50 degrees·nm [13]. The methodology of NMR measurements and methods of determining the radii of interfacial water clusters has been described in detail in [10–13]. At that poly-associates with a radius $R<2$ nm may be considered as clusters, while larger polyassociates — as domains or nanodrops as they contain several thousand molecules of water [11].

The changes in the Gibbs free energy due to the effects of the limited space and the native interface correspond to the process of freezing (melting) of bound water. The smaller are differences because freezing in the volume; farther away from the surface is a layer of water. At $T = 273$ K water freezes, the properties of which correspond to the bulk water, and with temperature decreasing (excluding the effect of hypothermia) the water layers, located closer to surface, freeze. For the free energy of bound water (ice) change the following relation is valid

$$\Delta G_{\text{ice}} = -0.036(273.15 - T), \qquad (2)$$

where the numerical coefficient is a parameter, associated with the temperature coefficient of Gibbs free energy for ice change [19]. Determining by the magnitude of signal intensity the temperature dependence of nonfreezing water $C_{uw}(T)$ concentration, in accordance with the procedure described in detail in [10–13], the quantities of strongly and weakly bound water and thermodynamic characteristics of these layers can be calculated.

Water interfacial energy at the interface with solid particles, or in aqueous solution was determined as the modulus of total lowering of water free energy due to the presence of the phase boundary [10–13] by the formula:

$$\gamma_S = -K \int_0^{C_{\text{uw}}^{\max}} \Delta G(C_{\text{uw}}) dC_{\text{uw}}, \qquad (3)$$

where C^{max}_{uw} is the total quantity of nonfreezing water at $T = 273$ K.

Results and Discussion

Signs of a moderate edema-swelling of encephalon are marked macroscopically (furrows smoothness, tissue flabbiness, effusion on the cut surface of a transparent liquid drops), the area of ischemic necrosis (stroke) is determined in the left parietal-temporal zone as a structureless necrotic brain tissue about 4×5 cm in size, without clear borders (Fig. 1, *a, b*).

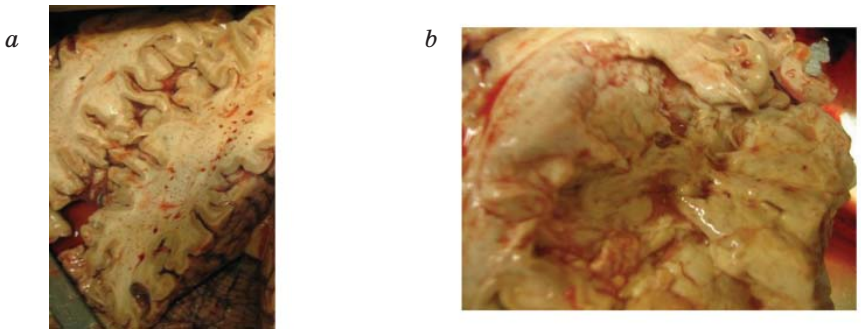

Fig. 1. **Brain:**
a — in health; *b* — an ischemic necrosis (stroke) zone without clear borders

The irregular blood filling of microvasculature vessels is noted on the light-optical level at pathomorphological investigation. There are blood redistribution into plasma and blood cells and intravascular erythrocytes aggregation in some part of vessels. The moderate sclerosis and plasmatic impregnation are observed in the vessel walls. Marked perivascular and pericellular edema, moderate net edema of varying prevalence are noticed. The degenerative changes of neurocytes with varying severity dominate: a significant portion of neurons are in swollen state, with karyorhexis, as a "melting" neurons and cells — "shadows". Extensive necrosis regions with karyolysis and neurocytolysis signs are registered. There is expressed glial cell response along the periphery of necrosis area (Fig. 2, *a*, *b*).

Fig. 3, *a*, *b* shows ^{1}H NMR spectra of the initial brain tissue sample registered at different temperature and device sensitivity, respectively. One broad signal is observed which chemical shift changes from $\delta_H = 4.5$ ppm at $T = 300$ K till $\delta_H = 5.8$ ppm at T = 220 K. It may be related to the strongly associated water [8–11]. Protons of lipid structures, as of biopolymers, do not appear in the spectra due to the short time of proton relaxation. Splitting into two signals with different intensities is observed in the spectra after thawing. This can be caused as by spatial inhomogeneity of the sample as by the existence of two forms of strongly associated water with different ordering which are the highest for the signal corresponding to larger value of the chemical shift. The signal intensity decreases with temperature reduction as a result of partial water freezing.

The width of the spectrum is significantly reduced after holding the tissue pieces in chloroform medium which also could fill the gaps between the individual pieces of tissue and penetrate into the bilipid layer of cell membranes (Fig. 3, *c*, *d*). Besides strongly associated water the group of signals lying in the range of $\delta_H = 1 \div 4$ ppm appear at the spectra. The most intense signal has a chemical shift $\delta_H = 1.25$ ppm which can be caused by the lipid component. The intensity ratio of water and lipids signals shows that their quantity is 5–6 wt% relative to the total water quantity. This is consistent with the amount of lipids in the brain determined by biochemical methods [5]. The appearance of lipids' signal in chloroform presence indicates that $CDCl_3$, dissolving in the substance of cell membranes, transfers them from the liquid crystal state (characterized by small time of nuclear magnetic relaxation) to more mobile — liquid state. It should be noted that the signal of weakly associated water may be located in the same spectral range [8–11]. However, we can assume that this form of water is absent or its NMR signal is very low at the chosen experimental conditions.

The cell structures in the brain are associated with intercellular interactions, which are implemented by neurotransmitters, and also by hydrogen, van der Waals and other types of interactions. In previous works on studying of the hydrated hydrophilic nanosilica interaction with hydrophobic organic substances [19, 20] or lactic zoogloea cell cultures with nanosilica TS-100 [21] it was found that the stable heterogeneous structures of micron size may be formed in a wide range of component concentrations where hydrophobic and hydrophilic sites coexist without phase stratification. This method can be used for brain tissue components encapsulating by silica. Nanoparticles reduce intercellular interactions penetrating into the intercellular gaps. The changes in the characteristics of intracellular water enable to estimate the influence of intercellular interactions on the

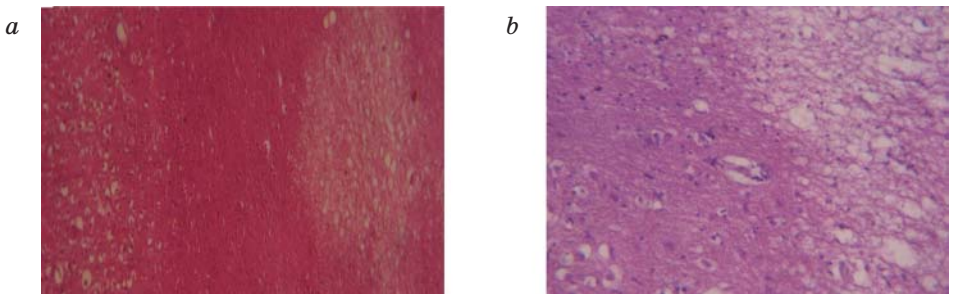

Fig. 2. **Brain fragments:**
a — necrosis zone with marked pericellular edema (×100);
b — "melting" neurons and cells — "shadows", necrosis zone with the neurons decomposition (×200).
Hematoxylin-eosin

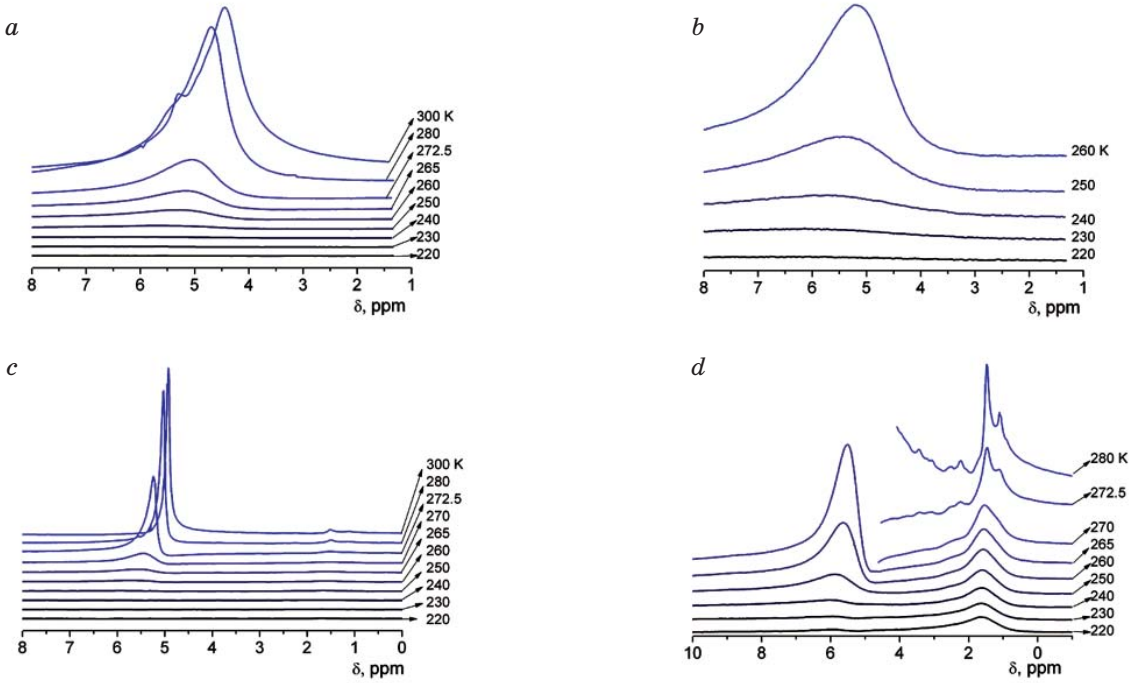

Fig. 3. **^{1}H NMR spectra of the tissue:**
at different temperature (*a, b*) and higher sensitivity of NMR spectrometer (*b, d*), native tissue sample (*a, b*) and exposed for 1 h in $CDCl_3$ medium (*c, d*)
Note: hereinafter there are the typical experiment results.

water mostly located within cells (glia and neurons).

Fig. 4 shows registered ^{1}H NMR spectra of brain tissue samples containing silica TS-100 in the air (*a, b*) and in $CDCl_3$ medium (*c, d*) at different temperatures. In comparison with the similar spectra on Fig. 3, the spectra feature on Fig. 4, *a–d* is a little bit larger signals width. This complicates the registration and separation of the signals of proton containing groups belonging to the lipid component. Significant reduction of intracellular water freezing temperature indicates the clusters ($R \leq 2$ nm) or domains ($R > 2$ nm) formation in cells, which size is determined according to the equation 1.

It is known that acids are dissolved well in the bulk water but its solubility drops sharply at its transition into nanostructured state (when water polyassociates are less than 20 nm of size) [17, 18]. This effect could be caused by reducing of hydration energy of acid molecules in strongly associated water clusters (domains) due to the necessity for significant hydrogen bonds restructuring. Inasmuch as the proton chemical shift in acids is significantly more (11 ppm in acid) then in strongly associated water (4–5 ppm), so in the presence in cells of water polyassociates differently dissolving TFA, several signals with different chemical shift value could be observed in ^{1}H NMR spectra.

The addition of 20 wt% TFA into the cell mass (Fig. 4, *e, f*) results in three signals (1–3 at Fig. 4, *e, f*) of water-acid solution with different component concentrations. There is the maximal acid concentration in strongly associated water clasters, corresponding to the signal 1, a bit smaller concentration is for the clusters manifested as the signal 2. The chemical shift values for the signal 3 are the same as in the samples without TFA. As its intensity is maximal it could be concluded that a significant portion of intracellular water practically does not dissolve TFA. A redistribution of signals intensity and their displacement in the region of larger chemical shift values take place in the spectrum with temperature decreasing. Mainly that water freezes which does not contain TFA. The signal intensity of H_2O-TFA solution increases again ($T = 210$ K) after reaching some minimal value at $T = 220$ K. This can be related with the existence of metabolic processes (with water molecules, acid or protons participation) that occur among solution clusters located inside a cell mass and adsorbed on the surface of the solid silica particles.

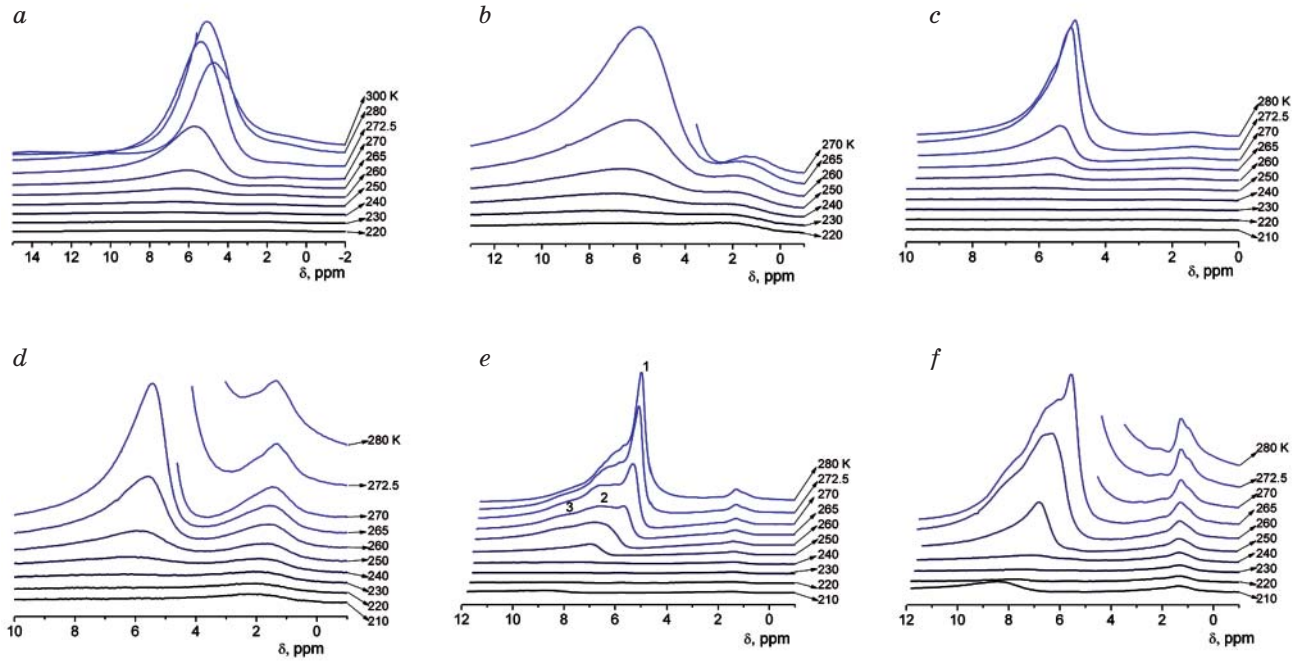

Fig. 4. **^{1}H NMR spectra of the tissue:**
at different temperatures (*a, c, e*) and spectrometer sensitivity (*b, d, f*); containing silica TS-100 in the air (*a, b*); $CDCl_3$ medium (*c, d*) and $CDCl_3$ medium with 20% TFA (*e, f*)

The layer characteristics of different forms of water ($C_{uw}{}^s$ and $C_{uw}{}^w$ for strongly and weakly bound water, respectively) and interfacial energy value (γ_S) which characterizes the total decrease in the free energy of water, caused by the presence of phase boundaries, and calculated on the basis of changes in the concentration of nonfreezing water depending on the temperature (Fig. 5, *a*) and Gibbs free energy changes depending on the concentration of nonfreezing water (Fig. 5, *b*) are shown in the table. Fig 5, *c* shows the bound water clusters distribution by radii.

According to the table data, the maximum value of the free energy reduction in the layer of strongly associated water (ΔG^S) is practically independent on the medium, in which measurements were accomplished. The exposure of the sample in chloroform medium leads to some reduction in the contribution of strongly associated water. Respectively, γ_S value decreases from 36 to 28.5 J/g. Addition of TFA to organic medium results in significant γ_S value increasing (2 times). Probably, it is related to salvation effect of water and acid interaction, which contributes to lowering the freezing temperature of water in aqueous acidic solution.

Water in the initial sample is presented as a system of clusters and domains, for which the maximum of the distribution responds to domains with R = 20 nm. Except this there is a small maximum with R = 2 nm. The exchange of the air on chloroform medium leads to decreasing of the main maximum and to increasing the total volume of domains with R = 100 nm. Thus, weakly polar organic medium reduces the energy of the water interaction with the internal interfaces. Acid addition results in relative increasing of the influence of domains and clusters of smaller radius (Fig. 5, *c*). This is due to the ice crystallization from an aqueous TFA solution when strong intermolecular water-acid interactions hinder the formation of hexagonal ice bulk crystals.

Despite the fact that silica nanoparticles penetrate into neuroglia intercellular space and into the gaps between neurons, thereby reducing intercellular interactions, the significant increasing in the interfacial energy of associated water is observed in the

investigated brain tissue samples (table). It can be assumed, that destruction of the gel glia structure is accompanied by formation of composite silica-cells particles with low content of weakly bound water. The difference in the values of interfacial energy of the initial brain tissue and its encapsulated form should be attributed to the energy predominance in the composite formation. At the same time there are significant changes in the characteristics of intermolecular interactions in the intercellular gaps. Accordingly, the main maximum on the distribution curve $\Delta C(R)$ shifts toward lower values and corresponds to domains with $R = 7$ nm (table, Fig. 5, *c*). The chloroform medium in the encapsulated sample stabilizes domains of larger radius. This process is accompanied by a significant decrease in γ_S value.

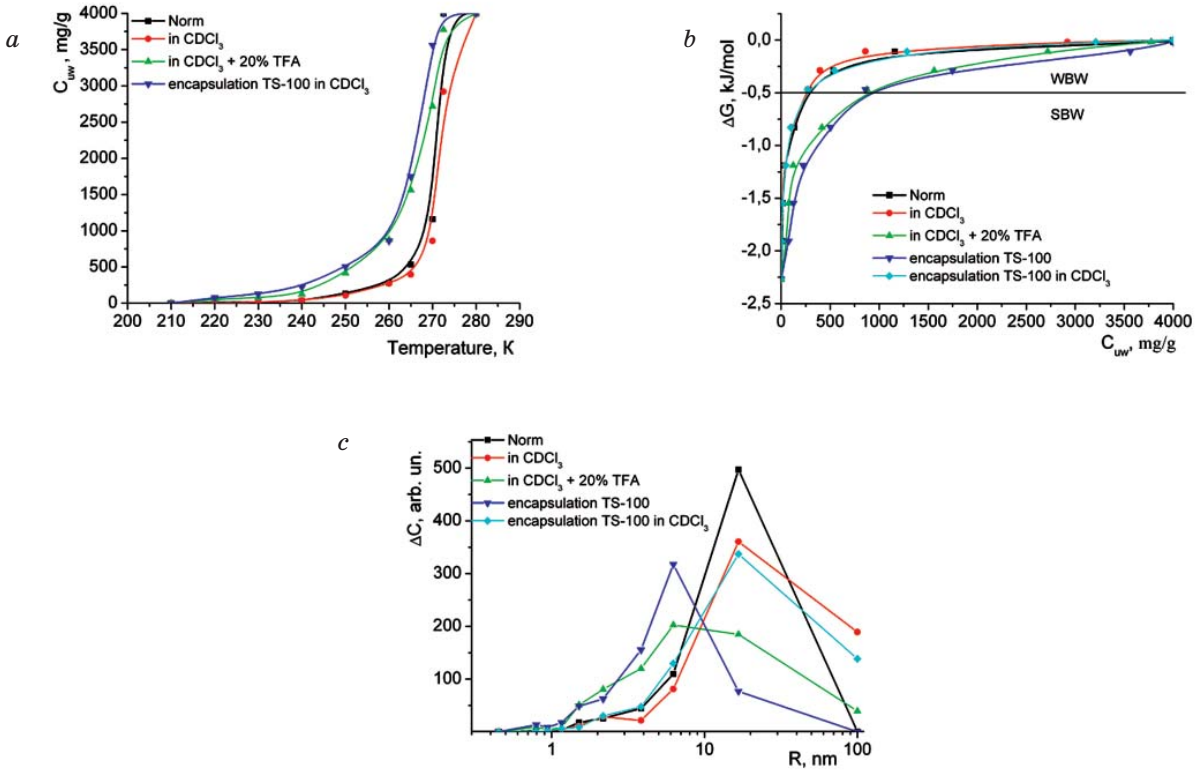

Fig. 5. **The temperature dependences:**
a — nonfreezing water concentration; *b* — changes of Gibbs free energy;
c — distribution of water clusters associated with brain tissue by radii

The characteristics of the water layers in the brain tissue samples in different media

Sample		Medium	C_{H_2O} (mg/g)	ΔG^s (kJ/mol)	$C_{uw}{}^s$ (mg/g)	$C_{uw}{}^w$ (mg/g)	γ_S (J/g)
*Norm		Air	4000	−2.25	250	3750	36
*Norm		$CDCl_3$	4000	−2.25	225	3775	28.5
*Norm		$CDCl_3$+20% TFA	4000	−2.25	900	3100	76
Brain tissue + silica TS-100	*Norm	Air	4000	−2.25	900	3100	89.5
	*Norm	$CDCl_3$	4000	−2.25	400	3600	34
	*Norm	Air	2000	−2.8	1000	1000	66
	**Lesion	Air	2000	−2.25	500	1500	39.5
	*Norm	$CDCl_3$	2000	−2.25	1200	800	69.4
	**Lesion	$CDCl_3$	2000	−2.25	300	1700	23.5

Notes: * — normal brain tissue; ** — brain tissue from the region of ischemic stroke.

Fig. 6 shows ^{1}H NMR spectra obtained at different temperatures for the investigated brain tissue samples containing 2 g/g of bound water for samples of initial tissue and of the tissue located in the ischemic stroke zone. Measurements were performed in air (Fig. 6, *a*, *b*) and $CDCl_3$ medium (Fig. 6, *c*, *d*). The temperature dependences of nonfreezing water concentration, changes in Gibbs free energy and clusters (domains) distribution by radii, calculated according to the equation of Gibbs-Thomson, are shown in Fig. 7, *a*–*c*.

For both samples, in air in ^{1}H NMR spectra one signal is registered with the chemical shift of 5–6 ppm which corresponds to better ordering of hydrogen bonds structure in the brain in comparison with liquid water, which usually has δ_H = 4,5–5 ppm [8]. The signal of lipid component appears in the spectra in chloroform medium at δ_H = 1–3 ppm. When temperature is lowering the signals intensity decreases due to water and lipid transition to the solid state.

A comparison of the $C_{uw}(T)$ dependences and strongly and weakly bound water amounts calculated on their basis (table) demonstrates that the dehydration leads to reduction of weakly bound water amount while strongly bound water amount increases significantly. For the brain tissue sample obtained from the area of ischemic stroke the contribution of weakly bound water is much greater as evidenced by a comparison of the respective $C_{uw}{}^s$, $C_{uw}{}^w$ and γ_S values.

The partially dehydrated sample of normal tissue (Norm) has greater contribution of water clusters with a radius R = 2 nm in comparison with initial sample (if compare Fig. 5, *c* and Fig. 7, *c*). The domains contribution with R = 20 nm increases when placing this sample in a weakly polar medium. The presence of ischemic necrosis area leads to stabilizing of water polyassociates with radius R = 20 nm, and in $CDCl_3$ medium — with radius R = 100 nm, which are characteristic for weakly bound water.

The measurements of an ability of strongly associated water polyassociates (clusters, domains) to dissolve TFA were performed for tissue samples in $CDCl_3$ medium (Fig. 8). Addition of 20% TFA, that can be dissolved in cell water, into $CDCl_3$ medium results in three signals (1–3) with chemical shifts in the range of δ_H = 5–10.5 ppm (Fig. 8). Taking into

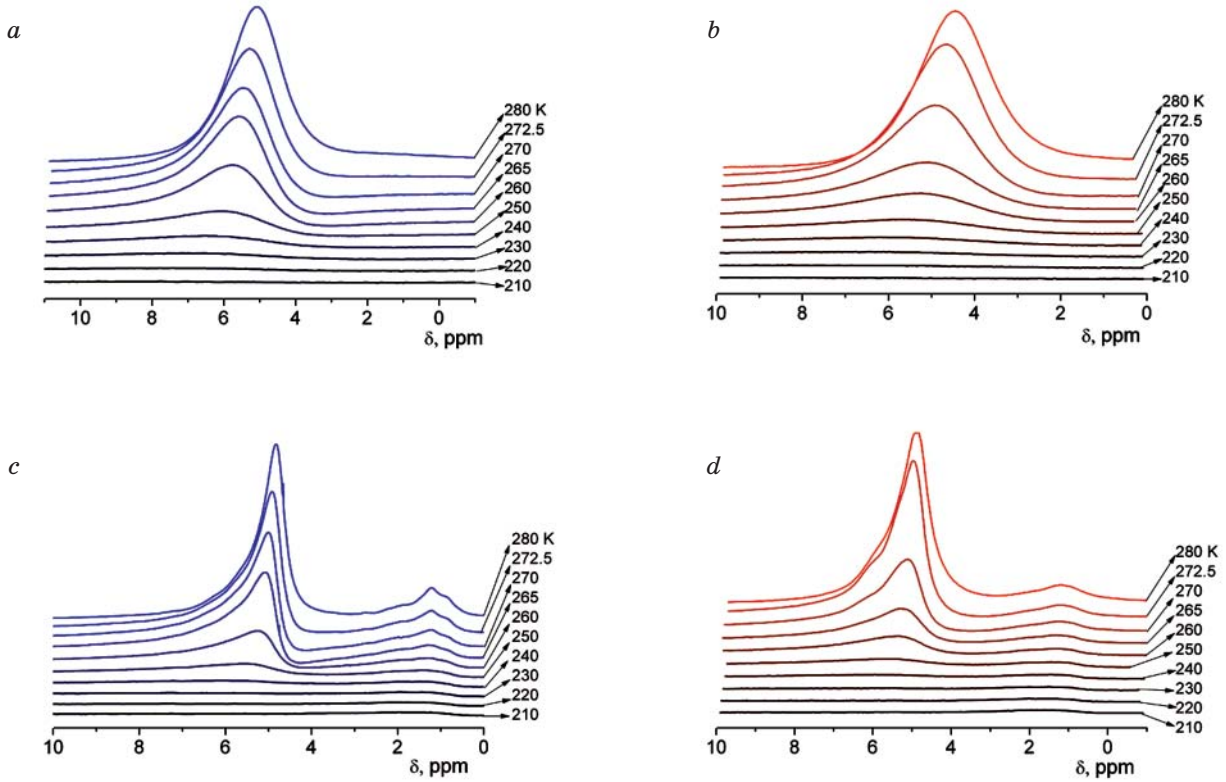

Fig. 6. **^{1}H NMR spectra of brain tissue samples containing silica nanoparticles TS-100:** for normal tissue at different temperatures (*a*, *c*); from the area of ischemic stroke (*b*, *d*) in the air (*a*, *b*) and in $CDCl_3$ medium (*c*, *d*) at C_{H_2O} = 2 g/g

account that the chemical shift of strongly bound water in brain tissue is δ_H = 4.5–6 ppm and δ_H = 11 ppm for pure TFA, it may be concluded that the signal 3 was caused by the water clusters (domains), which practically do not dissolve TFA (the TFA concentration is less than 10 wt% there); signal 2 (δ_H = 7–8 ppm) — by polyassociates, which are able to dissolve up to 30 wt% of TFA; and signal 1 — by concentrated solution of water–TFA. With temperature lowering the intensity of all signals decreases due to water freezing (likely, in the form of hexagonal ice), but at low temperatures so does — TFA.

The ratio between different types of water-TFA polyassociates differs significantly for normal tissue and tissue from ischemic necrosis area (Fig. 9). In the normal tissue the largest amount of interfacial water is a part of the clusters (domains) responsible for signal 2 while signal 3 is recorded only at low temperatures. Exactly this signal is dominant in a wide temperature range in tissue damaged by necrosis. For the damaged tissue also the signal 1 has relatively lower intensity.

Thus, almost all the water, located in the brain tissue, is associated and is a part of the domain and clusters, significant part of which have radii R = 2 and 20 nm. The chloroform medium stabilizes water polyassociates with radius less than R = 100 nm, and TFA stabilizes water polyassociates with radii R = 7–20 nm.

Addition of silica nanoparticles TS-100 into the brain tissue leads to formation of composite systems where parts of the tissue (and possibly separate cells) are surrounded by silica nanoparticles. This composite looks like a wet powder that facilitates to study the impact of the organic medium on the water polyassociates structure. In the composite system of brain tissue / silica the average size of water polyassociates is considerably less than in the initial tissue (R = 7 nm). The average domain size increases up to 20 nm in $CDCl_3$ medium. At least three types of domain differently dissolving acid are observed in the spectra in the presence of TFA.

Partial dehydration of the investigated brain tissue samples is accompanied by reducing in the amount of weakly bound water and some increasing in the amount of strongly bound water, that indicates a change of molecular interactions between the components of cell-nanoparticle composite system.

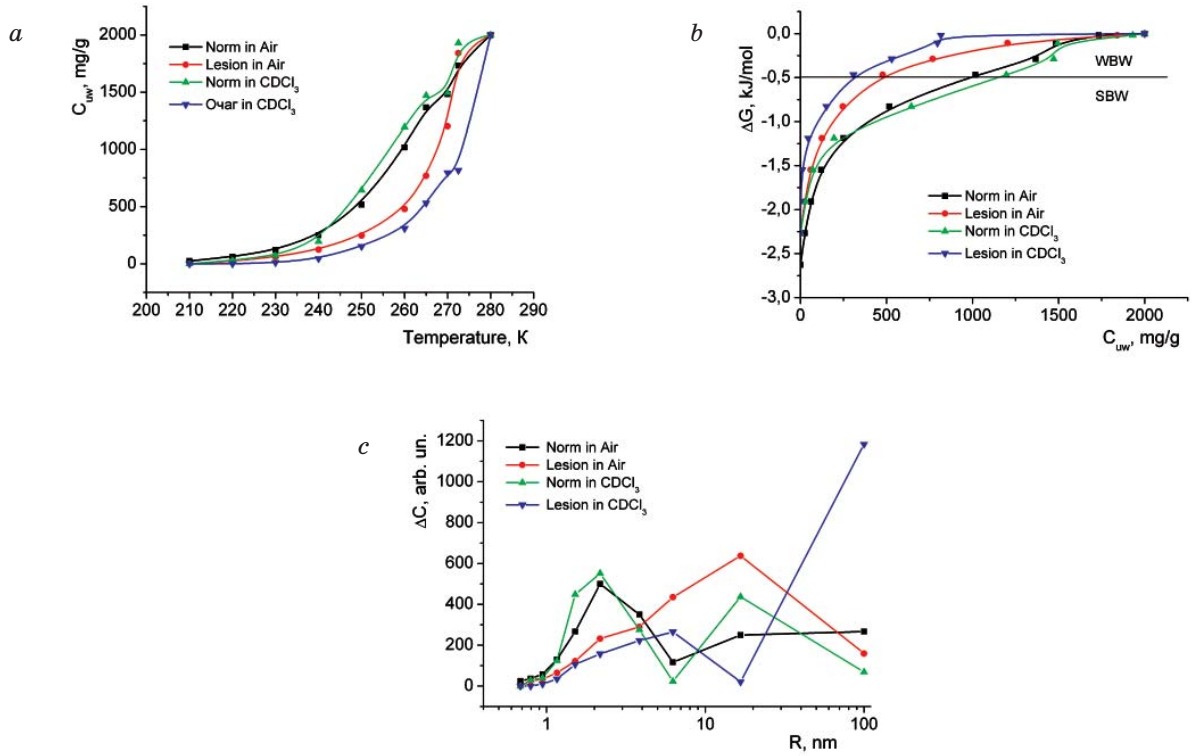

Fig. 7. **The temperature dependences:**
nonfreezing water concentration (*a*); changes in Gibbs free energy (*b*); and distribution by radii of water clusters (*c*); connected by normal brain tissue and by tissue from the ischemic necrosis area containing silica nanoparticles TS-100 (amount of residual water 2 g/g)

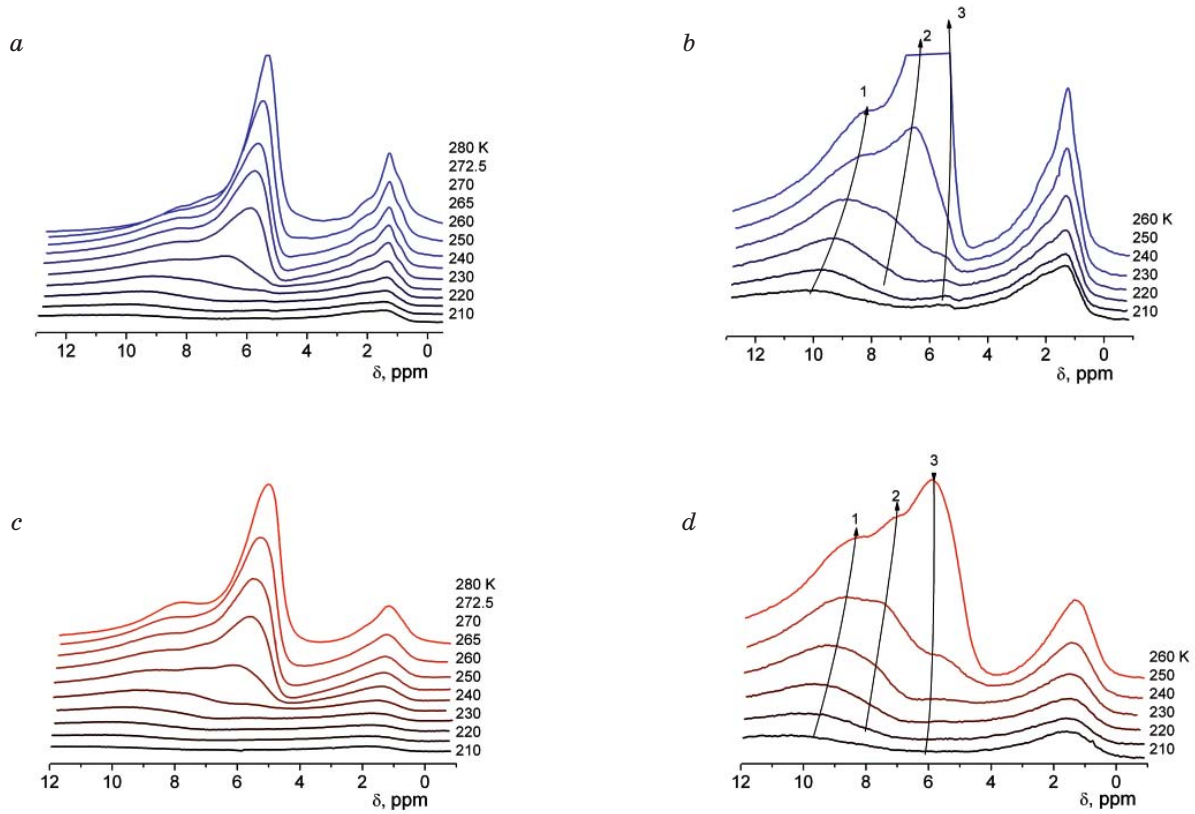

Fig. 8. **^{1}H NMR spectra:**
of brain tissue samples at different temperatures in $CDCl_3$ medium with addition of 20 wt% TFA for normal brain tissue (*a*, *b*) and for tissue from ischemic necrosis area (*c*, *d*)

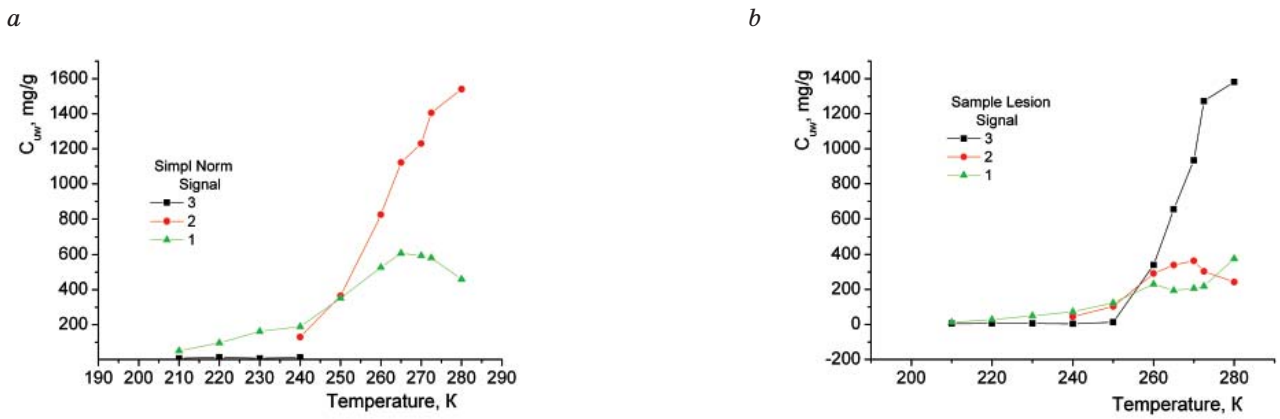

Fig. 9. **The temperature dependences for water concentration, being a part of the different types of water-TFA polyassociates:**
a — intact tissue, *b* — stroke

The presence of the ischemic necrosis area in the brain tissue increases the size of bound water polyassociates, which occurs as in air and in a weakly polar organic solvent (deuterochloroform) media.

The addition of TFA in an organic medium enables to differentiate the clusters (domains) of cell water with respect to their ability to dissolve the acid. In the normal brain tissue the bulk of the water is in a composition of polyassociates capable of dissolving up to 30% of acid. For the tissue obtained from ischemic necrosis area the bulk of the water is in the domains slightly dissolving the acid.

REFERENCES

1. Therapeutic electrical stimulation of the human brain and nerves. Ed. red. N. P. Bekhtereva. *Moskva: ACT; St. Petersburg: Sova; Vladimir: VKT*. 2008, 464 p. (In Russian).
2. *Azin A. L, Gruzdev D. V., Kublanov B. C.* The dynamics of intercellular transport in brain tissue (Radiophysical study approach). *Vestnik novykh meditsinskikh tekhnologiy*. 2002, 9 (4), 74–79. (In Russian).
3. *Wiegell M., Larsson H., Wedeen V.* Fiber crossing in human brain depicted with diffusion tensor MR imaging. *Radiology*. 2000, V. 217, P. 897–903.
4. *Bronge L.* Magnetic resonance imaging in dementia. A study of brain white matter changes. *Acta. Radiol., SuppL.* 2002, V. 428, P. 1–32.
5. *Berezov T. P., Korovkin B. F.* Biological Chemistry. *Moskva: Meditsina*. 1998, 704 p. (In Russian).
6. *Block. R. E.* Factors Affecting Proton Magnetic Resonance Line-widths of Water in Several Rat Tissues. Federation European Bio-chem. *Soc. Lett*. 1973, V. 34, P. 109–112.
7. *Carr H. Y. Purcell E. M.* Effects of Diffusion on Free Precession in NMR Experiments. *Phys. Rev*. 1954, V. 84, P. 630–638.
8. *Clifford J., Pethica B. A., Smith E. G.* A Nuclear Magnetic Resonance Investigation of Molecular Motion in Erythrocyte Membranes. In: L. Bolis and B. A. Pethica (Eds.). Membrane Models and the Formation of Biological Membranes. *Amsterdam: North Holland Publishing Co*. 1968, P. 19–42.
9. *Damadian R.* Tumor Detection by Nuclear Magnetic Resonance. *Science*. 1971, V. 171, P. 1151–1153.
10. *Gun'ko V. M., Turov V. V., Gorbik P. P.* Water on interfaces. *Kyiv: Naukova dumka*. 2009, 694 p. (In Russian).
11. *Gun'ko V. M., Turov V. V.* Nuclear Magnetic Resonance Studies of Interfacial Phenomena. *Taylor & Francis, New York*. 2013, 1076 p.
12. *Turov V. V., Gun'ko V. M.* The clastered water and ways of its applications. *Kyiv: Naukova dumka*. 2011, 313 p. (In Russian).
13. *Gun'ko V. M., Turov V. V., Bogatyrev V. M., Zarko V. I., Leboda R., Goncharuk E. V., Novza A. A., Turov A. V., Chuiko A. A.* Unusual Properties of Water at Hydrophilic/ Hydrophobic Interfaces. *Adv. Coll. Interf. Sci*. 2005, V. 118, P. 125–172.
14. *Aksnes D. W., Kimtys L.* Characterization of mesoporous solids by ^{1}H NMR. *Solid State Nuclear Magnetic Resonance*. 2004, V. 25, P. 146–163.
15. *Petrov O. V., Furo I.* NMR cryoporometry: Principles, application and potential. *Progr. NMR*. 2009, V. 54, P. 97–122.
16. *Kinney D. R., Chaung I-S., Maciel G. E.* Water and the Silica Surface As Studied by Variable Temperature High Resolution ^{1}H NMR. *J. Am. Chem Soc*. 1993, V. 115, P. 6786–6794.
17. *Turov V. V., Gun'ko V. M., Turova A. A., Morozova L. P., Voronin E. F.* Interfacial behavior of concentrated *HCl* solution and water clustered at a surface of nanosilica in weakly polar solvents media. *Coll. Surf. A: Physicochem. Engin. Asp*. 2011, 390 (1), 48–55.
18. *Turov V. V., Todor I. N., Lukianova N. Yu., Krupskaya T. V., Ugnivenko A. P., Chekhun V. F.* Effect of trifluoroacetic acid in water clustering partially dehydrated rat liver Guerin carcinoma. *Dopovidi NAN Ukrayny*. 2014, N 2, P. 129–133. (In Russian).
19. Thermodynamic properties of individual substances. Ed. V. P. Glushko. *Moskva: Nauka*. 1978, 495 p. (In Russian).
20. *Turov V. V., Gun'ko V. M., Zarko V. I., Goncharuk O. V., Krupska T. V., Turov A. V., Leboda R., Skubiszewska-Zięba J.* Interfacial Behavior of *n*-Decane Bound to Weakly Hydrated Silica Gel and Nanosilica over a Broad Temperature Range. *Langmuir*. 2013, V. 29, P. 4303–4314.
21. *Krupskaya T. V., Prylutskyy Yu. I., Evstigneev M. P., Tsapko M. D., Turov V. V.* ^{1}H NMR characnerization of nanoscale aqueous structure in zoogloea Tibetan milk mushroom: influence of hydration and hydrophobic environment. *Zh. pricladnoy spektroskopii*. 2015, 82 (3), 341–347. (In Russian).

СТАН ВОДИ В ТКАНИНІ ГОЛОВНОГО МОЗКУ ЗА ПРИСУТНОСТІ НАНОЧАСТИНОК КРЕМНЕЗЕМУ TS-100

Т. В. Крупська[1]
С. В. Пакришень[2]
О. В. Сєров[2]
О. Т. Волик[3]
В. В. Туров[1]

[1]Інститут хімії поверхні ім. О. О. Чуйка НАН України, Київ
[2]Патолого-анатомічне відділення Олександрівської клінічної лікарні, Київ
[3]Київський міжнародний університет, медико-фармацевтичний факультет

E-mail: krupska@ukr.net

Методом низькотемпературної ^{1}H ЯМР-спектроскопії вивчено будову гідратних шарів води, зв'язаної клітинами головного мозку, зміну цих параметрів за некротичних ушкоджень (інсульт) і за присутності трифторацтової кислоти, що дає змогу диференціювати кластери внутрішньоклітинної води за їхньою здатністю розчиняти кислоту. Розглянуто також вплив наночастинками кремнезему TS-100 на стан води у тканині головного мозку, а саме на параметри зв'язування води на повітрі та за присутності слабополярного розчинника.

Для кластерів сильноасоційованої міжфазної води отримано розподіли за радіусами і змінами вільної енергії Гіббса. Показано, що гідратні властивості нативної тканини відрізняються від властивостей за некротичних ушкоджень будовою кластерів слабоасоційованої води. В інтактній тканині вся вода є зв'язаною і входить до складу кластерів і доменів, значна частина яких має радіуси R = 2 і 20 нм. Середовище із хлороформом стабілізує водні поліасоціати з радіусом до R = 100 нм, а трифторацтова кислота — з радіусами R = 7–20 нм. Встановлено, що часткова дегідратація досліджуваних зразків тканини супроводжується зменшенням кількості слабозв'язаної води і деяким зростанням кількості сильнозв'язаної води, що свідчить про зміну молекулярних взаємодій між компонентами композитної системи клітини–наночастинки. Присутність осередку ішемічного некрозу призводить до зменшення зв'язування води через збільшення водних поліасоціатів середніх розмірів. Цей ефект спостерігається як на повітрі, так і в середовищі слабополярного органічного розчинника — дейтерохлороформу.

Ключові слова: ішемічний інсульт, сильно- і слабозв'язана вода, ^{1}H ЯМР-спектроскопія.

СОСТОЯНИЕ ВОДЫ В ТКАНИ ГОЛОВНОГО МОЗГА В ПРИСУТСТВИИ НАНОЧАСТИЦ КРЕМНЕЗЕМА TS-100

Т. В. Крупская[1]
С. В. Пакришень[2]
А. В. Серов[2]
А. Т. Волик[3]
В. В. Туров[1]

[1]Институт химии поверхности им. А. А. Чуйко НАН Украины, Киев
[2]Патолого-анатомическое отделение Александровской клинической больницы, Киев
[3]Киевский международный университет, медико-фармацевтический факультет

E-mail: krupska@ukr.net

Методом низкотемпературной ^{1}H ЯМР-спектроскопии изучено строение гидратных слоев воды, связанной клетками головного мозга, изменение этих параметров при некротических повреждениях (инсульт) и в присутствии трифторуксусной кислоты, позволяющей дифференцировать кластеры внутриклеточной воды по их способности растворять кислоту. Рассмотрено также влияние наночастиц кремнезема TS-100 на состояние воды в ткани головного мозга, а именно на параметры связывания воды на воздухе и в присутствии слабополярного растворителя.

Для кластеров сильноассоциированной межфазной воды получены распределения по радиусам и изменениям свободной энергии Гиббса. Показано, что гидратные свойства нативной ткани отличаются от свойств при некротических повреждениях строением кластеров слабоассоциированной воды. В интактной ткани вся вода является связанной и входит в состав кластеров и доменов, значительная часть которых имеет радиусы R = 2 и 20 нм. Среда с хлороформом стабилизирует водные полиассоциаты с радиусом до R = 100 нм, а трифторуксусная кислота — с R = 7–20 нм. Установлено, что частичная дегидратация исследуемых образцов ткани сопровождается уменьшением количества слабосвязанной и некоторым ростом количества сильносвязанной воды, что свидетельствует об изменении молекулярных взаимодействий между компонентами композитной системы клетки–наночастицы. Присутствие очага ишемического некроза приводит к уменьшению связывания воды за счет роста водных полиассоциатов среднего разме ра. Этот эффект наблюдается как на воздухе, так и в среде слабополярного органического растворителя — дейтерохлороформа.

Ключевые слова: ишемический инсульт, сильно- и слабосвязанная вода, ^{1}H ЯМР-спектроскопия.